

NASA Contractor Report 172424

P-104

IN-01

DATE OVERRIDE

97705

FINAL REPORT

Development of Laminar Flow Control Wing Surface Porous Structure

(NASA-CR-172424) DEVELOPMENT OF LAMINAR
FLOW CONTROL WING SURFACE POROUS STRUCTURE
Final Report (McDonnell-Douglas Corp.) 104
p Avail: NTIS EC A06/MF A01 CSCL 01B

N87-28502

Unclas
G3/01 0097705

DOUGLAS AIRCRAFT COMPANY
MCDONNELL DOUGLAS CORPORATION
LONG BEACH, CALIFORNIA

CONTRACT NAS1-17506
JULY 1984



National Aeronautics and
Space Administration

Langley Research Center
Hampton, Virginia 23665

on any reproduction of this data in whole or in part. Date for general release
will be three (3) years from date indicated on the document.

NASA Contractor Report 172424

FINAL REPORT

Development of Laminar Flow Control Wing Surface Porous Structure

**DOUGLAS AIRCRAFT COMPANY
MCDONNELL DOUGLAS CORPORATION
LONG BEACH, CALIFORNIA**

**CONTRACT NAS1-17506
JULY 1984**



**National Aeronautics and
Space Administration**

**Langley Research Center
Hampton, Virginia 23665**

on any reproduction of this data in whole or in part. Date for general release
will be three (3) years from date indicated on the document.

FOREWORD

This document summarizes the work performed by Douglas Aircraft Company, McDonnell Douglas Corporation, on Laminar Flow Control (LFC) structural concepts under NASA Contract NAS1-16234, entitled Wing Surface Structural Development. The contract activity is part of the overall Aircraft Energy Efficiency (ACEE) program supported by NASA through its Langley Research Center.

Acknowledgments for their support and guidance are given to the NASA LFC Project Manager, Mr. R. Wagner, and to the Project Technical Monitors, Mr. J. Cheely and Mr. D. Maddalon.

The Douglas personnel primarily responsible for this work were:

M. Klotzsche	ACEE Program Manager
W. Pearce	LFC Project Manager
C. Anderson	WSSD Project Manager
J. Thelander	Aerodynamics
W. Boronow	Environmental Systems
F. Gallimore	Materials and Processes
W. Brown	Structures
T. Matsuo	Structures
J. Christensen	Structural Mechanics
G. Primavera	Suction Systems

TABLE OF CONTENTS

<u>SECTION</u>		<u>PAGE</u>
	FOREWORD	i
	TABLE OF CONTENTS	ii
	FIGURE AND TABLES	v
	SYMBOLS AND ABBREVIATIONS	ix
1.0	INTRODUCTION	1
2.0	SUMMARY	2
3.0	STRUCTURAL DESIGN	4
3.1	INTRODUCTION	4
3.2	WING STRUCTURAL CONFIGURATION	5
3.3	PANEL GEOMETRY	12
3.4	ENVIRONMENTAL EFFECTS ON THE PANEL STRUCTURE	29
	3.4.1 Rain Erosion Tests	33
	3.4.2 Impact Damage Test	35
	3.4.3 Materials Compatibility Tests	37
	3.4.3.1 Liquid Evaluation	38
	3.4.3.2 Determination on New Test Conditions	39
	3.4.3.3 Laminate Evaluation	41
	3.4.3.4 Adhesive Evaluation	41
3.5	CONCLUSIONS AND RECOMMENDATIONS - STRUCTURAL DESIGN	42
4.0	SUCTION/CLEARING SYSTEM	44
4.1	INTRODUCTION	44
4.2	GENERAL DESIGN CRITERIA	44
4.3	FLOW REQUIREMENTS	45
	4.3.1 Suction Requirements	45
	4.3.2 Clearing Requirements	46

TABLE OF CONTENTS (continued)

<u>SECTION</u>		<u>PAGE</u>
4.4	CONCEPTS	46
4.4.1	Suction System Concepts	46
4.4.2	Clearing Systems Concept	48
4.4.3	Configuration Studies	48
4.5	ANALYSIS	52
4.5.1	Suction/Clearing Flow Calculation	52
4.5.2	Porosity Study	53
4.5.3	Control Valve Study	55
4.6	DETAIL DESIGN	55
4.6.1	Ducts and Channels	55
4.6.2	Orifices and Valves	57
4.7	CONCLUSIONS AND RECOMMENDATIONS - SUCTION AND CLEARING SYSTEMS	58
5.0	ICE PROTECTION AND CONTAMINATION AVOIDANCE SYSTEM	60
5.1	INTRODUCTION	60
5.2	CONFIGURATION AVOIDANCE AND ICE PROTECTION SYSTEM REQUIREMENTS	62
5.2.1	Fixed Leading Edge	62
5.3	PERFORMANCE AND DESIGN STUDIES	64
5.3.1	Intermittent Chordwise Design	64
5.3.2	Integration Suction/Contamination/Ice Protection Design	65
5.3.3	Pressure Drop Through Perforated Titanium	66
5.3.4	Environmental Contamination	69
5.4	CONCLUSIONS AND RECOMMENDATIONS - ICE PROTECTION AND CONTAMINATION AVOIDANCE	70
6.0	FABRICATION AND PROCESS DEVELOPMENT	71
6.1	INTRODUCTION	71

TABLE OF CONTENTS (continued)

<u>SECTION</u>		<u>PAGE</u>
6.2	FABRICATION TOOLING FOR CURVED PARTS	71
6.3	TITANIUM WELDING, PROCESSING, AND BONDING	78
6.3.1	Titanium Welding and Forming	78
6.3.2	Titanium Processing and Bonding	78
6.4	CONCLUSIONS AND RECOMMENDATIONS - FABRICATION DEVELOPMENT	79
7.0	SUMMARY OF CONCLUSIONS AND RECOMMENDATIONS	80
8.0	REFERENCES	84
9.0	APPENDIX I	85

LIST OF FIGURES

<u>FIGURE</u>		<u>PAGE</u>
3.1	Wing Arrangement	4
3.2	Suction Surface - Electron Beam Perforated Titanium	6
3.3	LFC Glove Panel Structure	6
3.4	Wing Arrangement for Spanwise Collection of Suction Airflow	7
3.5	Variation of \bar{t} with T/C Ratio for Two Wing Stations	8
3.6	Panel Buckling Load Versus Wing Rib Spacing	10
3.7	Typical Chordwise Distribution of Suction Velocity Required and Surface Pressure	11
3.8	Combined Spanwise and Chordwise Air Collection System	12
3.9	General Arrangement of LFC Panels	13
3.10	Buckling Allowables for Carbon Fiber/Titanium Panels	14
3.11	Material Combination Specimen	16
3.12	Three Footed Dial Indicator Gage	16
3.13	Panel Surface Measurement Locations	17
3.14	Panel Surface Measurement Values of Point Numbers Per Figure 3.13	18
3.15	LFC Surface Waviness Tolerance	20
3.16	Material Combination Specimen for 0.86 Inch Deep Panel	21
3.17	Panel Dimensions and Measurement Locations for Panel Surface Waviness Tests (0.86 Inch Deep Panel)	23
3.18	Panel Surface Deflection Values of Panels Without Thermal Compensation (0.86 Inch Deep Panels)	25
3.19	Panel Surface Deflection Values of Panels with Thermal Compensation (0.86 Inch Deep Panels)	26
3.20	Closing of Corners During Laminate Cure - Outside Corner	27
3.21	Typical Layup with Multi-Piece Plies in the Corrugation	28
3.22	Typical Panel with Individually Wrapped Corrugations	28
3.23	Panel Dimensions and Measurement Locations for Individually Wrapped Corrugations	31
3.24	Panel Surface Deflection of Individually Wrapped Corrugations (Without Thermal Compensation)	32
3.25	Flight Profile - True Airspeed Versus Altitude for 1990's LFC Transport	33
3.26	Rain Erosion Test Specimen - Panel Materials and Dimensions	34

LIST OF FIGURES (continued)

<u>FIGURE</u>		<u>PAGE</u>
3.27	Porous Surface Panel Ball Impact Test Results	36
3.28	Impact Test Specimen	36
3.29	Evaporation Rate of PGME in Still Air	39
3.30	Double Lap Shear Tests Graphite-Epoxy Immersed in Glycol	41
4.1	Suction System Manifolding	47
4.2	Wing Surface Panels	48
4.3	Wing Arrangement for Spanwise Collection of Suction Airflow	49
4.4	Spanwise Air Collection System	50
4.5	Chordwise Air Collection System	51
4.6	Flute-to-Channel Orifice Sizing - Constant Surface Porosity	52
4.7	Suction and Clearing Airflow Requirements	53
4.8	Flute-to-Channel Orifice Sizing with Variable Surface Porosity	54
4.9	Surface Porosity Requirement	54
4.10	Leading Edge Air Collectors	56
4.11	Duct Sizing	57
4.12	Conceptual Valve Design	58
5.1	Spanwise Dispensers	64
5.2	Intermittent Dispensers	66
5.3	Liquid Pressure Drop Through 0.0026 Inch Diameter Perforated Titanium	66
5.4	Liquid Pressure Drop Across 0.025 Inch Perforated Titanium with 0.0026 Inch Diameter at 0.026 Inch Spacing Using 60% PGME Plus 40% Water at Various Temperatures	68
5.5	Environmental Contamination of 0.0026 Inch Diameter Perforated Titanium - Specimen No. 1	69
5.6	Environmental Contamination of 0.0026 Inch Diameter Perforated Titanium - Specimen No. 2	70

LIST OF FIGURES (continued)

<u>FIGURE</u>		<u>PAGE</u>
6.1	Corrugated Panel Fabrication Steps	72
6.2	Hard Tooling for Curved Panels	73
6.3	Flexible Tooling for Curved Panels	73
6.4	Eight Harness Satin Weave Cloth	75
6.5	Ridges Caused by Silicone Expansion	77
6.6	Caul Plate Tooling	77

LIST OF APPENDIX I

A1-1	Upper Surface Pressure Distribution	87
A1-2	Upper Surface Isobars	88
A1-3	MARIA Crossflow Stability Analysis (No Suction)	89
A1-4	MARIA Crossflow Stability Analysis (With Suction)	90
A1-5	WSSD D3128 SUCTION REQUIREMENTS	91

LIST OF TABLES

<u>TABLE</u>		<u>PAGE</u>
3.1	LFC Transport Wing Dimensions	5
3.2	Dial Indicator Tabulated Panel Surface Measurement Values	19
3.3	Surface Deflection Values - Material Combinations Specimens	24
3.4	Surface Deflection Values - Material Combinations Specimens Individually Wrapped Corrugations	30
3.5	Rain Erosion Data	35
3.6	FM 73 Adhesive Strength After 2 and 4 Week Soak at 160°F	37
3.7	Double Lap Shear Strength After Two Week Exposure	38
3.8	Preconditioning of the Specimens	40

SYMBOLS AND ABBREVIATIONS

C	Wing Chord
C _q	Suction Coefficient
C _{root}	Root Chord
C _{tip}	Tip Chord
CAC	Chordwise Collection
CVS	Composite Vertical Stabilizer
DiEGBE	DiEthylene Glycol Butyl Ether
DFRC	Dryden Flight Research Center
DPS	Douglas Process Standard
EB	Electron Beam
EG	Ethylene Glycol
EGME	Ethylene Glycol Methyl Ether
FPD	Freezing Point Depressant
GPM	Gallons Per Minute
h _s	Height of Single Wave
h _m	Height of Multiple Waves
IP/CA	Ice Protection/Contamination Avoidance
K	Knots
KIAS	Knots Indicated Airspeed
LEFT	Leading Edge Flight Test
LFC	Laminar Flow Control
PD	Pressure Drop
PGME	Propylene Glycol Methyl Ether
PSF	Pounds Per Square Foot
PSFA	Pounds Per Square Foot Absolute

SYMBOLS AND ABBREVIATIONS (continued)

PSI	Pounds Per Square Inch
PSIG	Pounds Per Square Inch Gauge
R_c	Chord Reynolds Number
SAC	Spanwise Air Collection
SPF	Super Plastic Forming
TIG	Tungsten Inert Gas
T/C	Wing Thickness to Chord Ratio
\bar{t}	Combined Skin and Stringer Area Divided by the Panel Width Effective Thickness
V	Velocity
W	Airflow Rate lb/min/ft ²
WSSD	Wing Surface Structure Development
α	Coefficient of Thermal Expansion
μ	Standard Viscosity
μ_0	Viscosity at Test Condition
Λ	Leading Edge Sweep Angle
λ	Wavelength of Surface Waves
σ	Standard Density of Air
σ_0	Density at Test Condition

1. INTRODUCTION

This report discusses the work accomplished under NASA Contract NAS1-16234 Wing Surface Structure Development (WSSD). Due to funding cutbacks, the contract was terminated prior to the end of the preliminary design phase of the program. Consequently the major structural design and test efforts originally planned were not conducted. Significant work was accomplished, however, and a decision was made to document the work even though it was incomplete in some areas.

The principal activities during the preliminary design phase of the program were a review and updating of the wing design for the 1990's Laminar Flow Control (LFC) transport aircraft as defined in Reference 1 and development of the suction surface panels using the electron beam perforated titanium identified in Reference 1 as the preferred suction surface material.

Although the study was primarily on wing surface structure development, integration of the various systems associated with LFC was essential, and parallel system studies were undertaken to ensure that a practical structural arrangement would be designed and tested.

The design activity was divided into three parts by function: wing structure design, suction system design and analysis, and design and structural integration of the ice protection/insect contamination avoidance (IP/CA) system. These design activities were, of course, interdependent but are discussed separately in this report.

2. SUMMARY

The basis for the WSSD program was the 1990's LFC transport configuration defined by NASA Contract NAS1-14632, Evaluation of Laminar Flow Control Systems for Subsonic Commercial Transport Aircraft (Reference 1). In this design, LFC was used on the upper wing surface back to 85 percent chord. Electron beam perforated titanium was used as the suction surface material. The surface panel was supported by the spanwise external stringers of the main wing box. This created integral spanwise ducts for the suction airflow. Ice protection and insect contamination avoidance was provided by a retractable high lift shield incorporating a spray system designed to coat the wing leading edge with a protective freezing point depressant (FPD) liquid.

The preliminary design phase of the WSSD contract involved refining the design of the LFC panels, the necessary panel supporting structure, the suction/clearing system, and the IP/CA system for the wing configuration discussed in Reference 1. With the spanwise ducting arrangement, an excessive number of control valves were found to be necessary to meter the low airflow rates associated with LFC suction, yet be able to accommodate the relatively high flows required to clear the surface of the IP/CA fluid. This system also required deeper ducts than originally anticipated which reduced wing structural efficiency by decreasing the effective depth of the wing box structure.

After investigating the various design options for the structure and the surface suction/clearing system, the decision was made to use chordwise collector ducts over the main wing box and to retain spanwise collection ducts in the leading and trailing edge regions. This action not only made the matching of suction and clearing airflow requirements much easier, but also simplified the suction manifold design allowing easy access to metering controls and several improvements in the structure design.

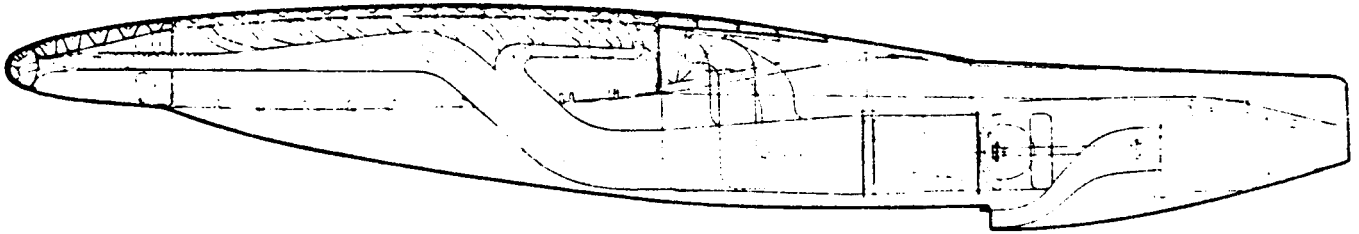
Numerous ancilliary activities in both design and fabrication supported the preliminary design activity. Two designs were created for dispensing the IP/CA fluid through the porous surface. A unique method of producing low cost tooling from silicone rubber was developed to reduce the time and money

required to fabricate the laminated substructures for the porous panels. The durability of the surface material was verified through ball impact and rain erosion tests, and the effects of the glycol based IP/CA fluid on various adhesive and laminate combinations were investigated. All of the epoxy based adhesives tested showed significant reductions in strength after prolonged exposure to the fluid. However, a nitrile-phenolic adhesive system was found to be more resistant and was selected for bonding the titanium skin to the laminated structure.

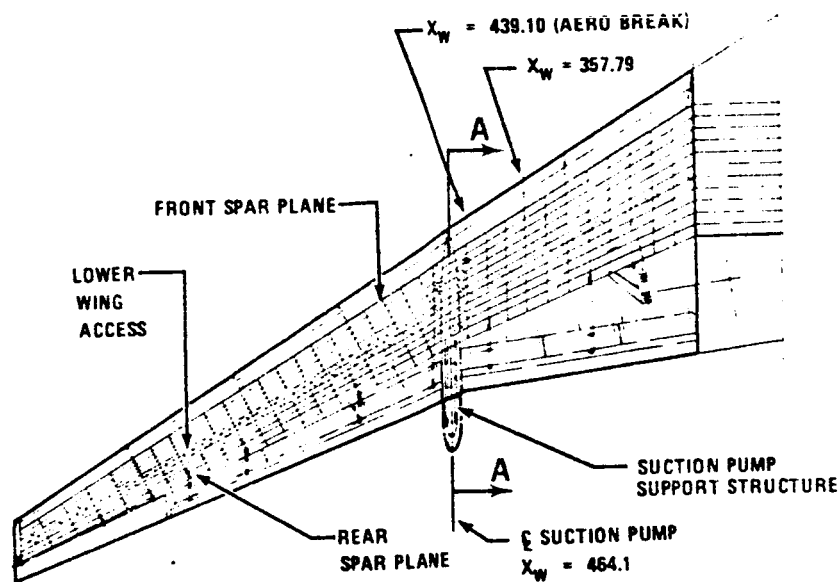
The WSSD program identified several areas where further work is needed in both the design and fabrication of surface panels.

3.1 INTRODUCTION

The LFC wing described in Reference 1 is shown in Figure 3.1 and is defined in Table 3.1.



SECTION A-A (ROTATED 90° COUNTERCLOCKWISE)

**WING ARRANGEMENT**

LAMINARIZATION TO 85 PERCENT CHORD
UPPER SURFACE ONLY

FIGURE 3.1

LFC TRANSPORT WING DIMENSIONS

Area	3100 Sq. Ft.
Span	176.1 Ft.
Aspect Ratio	10
Taper Ratio	0.25
Sweep (at Leading Edge)	30°
Thickness Ratio	0.107 Average
Front Spar Location	0.20 Chord at Tip 0.15 Chord at Root
Rear Spar Location	0.70 Chord

TABLE 3.1

LFC is provided to 85 percent chord on the upper surface only by suction through glove panels. These panels consist of an electron beam perforated titanium skin supported by a fiberglass corrugated substructure as shown in Figures 3.2 and 3.3. Panel support is provided by spanwise external stringers of the main wing box. This arrangement creates integral ducting that is used to handle the suction airflow. This provides a simple ducting scheme at the cost of structural efficiency and an increase in the complexity of manifold ducting to the suction source. Figure 3.4 shows the spanwise collection configuration which together with the surface panel shown in Figure 3.3 was the basis for the WSSD preliminary design. This phase of the WSSD program consisted of refining the design and adding more detail. The four areas of structural investigation were: wing structure configuration, panel geometry, environmental effects on the panel structure, and panel fabrication techniques. These are discussed in subsections 3.2, 3.3, 3.4, and section 6 respectively.

3.2 WING STRUCTURAL CONFIGURATION

The wing configuration shown in Figures 3.1 and 3.4 resulted from a decision to abandon LFC on both the upper and lower surfaces in favor of LFC suction on

SUCTION SURFACE ELECTRON-BEAM-PERFORATED TITANIUM

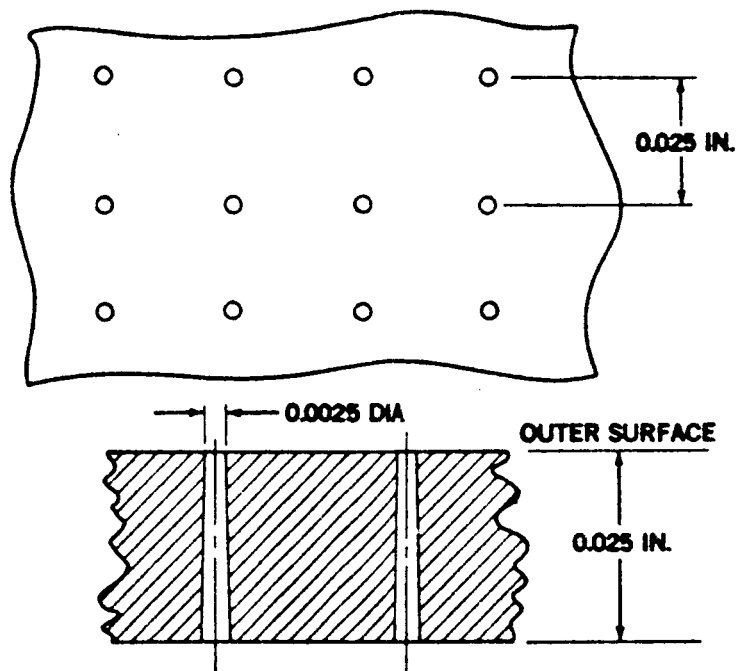
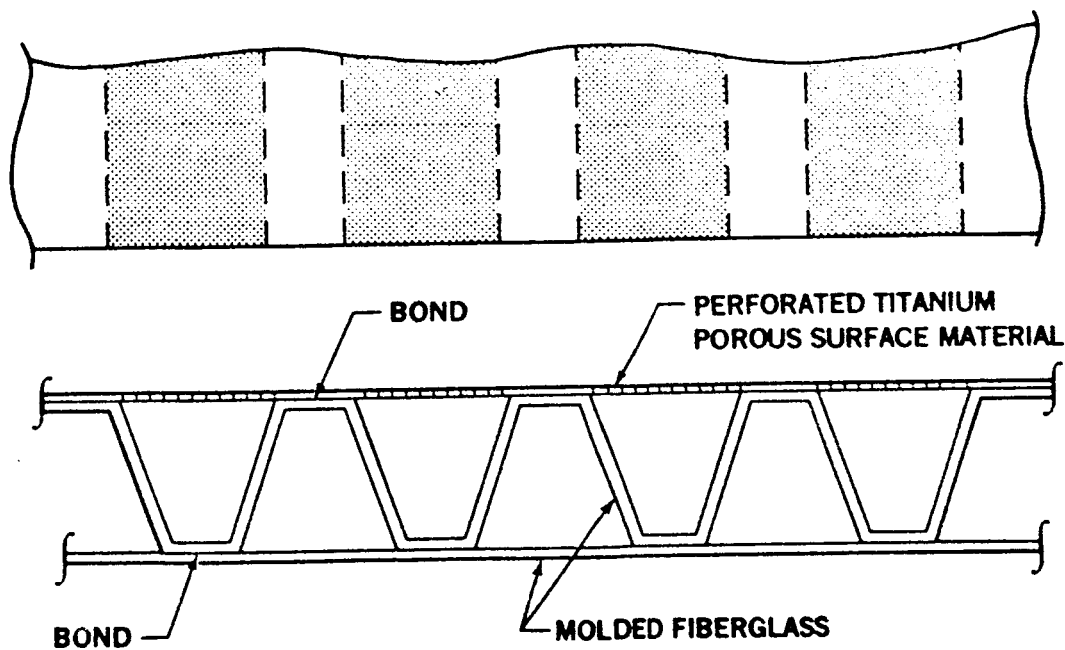


FIGURE 3.2



LFC GLOVE PANEL STRUCTURE

FIGURE 3.3

ORIGINAL PAGE IS
OF POOR QUALITY

ORIGINAL PAGE IS
OF POOR QUALITY

WING ARRANGEMENT FOR SPANWISE COLLECTION OF SUCTION AIRFLOW

UPPER SURFACE ONLY TO 85% CHORD

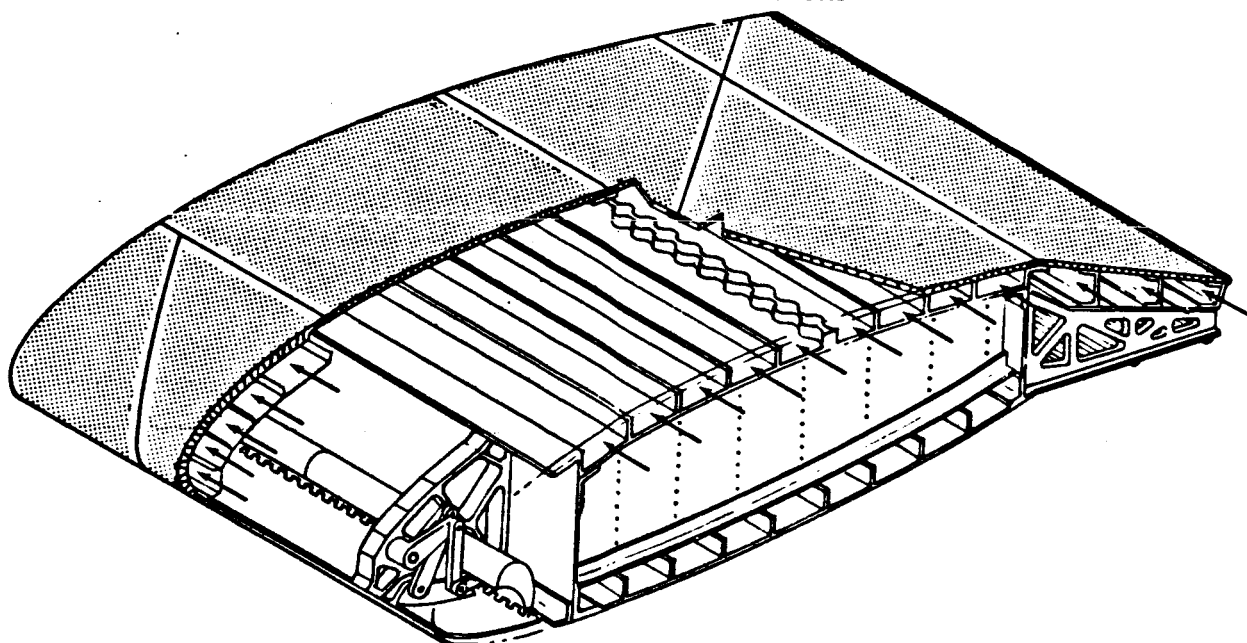


FIGURE 3.4

the upper surface only, back to 85 percent chord (see Reference 1). The initial study concluded that, in addition to other advantages, this system would be lighter because of the increase in effective structural wing thicknesses, and that additional savings could be gained by minimizing the height of the integral suction ducts. An investigation was therefore conducted in this WSSD program to determine the sensitivity of the wing weight to changes in effective wing thickness. Figure 3.5 shows a graph of effective wing thickness to chord ratio (T/C) versus the total bending material required with the skin and stiffeners smeared into an effective skin thickness (\bar{t}), for the original wing having suction on both surfaces.

VARIATION OF \bar{t} WITH T/C RATIO
FOR TWO WING STATIONS
LFC TO 70% CHORD ON BOTH SURFACES

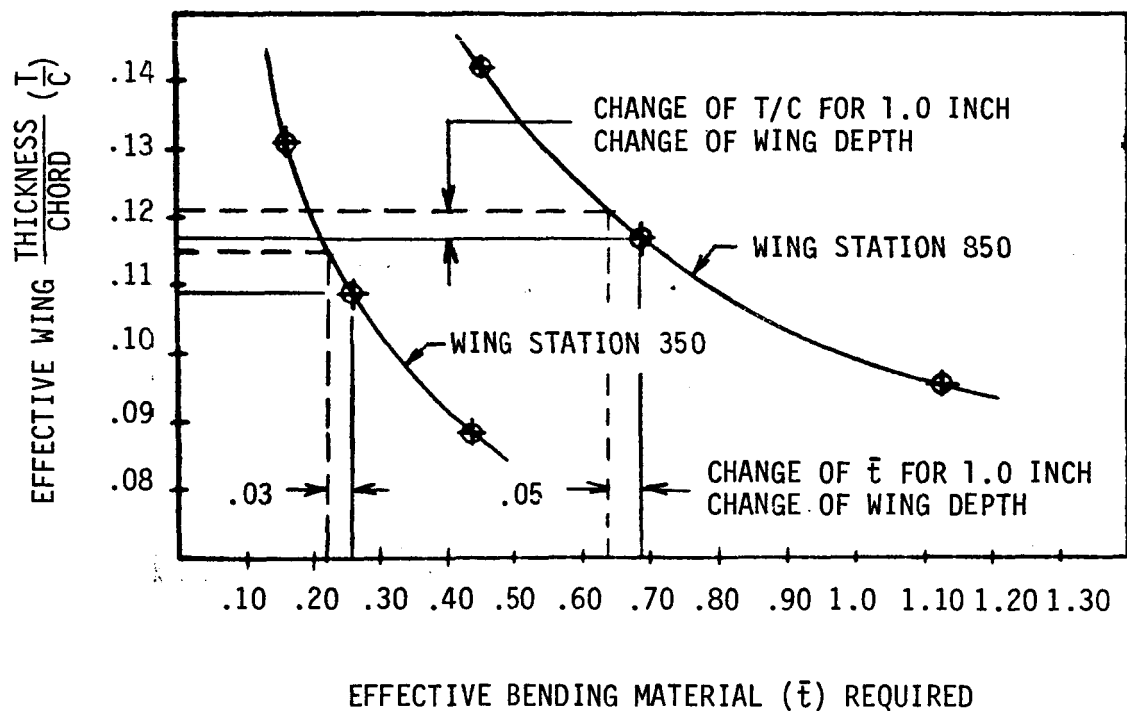


FIGURE 3.5

The change in the effective T/C and \bar{t} resulting from a 1.0 inch increase in the effective wing depth (thickness) is indicated by the dashed lines which show that \bar{t} decreases by 0.03 inch at wing station 850 and by 0.05 inch at station 350. This reduction in \bar{t} of 0.05 inch over the inboard wing box section whose area is 344 square feet, and a reduction of 0.03 over the outboard section whose area is 347 square feet, results in a weight saving for the entire wing of 890 pounds. This indicated that the wing weight was very sensitive to changes in effective T/C and that considerable efforts should be made to reduce the duct height. Although weight could be saved, reducing the height of the spanwise ducts could cause disadvantages. It would reduce the flow carrying capabilities of the ducts and would reduce the space available for duct control valves (see Section 4). Also, since reducing the duct height reduced the stringer height on the upper (compression) side of the wing, it results in reduced compression stability of the skin panels. This is illustrated in Figure 3.6 which shows a graph of wing rib spacing versus panel compression load for various stringer depths for a carbon fiber blade stiffened skin panel. The wing section properties are for 70 percent semispan on the wing, with suction on the upper surface only, and using spanwise air collection. This particular section was selected because it is where the maximum wing compression strains are expected to occur. The stringer depth at this point is nominally 1.4 inch and the overall area of bending material (t) is 0.33 square inch per inch of chord. It is evident from this graph that the desired ultimate strain rate of 0.004 inch per inch cannot be achieved without: increasing the stringer depth, decreasing the wing rib spacing, or adding bending material, any of which would increase wing weight. A different approach to the integration of the suction ducting and wing structure is therefore needed for the benefits of increased effective wing depth to be achieved. An alternative chordwise ducting arrangement was therefore investigated.

A diagram of the design suction and pressure distribution across the wing chord (Figure 3.7) shows that the external surface pressure, suction flow requirements, and the corresponding suction ducting pressure requirements are fairly constant in the region between 12 percent chord and 60 percent chord. This suggests that there is no fundamental need for chordwise metering and

FIGURE 3.6
OF FOUR CONTAIN

PANEL BUCKLING LOAD
VERSUS
WING RIB SPACING

SUCTION UPPER SURFACE ONLY
SPANWISE AIR COLLECTION

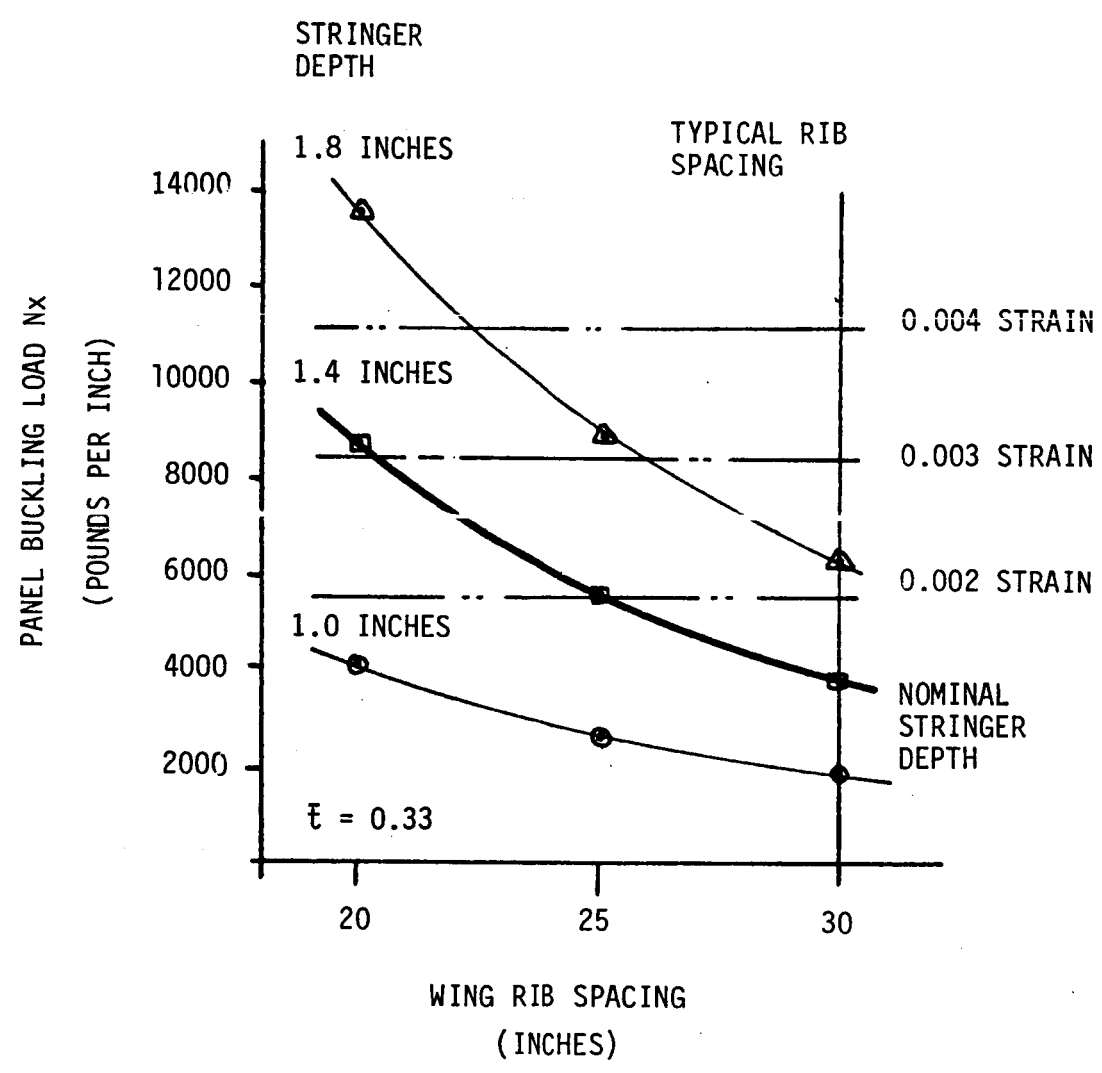


FIGURE 3.6

TYPICAL CHORDWISE DISTRIBUTION OF SUCTION VELOCITY REQUIRED AND SURFACE PRESSURE

ORIGINAL PAGE IS
OF POOR QUALITY

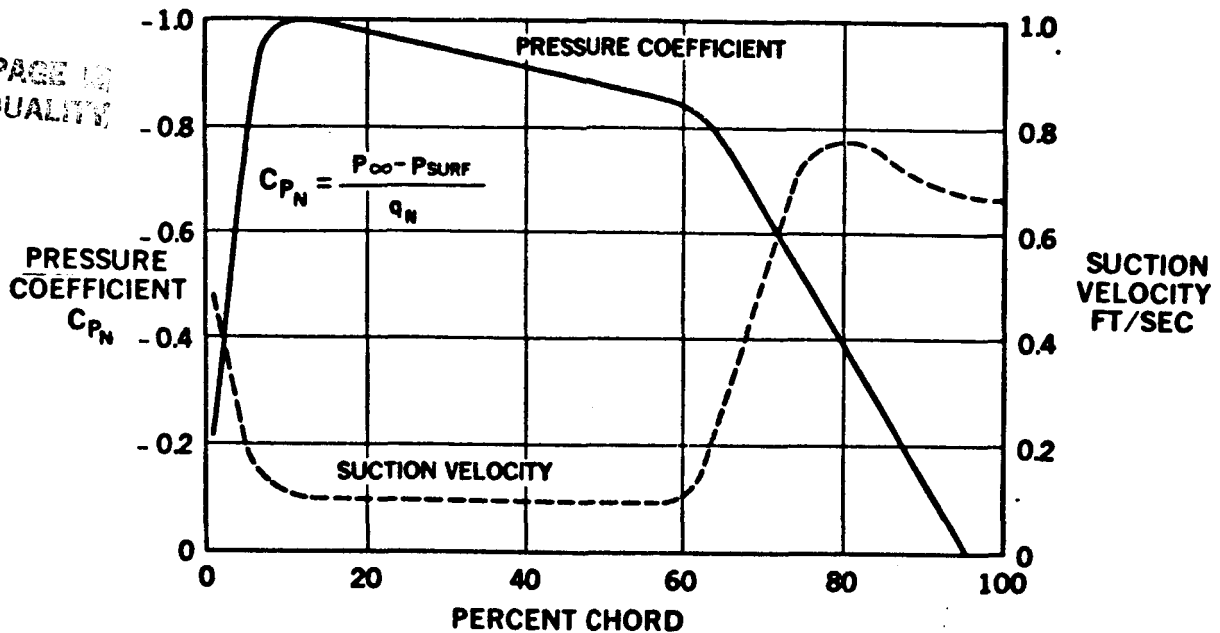


FIGURE 3.7

multiple ducting since the entire area could operate at the same suction level. If chordwise collection ducts were employed in this area, the integral ducts below the glove panel could be very shallow due to their much shorter length and reduced accumulated airflow. Additional weight could be saved by eliminating the multiple holes in the upper skin panel which feed suction air to the manifolds at the suction pumps. With the suction air collected and ducted spanwise forward of the front spar, large holes in the lower skin panel would also be eliminated and the manifolding in a dry wing bay would be unnecessary. Refer to Section 4 for details.

Figure 3.8 shows a system in which the air over the main wing box is collected by chordwise ducts while air from the leading and trailing edge regions, where the suction requirements are rapidly changing, is collected by spanwise ducts. Note the duct dividers can act as supports for the panel joints. These joints are at an angle to the external airflow to minimize the distance over which the air must travel without encountering suction when crossing a joint, thus the term chordwise air collection is not strictly true. Support of the chordwise joints is a desirable feature of this system because it would help to maintain the smoothness required over these joints which carry high spanwise compression loads.

COMBINED SPANWISE AND CHORDWISE AIR-COLLECTION SYSTEM

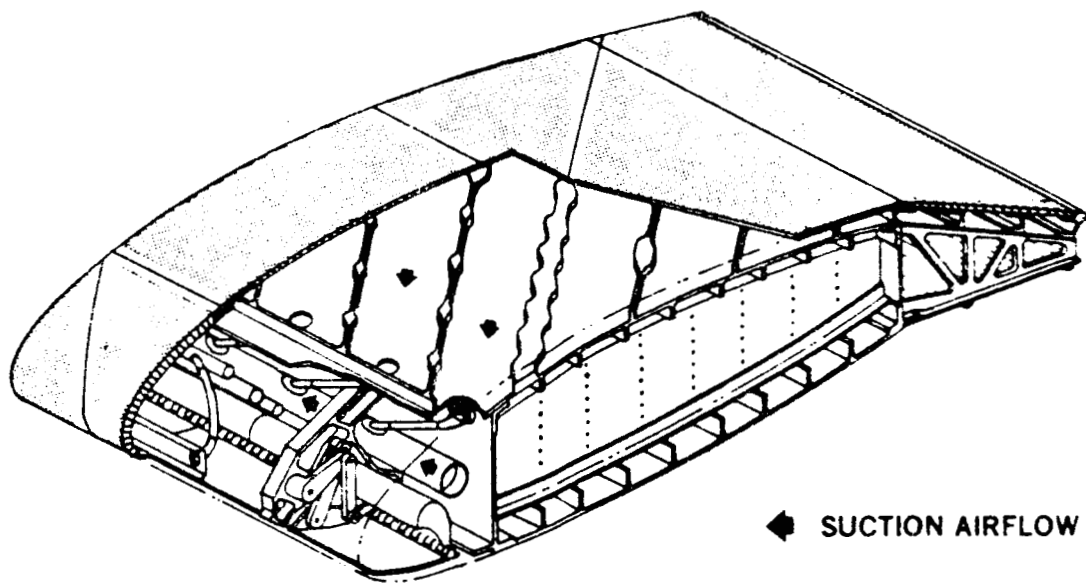


Figure 3.8

Another advantage is easier access to duct manifolding to allow suction pressure metering to compensate for spanwise pressure gradients.

After an extensive comparison of the two systems, the system using chordwise air collection over the main wing box was selected for the following reasons:

- o improved structure efficiency of the main wing box resulting in a reduction in wing weight, and
- o continuous support of the "chordwise" panel joints.

Additional reasons discussed in Section 4 are:

- o better matching of suction and clearing airflow requirements, and
- o simplified duct to suction source manifolding.

3.3 PANEL GEOMETRY

When perforated titanium was selected as the porous surface material, it allowed the surface panel to carry a larger share of the wing bending loads.

ORIGINAL PAGE 14
OF POOR QUALITY

This, in turn, suggested the use of carbon fiber in place of fiberglass for the corrugated substructure to improve the structural efficiency of the panel. One of the first questions to be addressed was how the use of carbon fiber would affect the panel geometry. It was apparent that the planform shape of the panels would still be trapezoidal with the long sides following percent chord lines and with the short sides parallel and at an angle to the airflow as suggested in Reference 1. Determining the appropriate size of the panels was a much more difficult problem because of the conflicting requirements of interchangeability, minimum number of joints, replacement frequency, and fabrication cost. Figure 3.9 shows a panel layout having four leading edge sections and eight panels over the remainder of the wing. These panels would be about 20 feet long and 5 feet wide. The choice of panel size is largely independent of the method of air collection used. The decision to use chordwise air collection over the main wing box did influence the choice of panel depth. With this configuration, the width of the chordwise ducts is

GENERAL ARRANGEMENT OF LFC PANELS

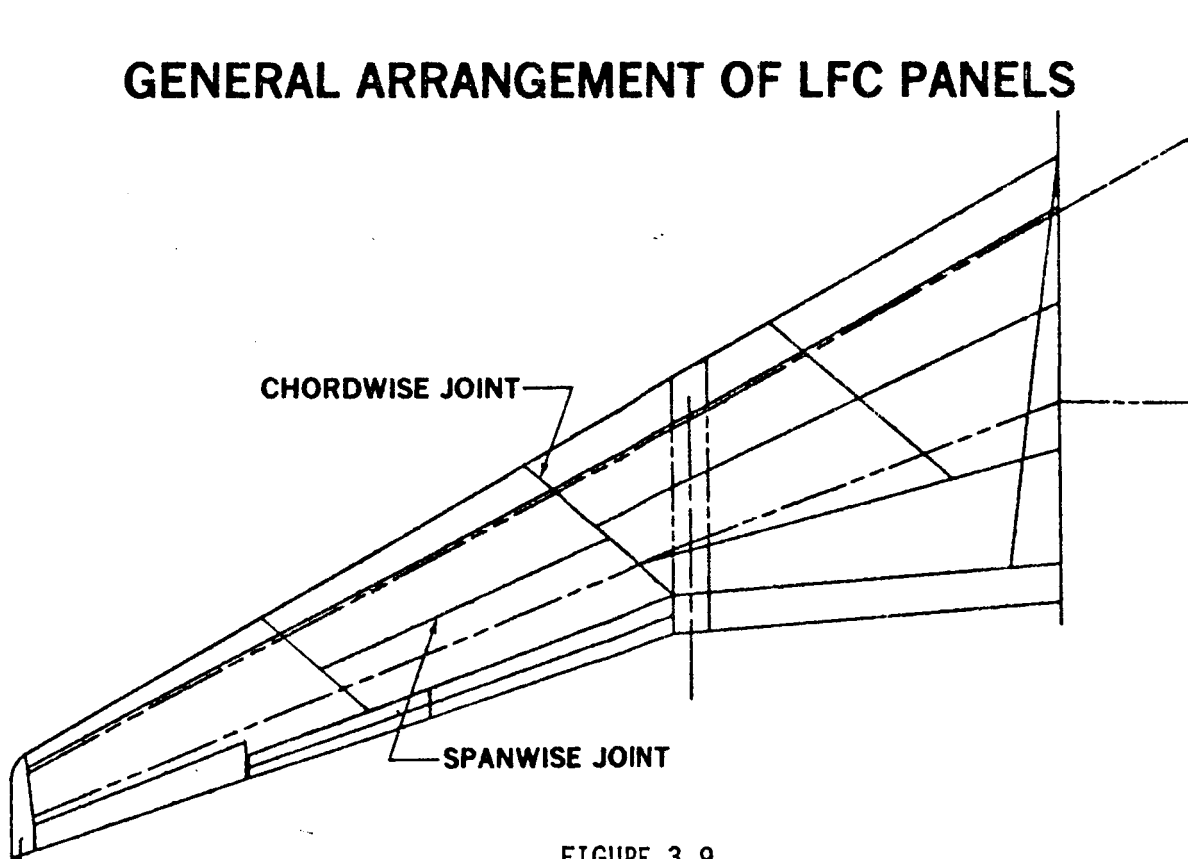


FIGURE 3.9

ORIGINAL PANEL
OF POOR QUALITY

also the panel support span which is the panel length used for panel buckling calculations. This length can be traded against panel depth to produce the lightest configuration which can achieve the design goal of 4,000 micro inches per inch ultimate strain. Figure 3.10 shows a graph of panel depth versus allowable buckling load for panels of 10, 12, and 15 inches in length.

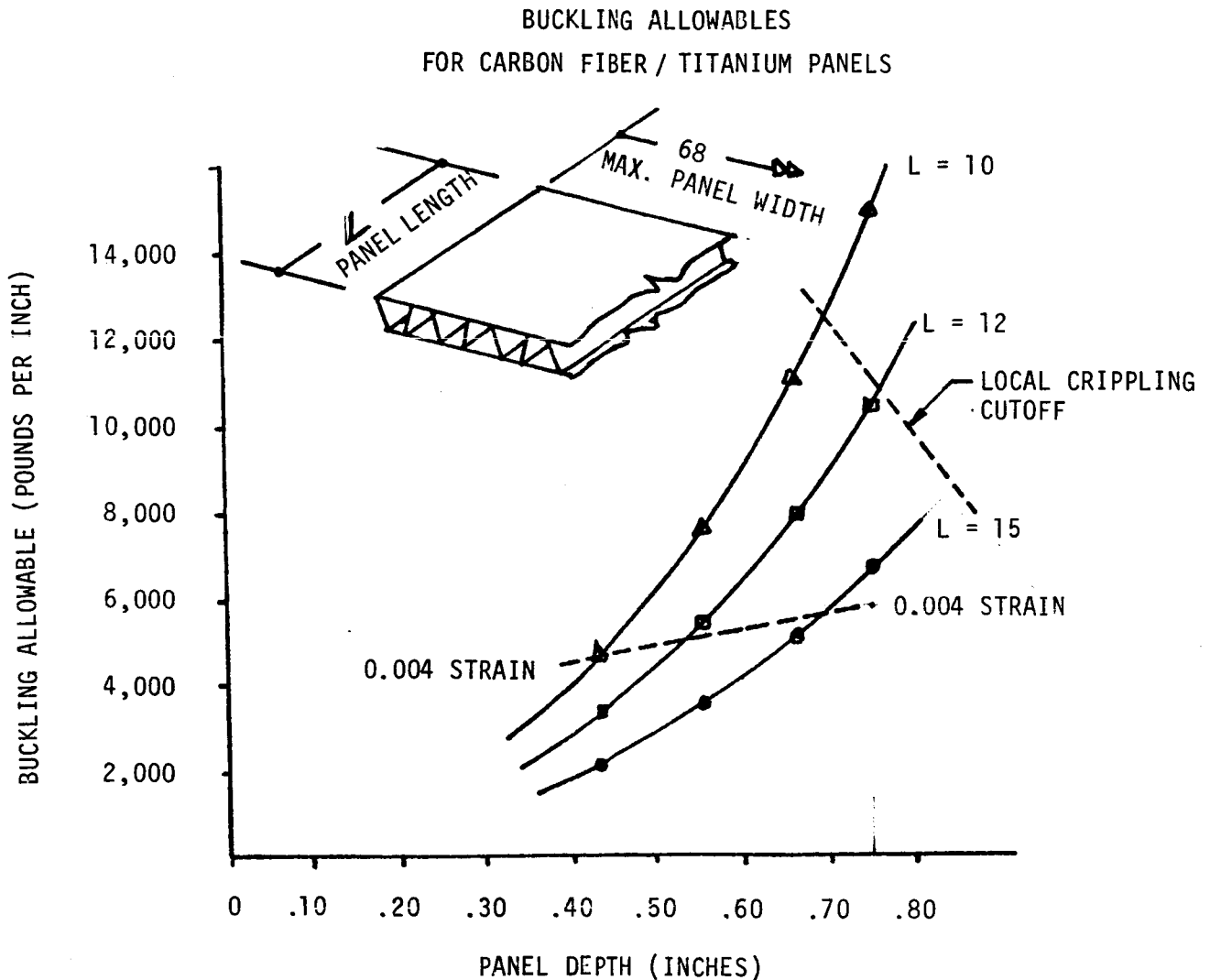


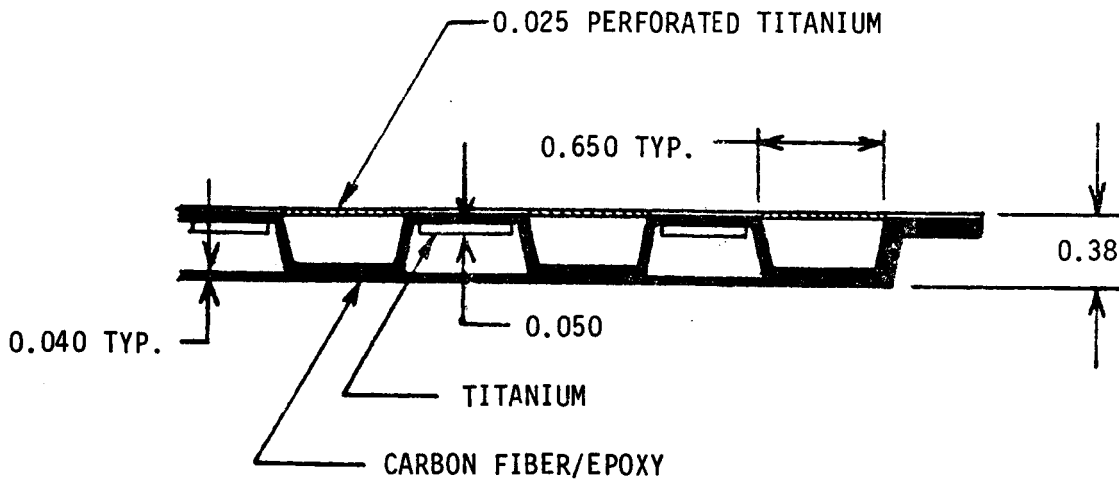
FIGURE 3.10

By extrapolation of Figure 3.10, it appeared that panels up to 0.9 inch deep, supported every 18-1/2 inches, could be used without having to increase the wall thickness to prevent local crippling. The use of existing tooling that gave a panel depth of 0.75 inch for most of the specimens fabricated was therefore realistic. A panel of this depth could carry about 6,000 pounds per inch at 0.004 strain with panel attachments at about 16 inch pitch. The panel depth was not too critical and could be changed if necessary during the detailed design of the panels and joints.

For laminar flow, the titanium surface must stay sufficient smooth throughout the LFC operating temperature range. Because the titanium, with a coefficient of thermal expansion of 4.85×10^{-6} in/in/°F, would be bonded at 250°F to a carbon fiber substructure having a much lower thermal expansion coefficient, the smoothness of the surface at the low cruise flight temperatures could be affected by differential contraction causing curvature of the bonded layers.

A thermal analysis was conducted which verified that the combination of titanium and carbon fiber when bonded at 250°F and cooled to 70°F would induce moments at the edges of the titanium which would cause a convex wave across the suction flute. This analysis was expanded to show that adding a local layer of titanium under the carbon fiber at each bonding land to produce thermally balanced titanium/carbon/titanium combination could eliminate the waves. Crippling and rain erosion test specimens were built with this thermal balancing strip added. The testing of these specimens is discussed in Section 3.4.1. An additional panel approximately 7 x 9 inches was made concurrently with the rain erosion and crippling specimens. A cross-section of this panel is shown in Figure 3.11. After fabrication, the panel exhibited overall bowing of approximately 0.010 inch across its width; e.g., normal to the direction of the flutes. Bowing in the direction of the flutes was negligible. The specimen also showed evidence of surface waves. To check waviness, the surface was measured at room temperature, at -65°F, and again at room temperature using a three footed dial indicator gage of the type commonly used for such measurements. See Figure 3.12.

The readings were taken at 33 locations as shown in Figure 3.13.



NOTE: DIMENSIONS ARE IN INCHES

FIGURE 3.11

THREE FOOTED DIAL INDICATOR GAGE

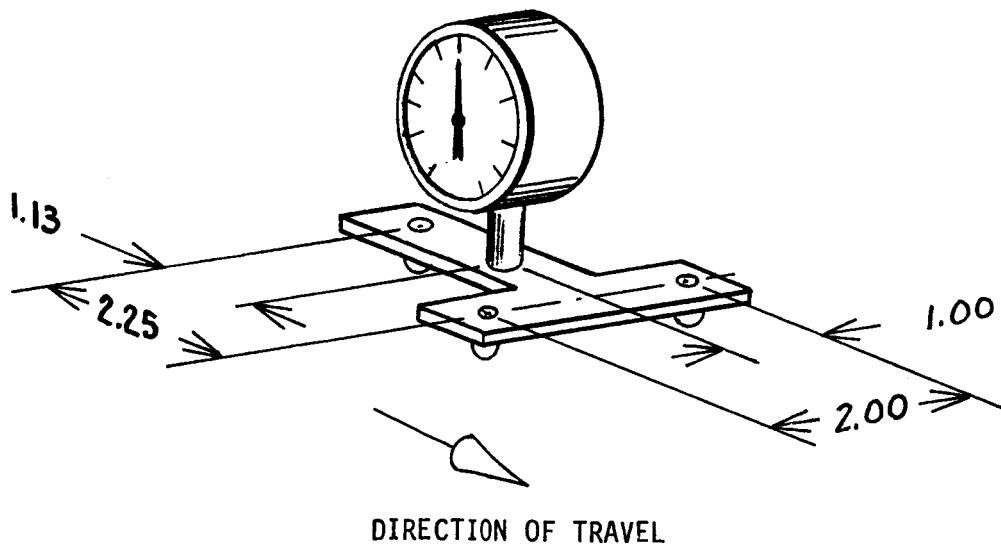


FIGURE 3.12

PANEL SURFACE
MEASUREMENT LOCATIONS

ORIGINAL PAGE IS
OF POOR QUALITY

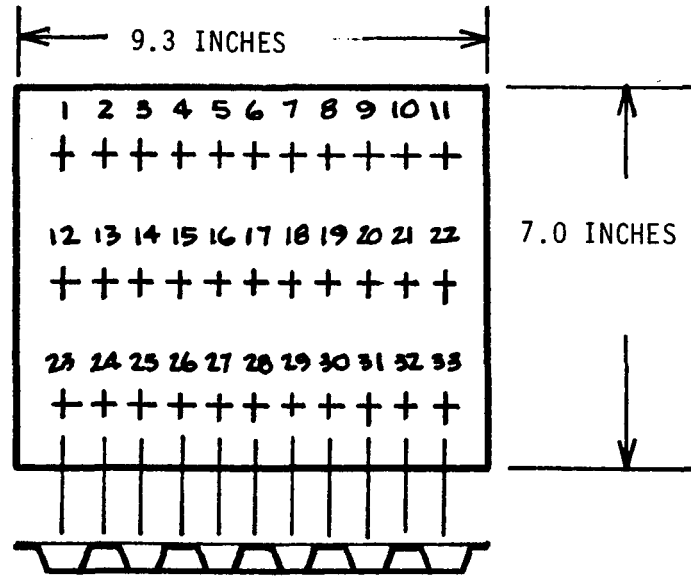


FIGURE 3.13

The readings are shown in graphic form in Figure 3.14 and in tabular form in Table 3.2. At room temperature the waves were unexpectedly concave between the bond lands with a depth of less than 0.001 inch. A graph of the allowable wave height for single or multiple waves of various lengths as specified by aerodynamics is shown in Figure 3.15. The panel is well within the 0.002 to 0.0032 inch allowable depth for wave lengths equal to the flute pitch. The large readings at 1, 10, 13, 21, 24, and 32 were believed to be due to curling of the unbalanced edges of the panel causing one of the feet of the dial indicator gage to rise as it neared the panel edge which gives the same reading as the probe dropping into a low spot. The readings at -65°F show that at low temperatures the waves became convex between the bond lands as originally expected. This suggests that the thermal balancing strips were inadequate and that the "bimetallic strip effect" was overcoming the initial reverse waviness condition. Bonding the titanium to the bowed substructure could introduce compressive loads in the titanium and each unsupported section of the titanium between bond lands would act like a column which had a slight initial eccentricity due to the residual panel curvature. Since no measurement was made of the bowing of the substructure prior to bonding on the titanium, no estimate of the preloads was possible.

ORIGINAL PANEL
OF POOR QUALITY

PANEL SURFACE MEASUREMENT VALUES

POINT NUMBERS PER FIGURE 3.13

PANEL DIMENSIONS & MATERIALS PER FIGURE 3.11

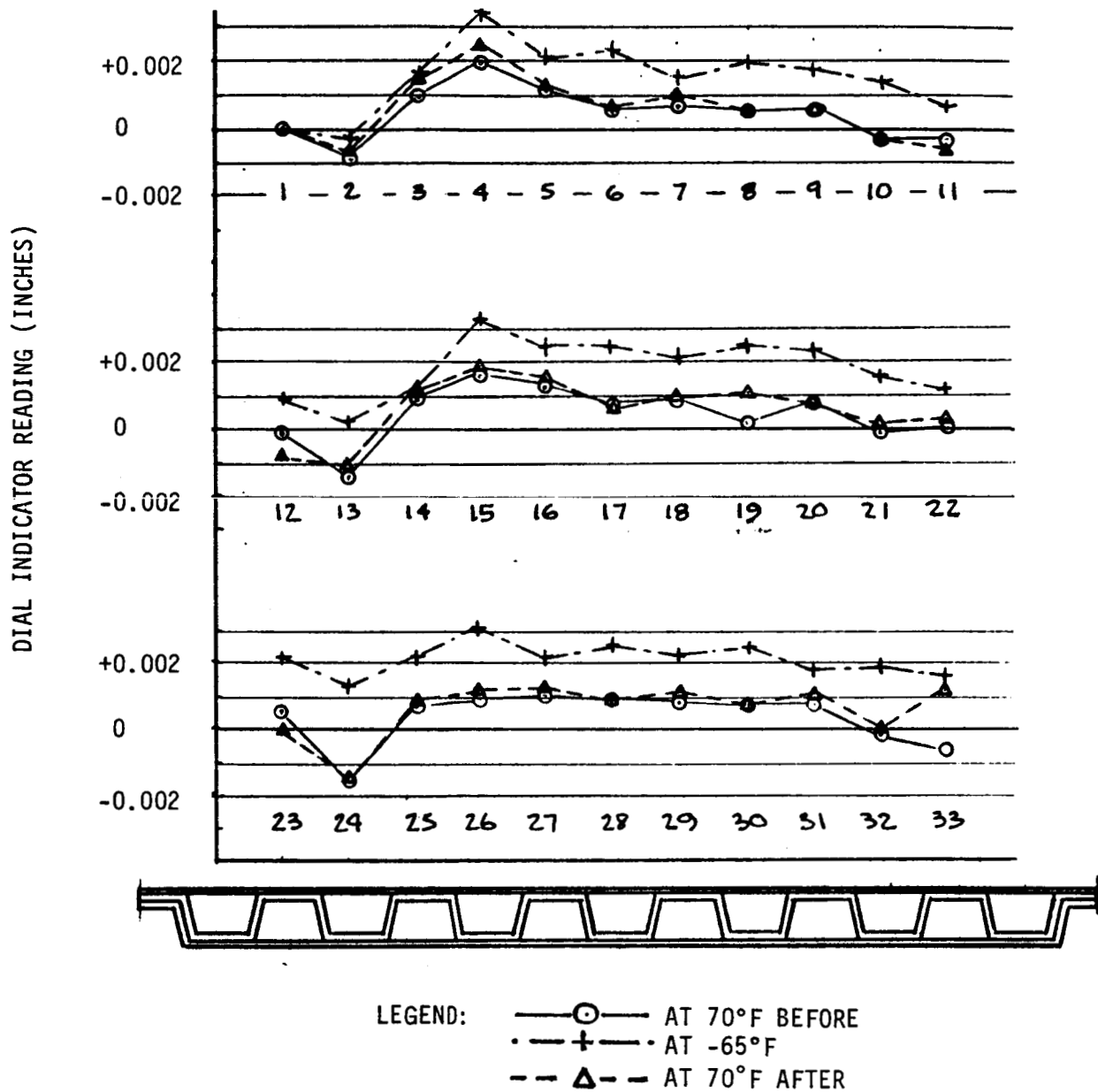


FIGURE 3.14

ORIGINAL PAGE IS
OF POOR QUALITY

DIAL INDICATOR
TABULATED PANEL SURFACE MEASUREMENT VALUES

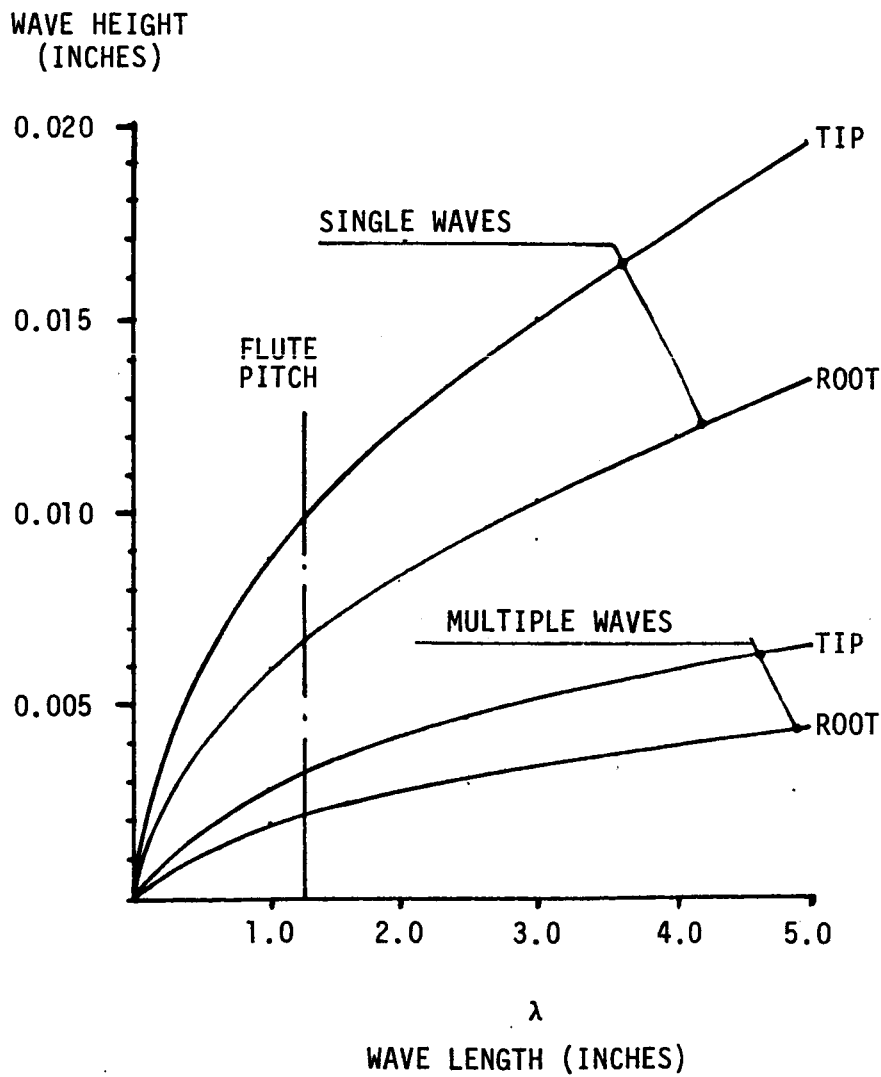
PANEL SURFACE MEASUREMENTS (INCHES)

	1	2	3	4	5	6	7	8	9	10	11
AT 70°F BEFORE -65°F SOAK	.0000	-.0009	.0010	.0020	.0012	.0007	.0007	.0006	.0007	-.0003	-.0003
AT -65°F	.0000	.0017	.0017	.0035	.0021	.0022	.0017	.0020	.0018	.0014	.0011
AT 70°F AFTER -65°F SOAK	.0000	-.0007	.0016	.0025	.0014	.0009	.0012	.0008	.0008	-.0003	-.0005
	12	13	14	15	16	17	18	19	20	21	22
AT 70°F BEFORE -65°F SOAK	-.0001	-.0013	.0010	.0017	.0014	.0009	.0009	.0001	.0010	-.0002	-.0001
AT -65°F	.0010	.0002	.0012	.0033	.0025	.0025	.0021	.0026	.0023	.0018	.0013
AT 70°F AFTER -65°F SOAK	-.0008	-.0010	.0013	.0019	.0015	.0008	.0011	.0012	.0009	.0003	.0004
	23	24	25	26	27	28	29	30	31	32	33
AT 70°F BEFORE -65°F SOAK	.0006	-.0016	.0007	.0008	.0009	.0008	.0008	.0007	.0006	-.0002	.0006
AT -65°F	.0022	.0013	.0022	.0030	.0021	.0025	.0022	.0024	.0018	.0020	.0018
AT 70°F AFTER -65°F SOAK	.0000	-.0017	.0010	.0011	.0012	.0009	.0011	.0008	.0011	.0000	.0012

TABLE 3.2

ORIGINAL PAGE IS
OF POOR QUALITY

LFC SURFACE WAVINESS TOLERANCE



$$h/\lambda = \left[\frac{59,000 \times \cos^2 \Lambda}{\lambda/c (R_c)^{1.5}} \right]^{0.5}$$

$$C_{TIP} = 7.04 \text{ FT}$$

$$C_{ROOT} = 30.83 \text{ FT}$$

$$R_c = 1.9 \times 10^6$$

$$(M = 0.8 @ 30,000 \text{ FT})$$

$$\Lambda = 30^\circ$$

FOR MULTIPLE WAVES

$$h_{MULT.} = \frac{h}{3} \text{ SINGLE}$$

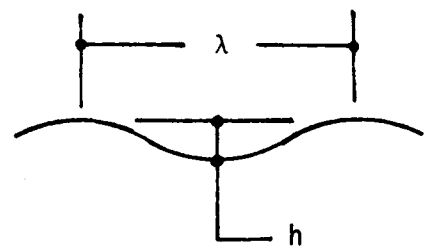


FIGURE 3.15

The panel depth study previously discussed indicated that deeper surface panels could be used without increasing wall thickness, so an additional four test panels were made to the deeper configuration shown in Figure 3.16. Titanium thermal balancing strips were used in only two of the panels.

The purpose of these panels was to answer the following questions:

1. Is the bowing on the substructure a general question associated with carbon fiber, corrugated panels?
2. Is the phenomenon of concave surface waves repeatable?
3. Are the surface waves caused by loads introduced into the titanium by bonding to the bowed substructure?
4. Do the titanium thermal balancing strips reduce the surface waviness?
5. Does increasing the depth of the panel affect the surface quality?

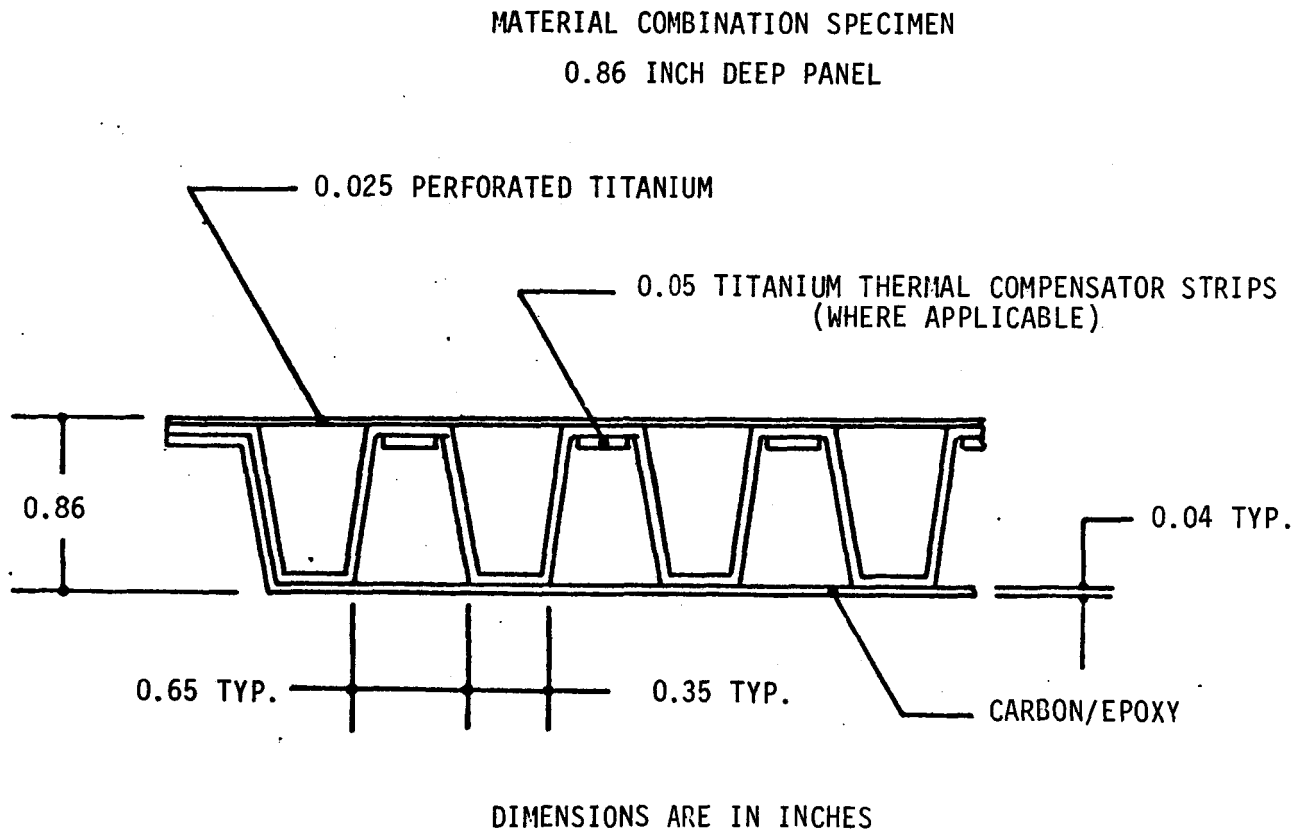


FIGURE 3.16

Before being bonded to the titanium surface, the substructures for these panels exhibited bowing similar to that observed on the previous shallower panel. These substructures were about 10 x 12 inches and the bow ranged from 0.10 to 0.12 inch over a 7 inch span measured across the flutes. Bowing along the flutes was negligible in all cases. After bonding to the titanium, the bowing was reduced to between 0.008 and 0.010 inch over the same 7 inch span. Figure 3.17 shows where the measurements were taken on the panels. Table 3.3 and Figures 3.18 and 3.19 show the surface waviness measurements for the panel with most waviness in each configuration, using both the three footed dial indicator and a Zeiss computer coordinated measuring machine which measures the absolute deviation of the surface from a plane established through three points.

An examination of Figures 3.18 and 3.19 shows that the titanium thermal compensation strips did reduce the waviness, but may have contributed to the additional bowing evident in these panels due to the increased overall unbalance of the materials. After bonding on the titanium, the remaining panel bow was less than 0.004 inch over a 7 inch span for panels without thermal balancing strips, and a maximum of 0.010 inch for panels with them. The waviness for both panel configurations is again less than the maximum allowed for multiple waves.

At that point, the following conclusions were made:

1. The bowing of the corrugated substructure was apparently inherent in the design.
2. The titanium thermal balancing strips reduced waviness but increased panel bowing.
3. The surface waviness was not affected by a change in panel depth.

Several theories on the cause of bowing of the panel substructure were advanced. These included unbalanced internal stresses due to the use of eight harness satin weave biwoven cloth (Narmco 5208/T300), resin imbalance due to the method of bagging and curing, and uneven cure rates due to uneven heating. Each theory was considered and a substructure was fabricated to prove or

PANEL DIMENSIONS AND MEASUREMENT LOCATIONS
FOR
PANEL SURFACE WAVINESS TEST
(0.86 INCH DEEP PANEL)

NOTE: DIMENSIONS ARE IN INCHES

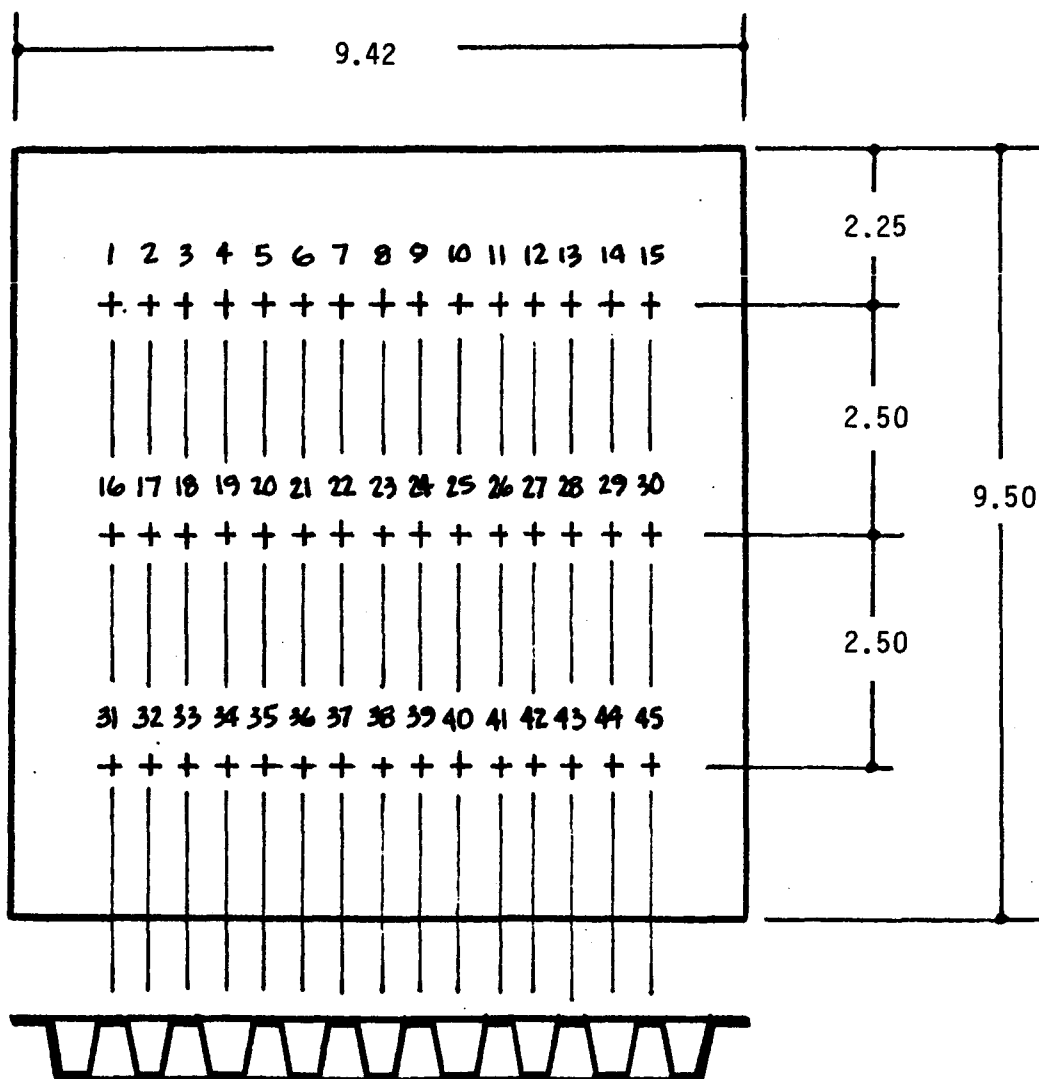


FIGURE 3.17

SURFACE DEFLECTION VALUES
MATERIAL COMBINATION SPECIMENS

With Thermal Balance

No Thermal Balance

POINT	DIAL INDICATOR	ZEISS	POINT	DIAL INDICATOR	ZEISS
1	+.0005	+.0053	1	* .000	+.0016
2	-.0004	+.0014	2	-.0004	* +.0000
3	* 0	* +.0000	3	-.0007	-.0004
4	+.0004	-.0017	4	-.0015	-.0019
5	+.0011	-.0018	5	-.0009	-.0020
6	+.0011	-.0030	6	-.0005	-.0020
7	+.0015	-.0030	7	-.0006	-.0021
8	+.0010	-.0037	8	-.0007	-.0024
9	+.0005	-.0037	9	-.0003	-.0020
10	+.0005	-.0037	10	-.0006	-.0021
11	+.0013	-.0023	11	-.0006	-.0013
12	+.0016	-.0016	12	-.0007	-.0012
13	+.0011	* -.0000	13	-.0005	* .0001
14	+.0007	+.0003	14	0	.0000
15	+.0022	+.0029	15	+.0008	+.0018
16	+.0020	+.0050	16	-.0001	+.0018
17	-.0005	+.0003	17	-.0003	+.0003
18	0	-.0010	18	-.0002	+.0002
19	+.0003	-.0028	19	-.0012	-.0016
20	+.0008	-.0035	20	-.0010	-.0018
21	+.0009	-.0047	21	-.0007	-.0022
22	+.0013	-.0049	22	-.0005	-.0022
23	+.0010	-.0056	23	-.0008	-.0027
24	+.0007	-.0058	24	-.0002	-.0021
25	+.0003	-.0060	25	-.0004	-.0022
26	+.0008	-.0051	26	-.0005	-.0015
27	+.0015	-.0046	27	-.0012	-.0016
28	+.0004	-.0031	28	-.0008	-.0007
29	+.0004	-.0031	29	0	+.0002
30	+.0006	-.0011	30	+.0010	+.0016
31	+.0009	+.0067	31	-.0001	+.0014
32	+.0018	+.0020	32	-.0004	* 0
33	-.0002	* +.0002	33	-.0002	0
34	+.0005	-.0024	34	-.0009	-.0016
35	+.0003	-.0035	35	-.0008	-.0021
36	+.0003	-.0050	36	-.0007	-.0025
37	+.0006	-.0049	37	-.0005	-.0025
38	+.0018	-.0057	38	-.0009	-.0029
39	+.0011	-.0066	39	-.0001	-.0023
40	+.0003	-.0072	40	0	-.0023
41	+.0008	-.0066	41	-.0004	-.0016
42	+.0013	-.0067	42	-.0014	-.0020
43	-.0012	-.0052	43	-.0010	-.0011
44	-.0001	-.0056	44	0	-.0001
45	+.0005	-.0034	45	+.0011	+.0013

* DEF. POINT OR PLANE INDICATED THUS

TABLE 3.3

PANEL SURFACE DEFLECTION VALUES OF
PANELS WITHOUT THERMAL COMPENSATION
(0.86 INCH DEEP PANELS)

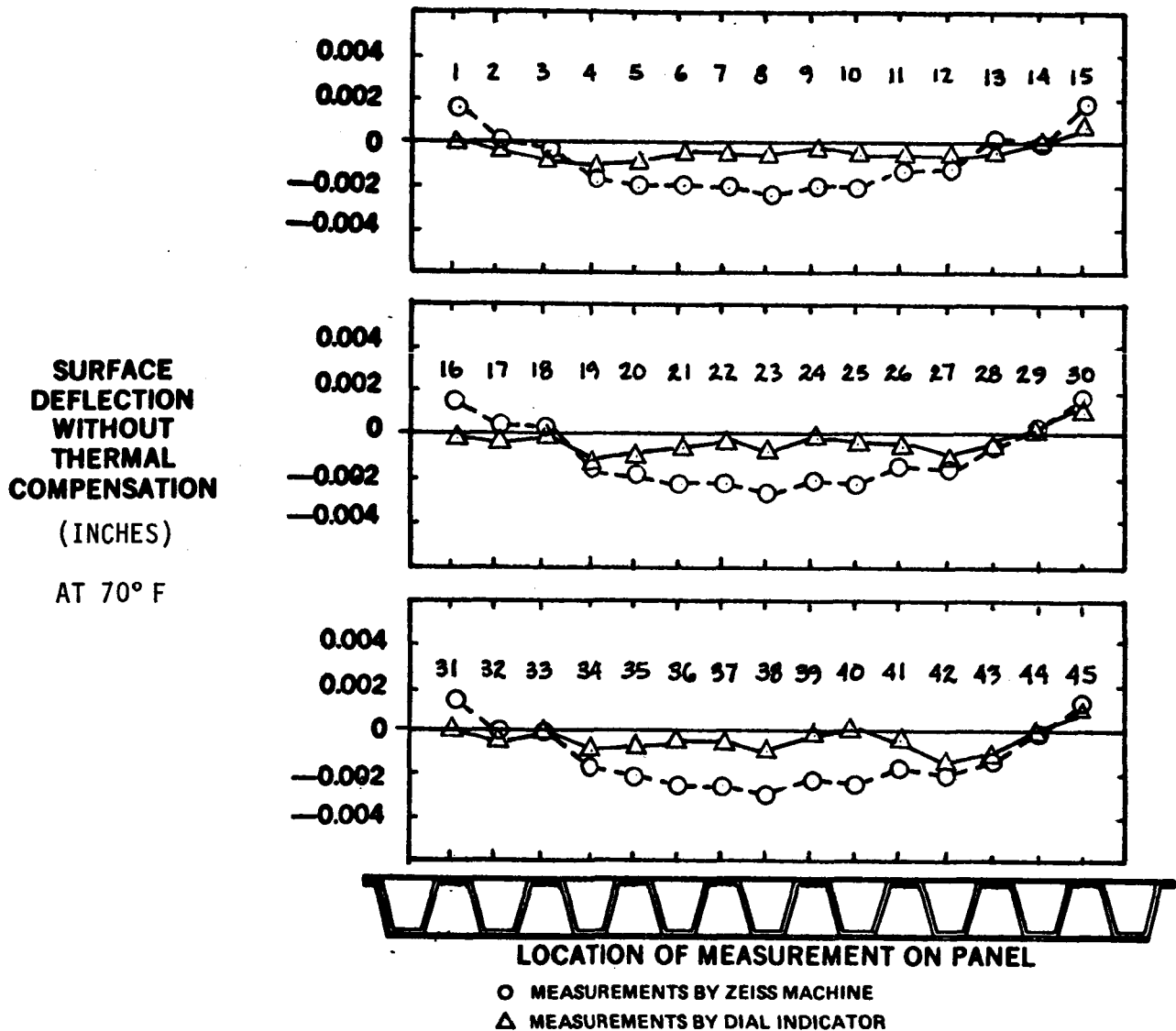


FIGURE 3.18

PANEL SURFACE DEFLECTION VALUES OF
PANELS WITH THERMAL COMPENSATION
(0.86 INCH DEEP PANELS)

ORIGINAL PAGE IS
OF POOR QUALITY

SURFACE
DEFLECTION
WITH
THERMAL
COMPENSATION
(INCHES)
AT 70°F

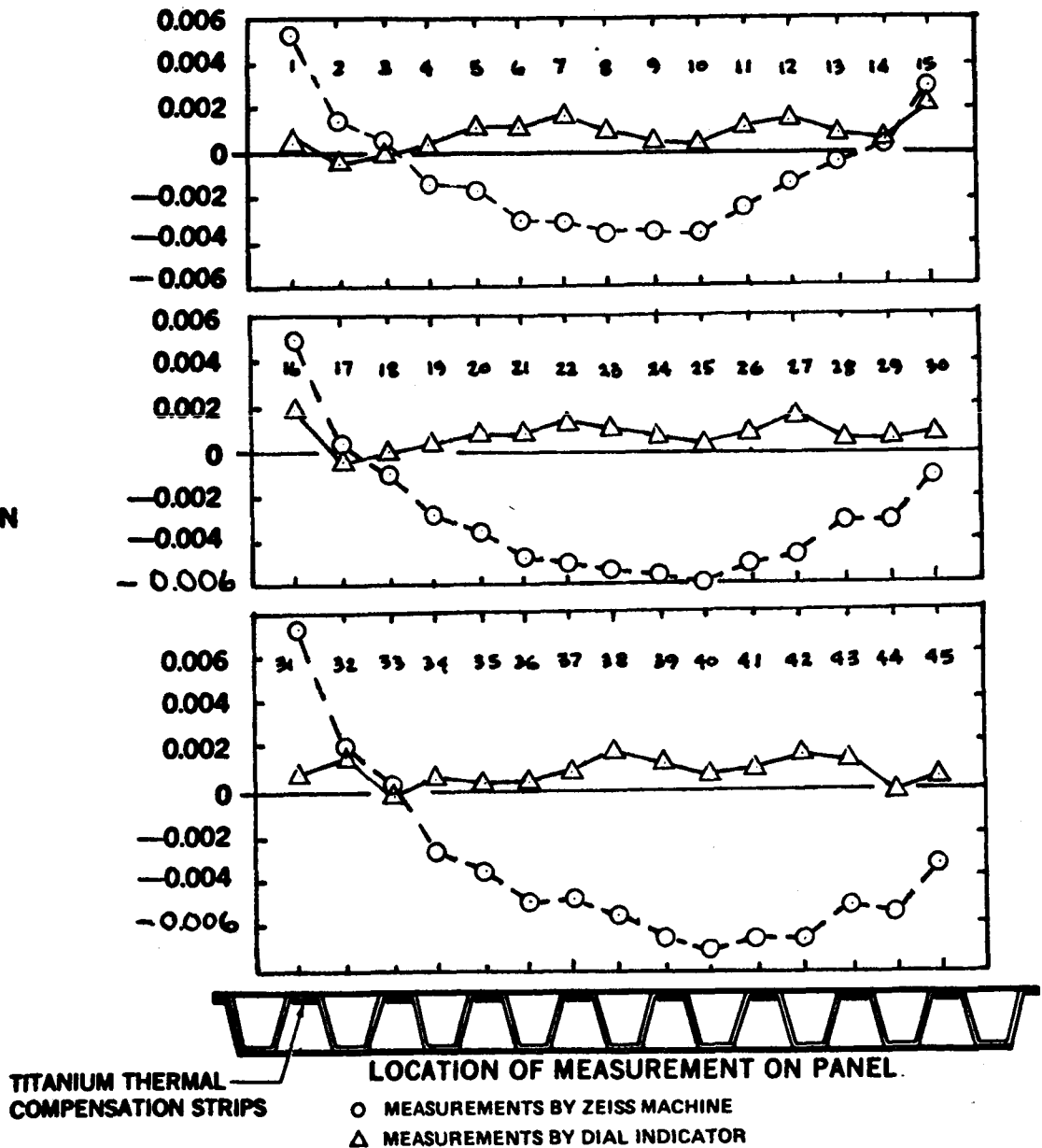


FIGURE 3.19

ORIGINAL FIGURE
OF POOR QUALITY

disprove it and about half a dozen specimens were made. All were bowed except one in which the corrugation and the carbon face sheet were layed up with a teflon separator sheet between them so they could not bond together. When this part was cured, it was discovered that the corrugation was approximately 0.25 inch narrower overall than the face sheet over a span of 9 inches across the corrugations. Obviously, if they had been cured as one unit the panel would have bowed as the corrugations tried to shrink against the resistance of the face sheet. It was then realized that the shrinkage was caused by the laminations in the corners of the corrugation being squeezed together as the part is cured, due to pressure against the mold as shown in Figure 3.20. As the outer fibers in the bend are squeezed to a smaller radius, their length is reduced, resulting in compressive stress. When removed from the mold, this compressive stress is relieved by closure of the corner angle. The effect of this occurring at all bends is an overall reduction in width. To avoid this occurrence, a corrugated substructure was fabricated in which each of the three plies was

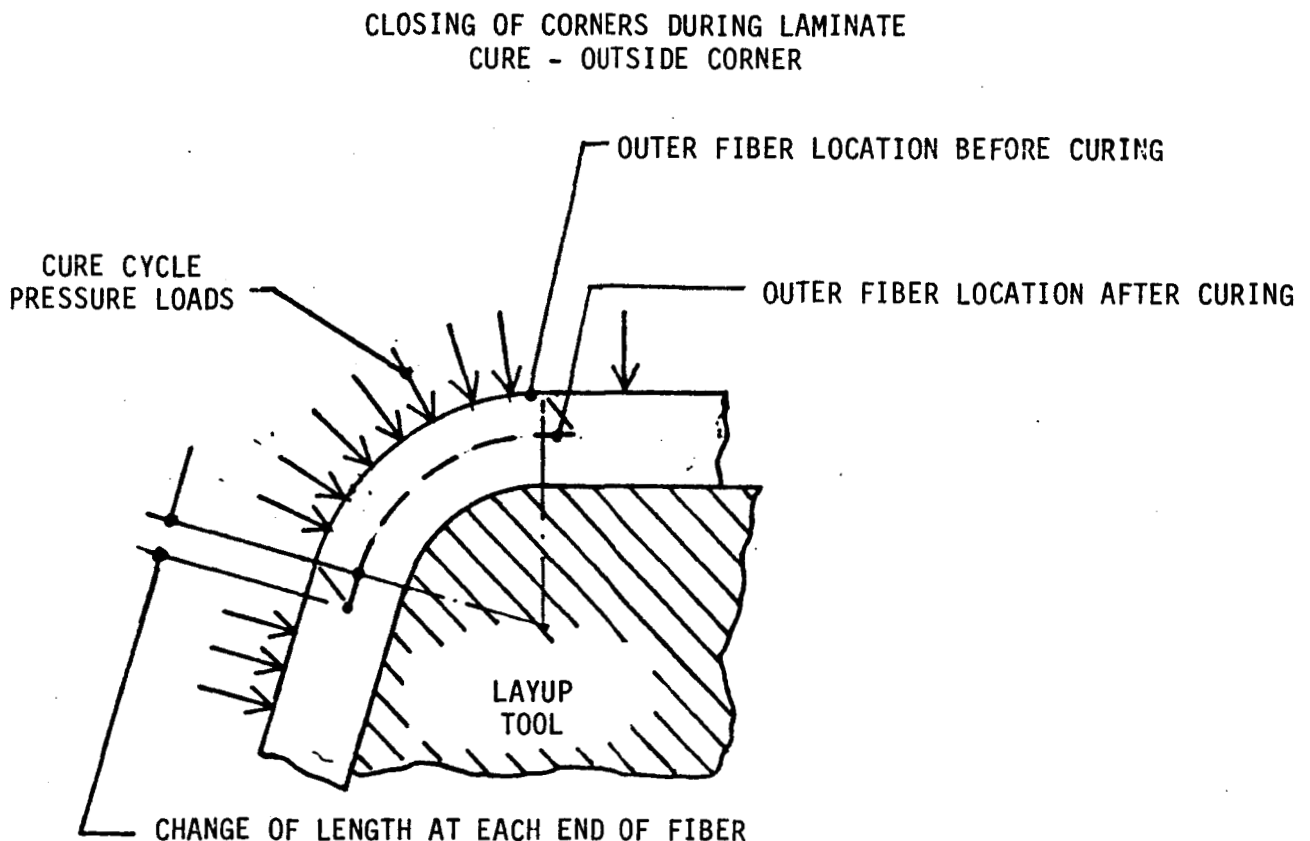


FIGURE 3.20

made in several pieces as shown in Figure 3.21. This was done to allow movement of the plies so that the buildup of internal loads would be eliminated. When cured, this panel was bowed about the same amount as previous ones, probably because relative movement could not occur due to friction forces between the layer under pressure. Alternatively, if the internal forces could not be eliminated, they would possibly be made to counteract each other by using closed loop corrugations as shown in Figure 3.22.

TYPICAL LAYUP WITH MULTI-PIECE PLIES IN THE CORRUGATION

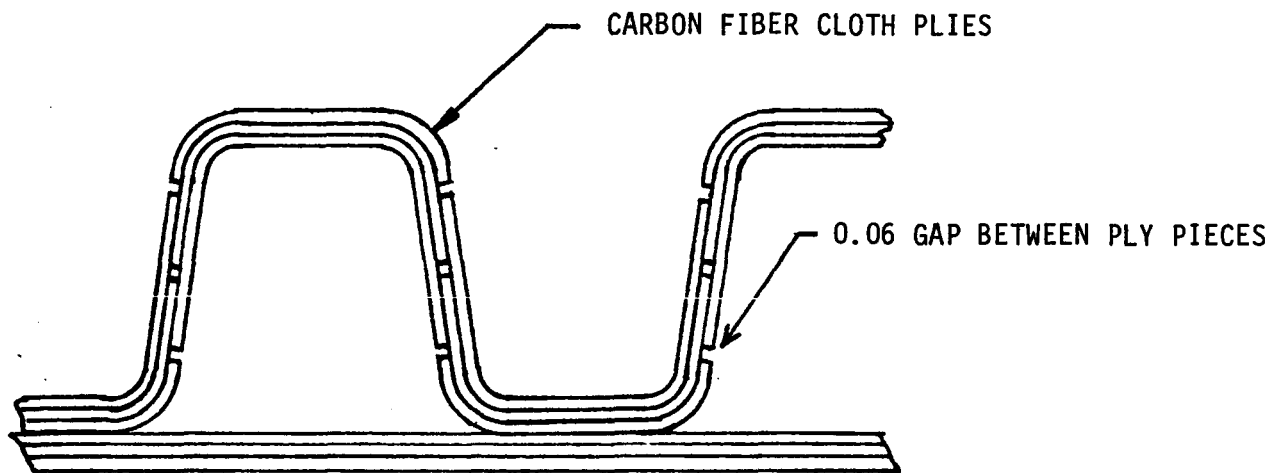


FIGURE 3.21

TYPICAL PANEL WITH INDIVIDUALLY WRAPPED CORRUGATIONS

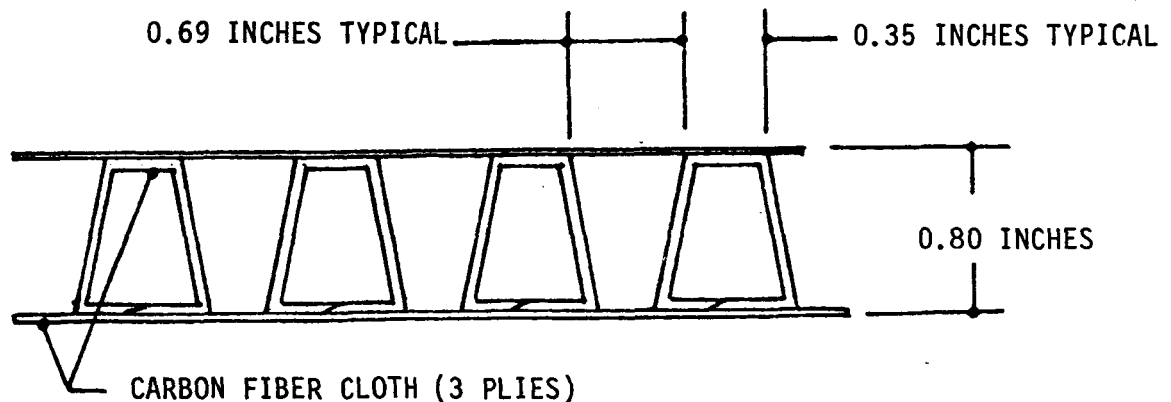


FIGURE 3.22

Four panels were made up using this individually wrapped corrugation concept. Fabrication of these panels was found to be very time consuming. Wrapping the stiff carbon fiber cloth around the tooling mandrel and keeping it in place was difficult and keeping the titanium thermal balancing strips in place was nearly impossible. It therefore was decided that the titanium strips would not be used with this panel configuration. The panels were measured for surface waviness at room temperature and the results for the two waviness panels are shown in Table 3.4 and Figures 3.23 and 3.24. The bowing which was characteristic of the previous panels was not evident, but the panels did have waviness at the flute pitch. These waves were 0.001 to 0.002 inch in depth, which is greater than the waves in panels with continuous corrugations, but is still within the allowable limits for multiple waves, as shown in Figure 3.15. The difficulty in getting a consistently tight wrap of cloth around the tooling mandrel may have contributed to the increased surface waviness. The problem of holding contour with panels having continuous corrugations and the difficulty encountered in fabricating the individually wrapped corrugations cast some doubt on the advisability of using carbon fiber for the panel substructure. Much less difficulty has been experienced previously using a fiberglass substructure, due mainly to its lower stiffness, but also influenced by its increased thermal expansion characteristics.

It was concluded that further experimental development should proceed using a fiberglass substructure with carbon fibers introduced only in sufficient quantity to balance thermal expansion. For production components, an all titanium panel should be investigated.

3.4 ENVIRONMENTAL EFFECTS ON THE PANEL STRUCTURE

Testing consisted primarily of material properties tests and environmental tests. The number of tests required was minimized by the use of Douglas qualified materials whenever possible. The tests included rain erosion, impact damage, and resistance of the materials involved to propylene glycol methyl ether, which was the preferred ice protection/contamination avoidance fluid. In addition, compression crippling tests and field fastener strength tests were done.

SURFACE DEFLECTION VALUES
MATERIAL COMBINATION SPECIMENS
INDIVIDUALLY WRAPPED CORRUGATIONS

PANEL ZCA10189-2

PANEL ZCA 10189-4

POINT	DIAL	ZEISS	POINT	DIAL	ZEISS
1	* 0	* .0001	1	* 0	* 0
2	.0013	-.0005	2	0	-.0011
3	.0015	+.0003	3	.0012	-.0026
4	.0010	-.0005	4	.0011	-.0010
5	.0012	+.0003	5	.0011	-.0009
6	.0023	.0002	6	.0017	-.0009
7	.0021	.0003	7	.0007	-.0013
8	.0014	-.0011	8	-.0005	-.0026
9	.0010	-.0006	9	.0002	-.0019
10	.0006	-.0012	10	.0002	-.0015
11	.0010	* 0	11	-.0002	* -.0001
12	-.0003	-.0010	12	-.0001	-.0006
13	.0015	-.0016	13	+.0005	-.0016
14	.0012	-.0010	14	+.0001	-.0010
15	.0004	-.0028	15	-.0002	-.0029
16	.0009	-.0015	16	+.0009	-.0018
17	.0030	-.0006	17	.0026	-.0013
18	.0022	-.0011	18	.0006	-.0025
19	.0005	-.0032	19	-.0013	-.0044
20	.0006	-.0021	20	.0002	-.0026
21	-.0005	-.0040	21	.0008	-.0026
22	.0007	-.0018	22	.0001	-.0012
23	.0006	* 0	23	-.0003	* 0
24	.0015	-.0011	24	.0002	-.0012
25	.0008	-.0009	25	+.0011	-.0004
26	-.0002	-.0025	26	+.0008	-.0015
27	.0014	-.0003	27	+.0008	-.0011
28	.0023	-.0009	28	.0013	-.0018
29	.0019	-.0006	29	.0007	-.0020
30	.0003	-.0023	30	-.0006	-.0032
31	.0008	-.0015	31	.0001	-.0024
32	.0010	-.0019	32	.0003	-.0022
33	.0008	-.0013	33	-.0002	-.0011

Reference point or plane (3 points) indicated thus *.

TABLE 3.4

ORIGINAL PAGE IS
OF POOR QUALITY

PANEL DIMENSIONS AND MEASUREMENT LOCATIONS FOR
INDIVIDUALLY WRAPPED CORRUGATIONS

NOTE: DIMENSIONS ARE IN INCHES

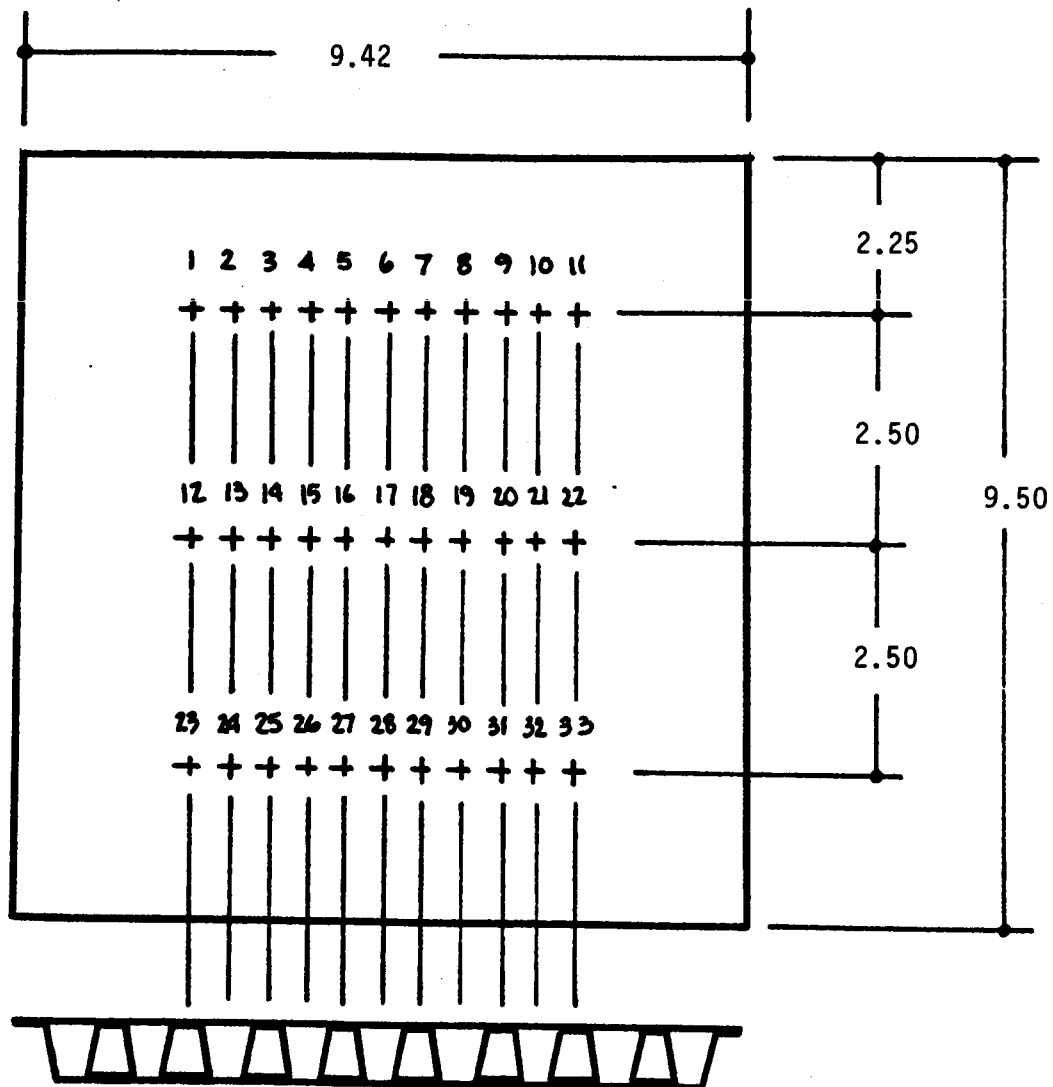
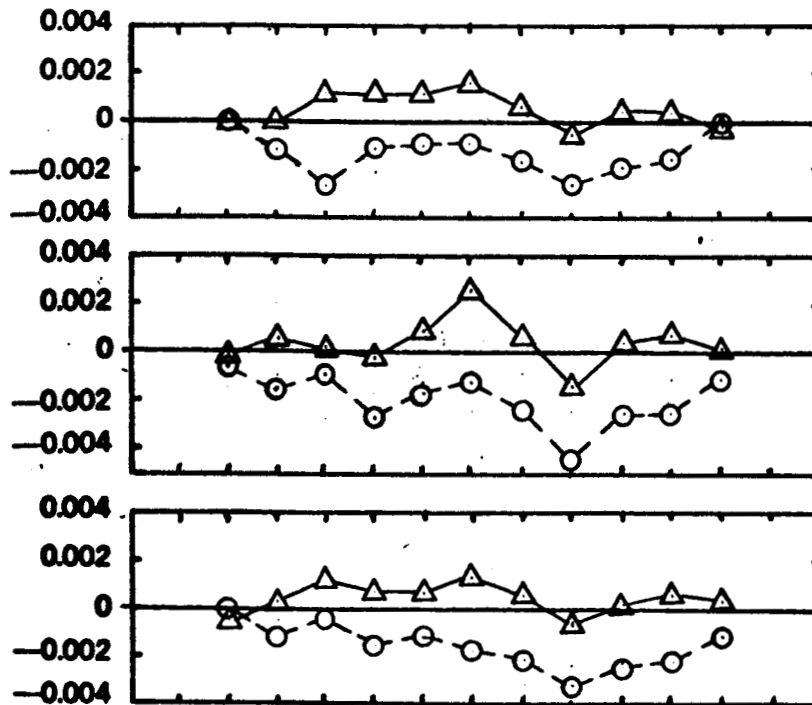


FIGURE 3.23

PANEL SURFACE DEFLECTION OF
INDIVIDUALLY WRAPPED CORRUGATIONS
(WITHOUT THERMAL COMPENSATION)

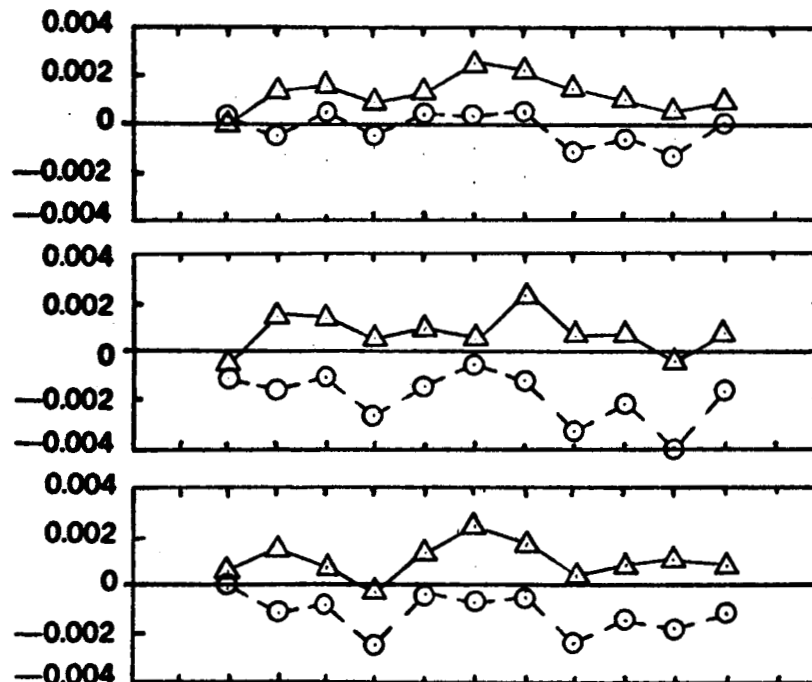
ORIGINAL PAGE IS
OF POOR QUALITY

SURFACE
DEFLECTION
WITHOUT
THERMAL
COMPENSATION
at 70°F
(inches)



PANEL ZCA 10189-4

SURFACE
DEFLECTION
WITHOUT
THERMAL
COMPENSATION
at 70°F
(inches)



PANEL ZCA 10189-2

LOCATION OF MEASUREMENT ON PANEL

- MEASUREMENTS BY ZEISS MACHINE
- △ MEASUREMENTS BY DIAL INDICATOR

FIGURE 3.24

3.4.1 Rain Erosion Tests

ORIGINAL PLATE OF
OF POOR QUALITY

There are no federal requirements governing rain damage to commercial aircraft. However, an estimate of conditions that might be encountered may be arrived at by studying a typical aircraft operating envelope, Figure 3.25, and possible environmental conditions.

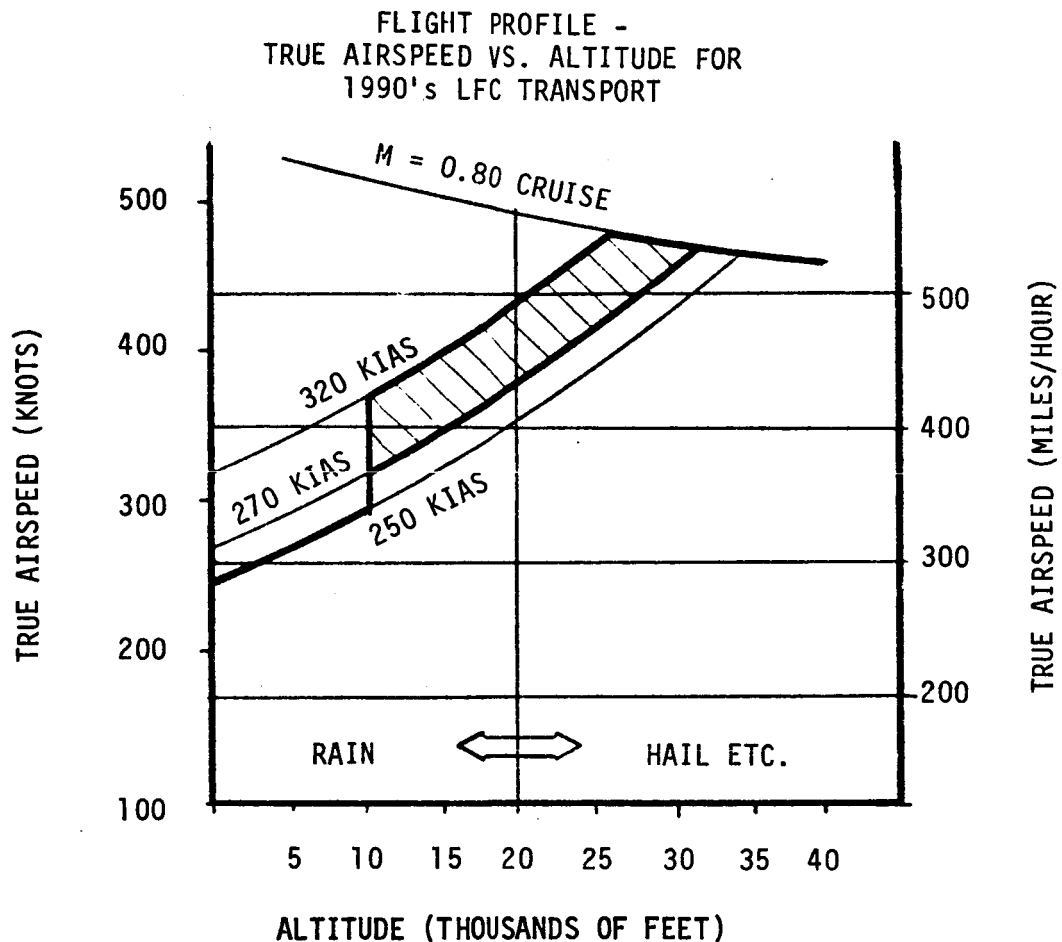


FIGURE 3.25

The figure shows a projected airspeed versus altitude plot for a 1990's LFC transport aircraft. Below 10,000 feet, air traffic regulations limit the aircraft speed to 250 knots indicated airspeed, which corresponds to a maximum of 280 knots or 340 miles per hour true airspeed at 10,000 feet. Above 10,000 feet, the climb speed would be between 270 and 320 knots indicated airspeed as shown. Given that the probability of encountering rain is reduced above

20,000 feet, and assuming a maximum climb speed of 320 knots indicated, the medium true airspeeds over which an encounter could occur is in the range of 370 to 425 knots or 430 to 495 miles per hour, depending on altitude. Flights at high speed through rain are normally avoided, however, one could reasonably expect the panels to be required to withstand rain impact at the low end of this speed range.

Eight specimens having the cross-section shown in Figure 3.26 were constructed and tested in the rotating arm rain erosion testing device at Wright Patterson Air Force Base. This test was conducted at the beginning of the WSSD program, thus the specimen reflects an earlier panel design. The test conditions and results of the test are shown in Table 3.4. Four of the specimens were subjected to a 1 inch per hour rainfall at 400 miles per hour for 100 minutes and showed no visible damage. The remaining four specimens were tested under the same conditions, but at 500 miles per hour and showed significant damage after 75 to 80 minutes. The damage included deformation of the titanium between the bond lands and separation of the titanium from the graphite substructure at the bondline. The time of onset of visible damage at this speed was not recorded. Under real conditions rain would impinge normal to the panel surface only at the very leading edge of the wing where the panel has additional resistance to deformation due to curvature. Speeds above 400 miles per hour may therefore be acceptable even under these extreme conditions, and certainly if the flute width is limited to 0.65 inch, a prolonged flight in heavy rain at a true airspeed of 400 miles per hour will not damage the LFC surface.

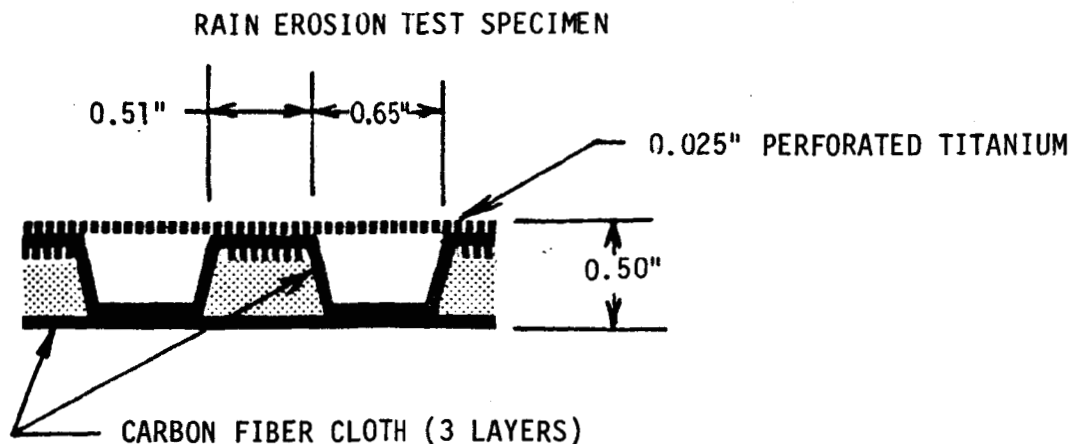


FIGURE 3.26

RAIN EROSION DATA					
400 and 500 mph 1 inch/hour simulated rainfall (1.8 mm drops)					
AFWAL Rig No.	Douglas No.	Material Description	Velocity (mph)	Time of Exposure (min)	Comments
12085	1	Perforated Ti Sheet/Bi woven Graphite	500	100.0	Center post delamination at 80.0 min, no erosion
12086	2	Perforated Ti Sheet/Bi woven Graphite	500	100.0	Outboard post delamination at 80.0 min, no erosion
12087	3	Perforated Ti Sheet/Bi woven Graphite	500	75.0	Inboard post delamination, no erosion
12088	4	Perforated Ti Sheet/Bi woven Graphite	500	75.0	Center and inboard post delamination, no erosion
12089	5	Perforated Ti Sheet/Bi woven Graphite	400	100.0	No visible damage
12090	6	Perforated Ti Sheet/Bi woven Graphite	400	100.0	No visible damage
12091	7	Perforated Ti Sheet/Bi woven Graphite	400	100.0	No visible damage
12092	8	Perforated Ti Sheet/Bi woven Graphite	400	100.0	No visible damage

TABLE 3.5

3.4.2 Impact Damage Test

An impact test specimen was fabricated having the cross-section shown in Figure 3.22. This specimen was subject to impacts of 5, 10, 15, 20, and 50 inch pounds on both the bonding land and the center of the suction flute using a Gardner impact testing machine. Figure 3.27 shows the results graphically and a picture of the tested panel is shown in Figure 3.28. At 20 inch pounds or less no internal damage was evident, but impacts of 50 inch pounds on the bondline caused significant delamination and splintering of the carbon fiber substructure. More testing in the 20 to 50 inch pound range would establish the level at which damage to the substructure begins to occur. Wind tunnel tests have shown that when dents of the size shown are filled and smoothed, the local lack of porosity does not affect laminar flow up to the maximum Reynolds number tested (9.5×10^6 or 1.36×10^6 per foot). Filler materials are available that will not crack or fall out when subjected to the range of temperatures encountered in normal aircraft use.

POROUS SURFACE PANEL BALL IMPACT TEST RESULTS

ORIGINAL PAGE IS
OF POOR QUALITY

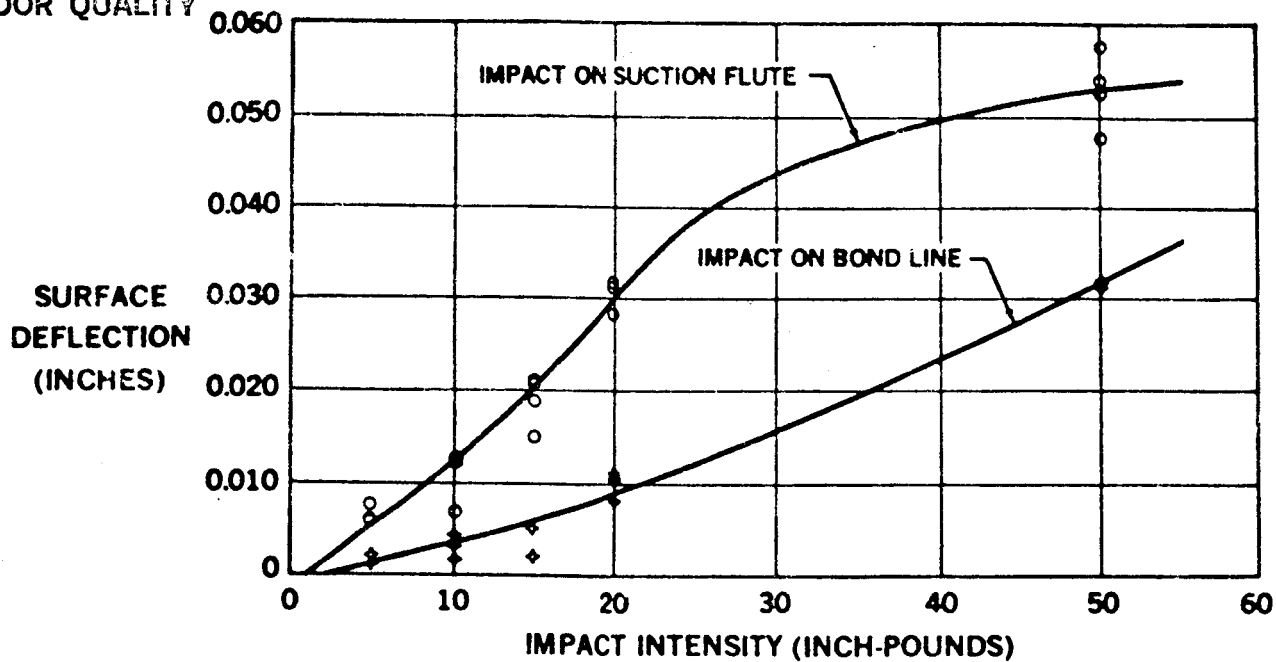
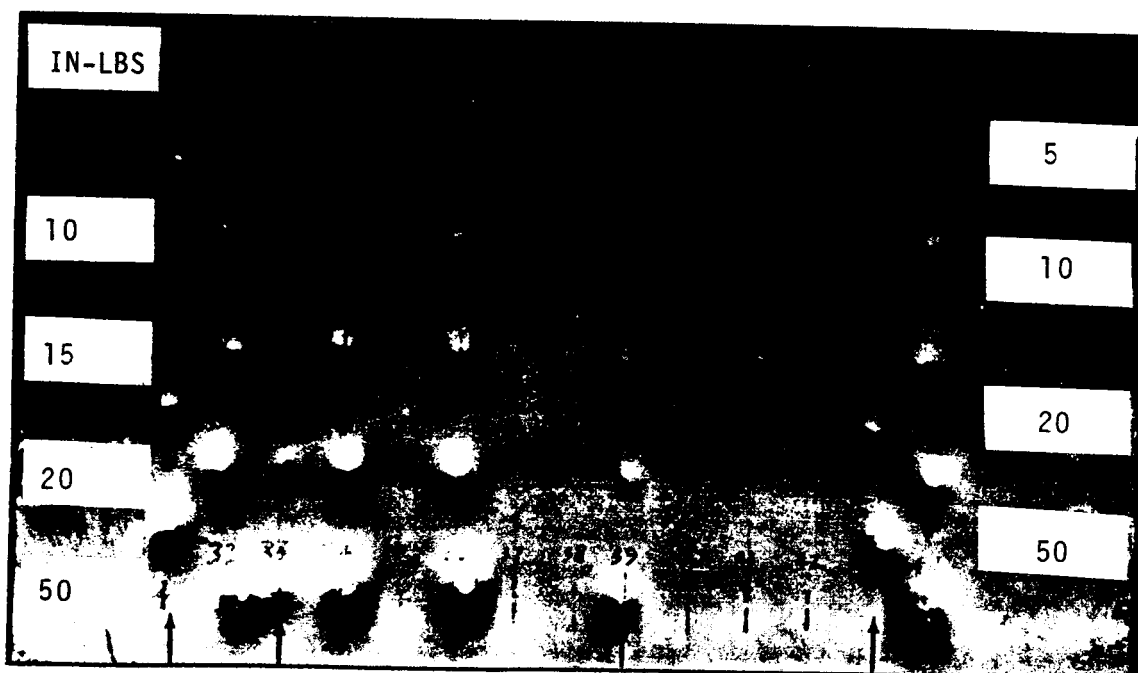


FIGURE 3.27



IMPACT TEST SPECIMEN
TAD ZCA10185 - DJ2191BG

FIGURE 3.28

3.4.3 Materials Compatibility Tests

The preferred freezing point depressant (FPD) liquid for ice protection and contamination avoidance (IP/CA) is propylene glycol methyl ether (PGME). See Section 5. Initial compatibility tests conducted for the Leading Edge Flight Test (LEFT) program indicated that PGME attacks both FM73, the adhesive currently being used on both the LEFT and WSSD programs, and the fiberglass laminate used on the LEFT article. When titanium to fiberglass bonded specimens were soaked in PGME for two and four weeks at 160°F, their strengths were reduced as shown below:

FM 73 ADHESIVE STRENGTH

Specimen Type	Percent of Original Strength Remaining	
	2 Week Soak @ 160°F	4 Week Soak @ 160°F
Lap Shear (FM73 Adhesive)	15	6
Peel (FM73 Adhesive)	58	-
Short Beam Shear (Fiberglass Laminate)	39	18

TABLE 3.6

These test conditions were considered to be unrepresentative and far too severe. As a result, a new test program was introduced to do the following:

1. Evaluate strength reductions of these materials with alternative IP/CA liquids under severe accelerated depreciation conditions.
2. Determine a more representative set of test conditions.
3. Evaluate the effects of PGME on other laminates.
4. Evaluate the effects of PGME on other adhesives.

3.4.3.1 Liquid Evaluation

Four liquids were originally considered for evaluation. They were: propylene glycol methyl ether (PGME), ethylene glycol methyl ether (EGME), diethylene glycol butyl ether (DiEGBE), and ethylene glycol (EG). A subsequent examination of the physical properties of DiEGBE and EG indicated that they were not suited to our use. Therefore, all but the early tests considered PGME and EGME only.

Lap shear tests were conducted to compare the residual strength of the FM73 adhesive after soaking the specimens in the various liquids. The results are shown below:

DOUBLE LAP SHEAR STRENGTH AFTER TWO WEEK EXPOSURE
(FM73 TO TITANIUM)

Liquid	Percent of Dry Strength Remaining		
	Soak @ 100°F*	Soak @ 130°F*	Soak @ 160°F*
PGME	100	57	15
EGME	---	86	--
DiEGBE	---	62	--
EG	---	85	--

* Preconditioning temperature, tests were conducted at room temperature.

TABLE 3.7

Although PGME is preferable for IP/CA conditions, the alternative liquids resulted in higher residual strength. EGME should therefore be for use as the FPD liquid considered if the residual strength under more realistic conditions becomes critical.

3.4.3.2 Determination of New Test Conditions

ORIGINAL PAGE 21
OF POOR QUALITY

Total immersion of the test specimens at 160°F for two or four weeks was an extremely severe test condition. If subsequent tests were to be conducted using more realistic conditions, they must account for the extent of exposure, liquid evaporation, the maximum temperature expected, and the number of wet/dry cycles expected under in-service conditions.

Tests were run to determine whether PGME would evaporate from a flute without the benefit of flowing air. The results are plotted below for a quantity of 10 grams of liquid in a container with 25 square centimeters of liquid exposed to air. The results indicated that the PGME would not evaporate fast enough from the flutes without some form of flute ventilation.

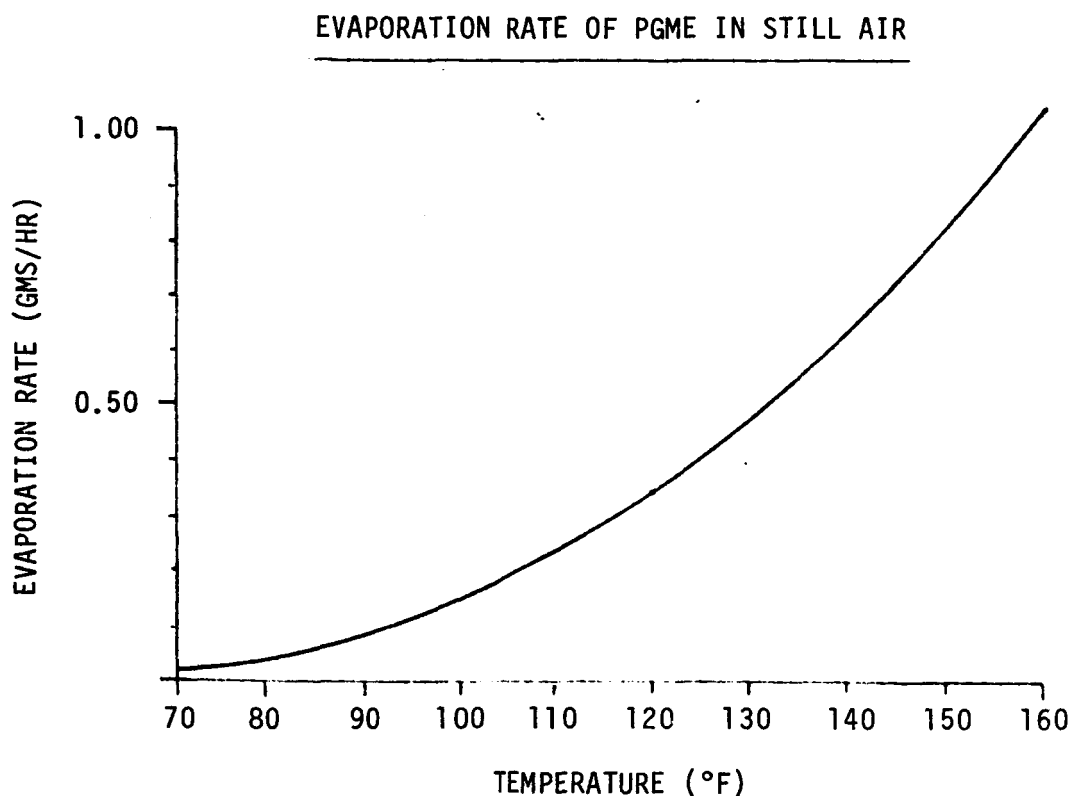


FIGURE 3.29

A small section representative of the LFC porous panels was given to NASA Dryden Flight Research Center to determine the maximum surface temperatures that might be encountered during a typical hot day. With the test panel directly exposed to solar radiation, maximum surface temperatures of 170°F and 180°F were recorded several times during the month of June.

For a typical LFC wing, such as shown in figure 3.8, if a small amount of FPO liquid remained in the flutes it would directly contact a bond line only in those flutes which are at the very leading edge. Since this area receives direct sunlight only in the morning or late afternoon, it was concluded that the combination of bondline soaking and extreme temperature such as 180°F would not occur and that 160°F would be realistic as a maximum temperature for preconditioning specimens.

Development of a soaking cycle that would be representative of an LFC aircraft in service was considered, but the large number of cycles would be impractical in terms of time and cost. The decision was made to use continuous immersion at temperature in lieu of wet/dry cycling for preconditioning the test specimens.

Based on the factors discussed above, subsequent test specimens were preconditioned as shown in Table 3.8 and tested at room temperature.

PRECONDITIONING OF TEST SPECIMENS

	No Soak	1 Week Soak	2 Week Soak
70°F	Control		
120°F - 140°F		Intermediate Time and Temperature	High Time - Intermediate Temperature
160°F		Intermediate Time - High Temperature	High Time and Temperature

TABLE 3.8

3.4.3.3 Laminate Evaluation

ORIGINAL PAGE IS
OF POOR QUALITY

Short beam shear tests were conducted on carbon fiber laminate specimens soaked in PGME and EGME for one and two weeks at temperatures from 70°F to 160°F as specified in Section 3.4.3.2. The failing shear stress was between 9,880 and 12,830 pounds per square inch (psi) throughout the full range of test liquids, soak times, and soak temperatures.

3.4.3.4 Adhesive Evaluation

Initially, aluminum to aluminum single lap shear tests were conducted using eight candidate adhesives, but correlation tests showed that the results obtained with aluminum were not indicative of the results that could be expected with titanium. Five of the adhesives were then selected for bonding

DOUBLE LAP SHEAR TESTS GRAPHITE-EPOXY IMMERSED IN GLYCOL

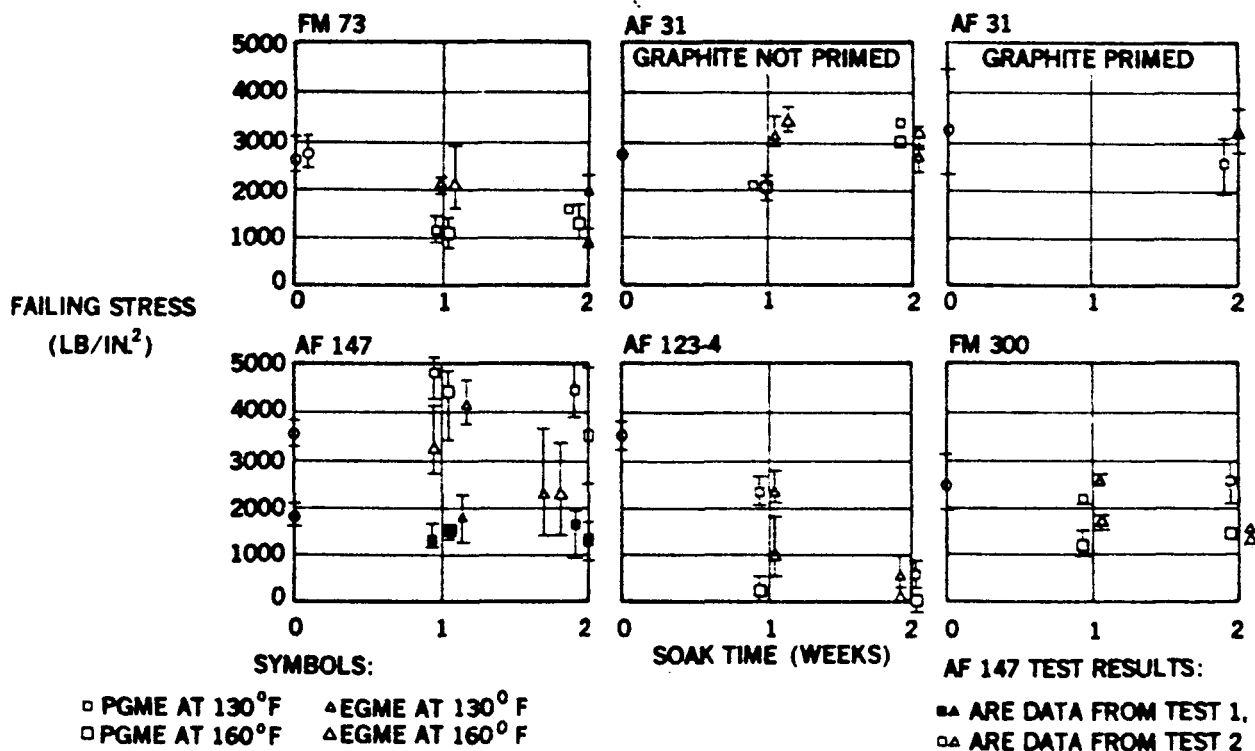


FIGURE 3.30

carbon fiber laminates to titanium to create double lap shear test specimens. The specimens were preconditioned by soaking in PGME or EGME using the time/temperature schedule shown in Table 3.8. The results of these tests are shown in Figure 3.30. An examination of these results and the tested specimens produced the following findings:

1. The epoxy based adhesives flowed out of the bond area leaving an adhesive depleted joint.
2. The phenolic based adhesive (AF31) stayed in the joint and maintained a strength of about 2000 psi. The strength could probably be raised to 3000 psi by post-curing.
3. The interlaminar strength of the carbon fiber laminate limited the shear strength of the specimens to about 3000 psi.
4. PGME and EGME had about the same effect on the adhesives.

As a result of these tests, AF31 was selected as the adhesive for the WSSD program with PGME as the prime IP/CA liquid.

3.5 CONCLUSIONS AND RECOMMENDATIONS - STRUCTURAL DESIGN

The WSSD program generated valuable information which will be useful in future LFC development programs.

Differing coefficients of thermal expansion between the titanium surface material and the substructure material affected the surface smoothness of the panels; however, acceptable surface smoothness was obtained using carbon fiber material for the substructure. Acceptable smoothness was achieved with either continuous corrugations or individual corrugations in the substructure; however, continuous corrugations generated internal stresses which caused problems in maintaining the overall contour. Theoretically, the surface could be made smoother if some form of thermal compensation were employed, but the use of titanium strips was difficult and increased the deviation from the panel contour also. The possibility of using a combination of glass and carbon fibers to achieve a coefficient of expansion equal to that of titanium should be investigated.

If 0.025 inch thick titanium is used as the surface material, acceptable damage resistance can be achieved by limiting the flute spacing to 1 inch on center. Additional development to increase impact resistance and testing in the 20 to 50 foot-pound range is recommended.

Epoxy based adhesives are unsuitable for this application due to their high flow characteristics and incompatibility with the glycol based liquids being used. Of the adhesives tested, the phenolic adhesive AF31 was best suited to our needs. This area of inquiry should be kept open to take advantage of new materials as they are introduced.

For LFC experimental testing, it is recommended that fiberglass with sufficient carbon material to avoid differential thermal expansion effects should be given prime consideration for the fluted sub-surface structures.

For a production aircraft, all titanium panels fabricated by superplastic forming and diffusion bonding techniques should be considered. While this requires expensive tooling it would avoid costly labor sensitive layup of laminated substructures. Before the necessary trade studies can be made in this area, techniques must be developed for analyzing the strength of corrugated panels made with orthotropic materials and/or mixes of materials. It is desirable that these methods and those used for analyzing metallic corrugated structures be automated because of the rather tedious mathematics involved.

A major design effort should be directed toward developing panel joints which can carry the requisite loads while maintaining the necessary joint smoothness. The panel and joint designs must consider interchangeability requirements.

4. SUCTION/CLEARING SYSTEM

4.1 INTRODUCTION

The suction/clearing system were examined to ensure that the LFC panel development work was practical from this aspect. The fundamental purpose of the suction/clearing system is to achieve and maintain laminar flow over the wing surface. Negative pressure or suction is applied to the boundary layer through perforations in the titanium wing skin. To ensure success of laminarization with suction, the skin must be kept clean so that no contaminants can act as roughness to trip the boundary layer. The porous surface must also be free of any obstructions that would reduce the effective open area and alter the suction flow characteristics. To keep the skin clean and protected from ice, a liquid film system is used. After the liquid has been applied, the surface must be cleared before suction is applied.

The clearing function of the system provides a positive differential pressure across the skin to remove any liquid trapped in the holes. This pressure is applied from takeoff up to the initial cruising altitude.

One objective in the design of the suction/clearing system was to integrate the components into the structure of the wing as much as possible. Previous studies indicated that incorporating as much ducting as possible into the structure resulted in a simple, efficient, reliable system with few moving parts. This type of system would also minimize the weight penalty. To this end, the suction and clearing functions of the system have as many common system components as possible

4.2 GENERAL DESIGN CRITERIA

General design criteria to be met in designing the suction/clearing system were as follows:

- a. Low Resistance: The energy required to provide suction or clearing pressure is a direct function of system resistance. Designing the system to have low pressure drop reduces the size of the suction and clearing pressure source.

- b. Maximum Duct Velocity of $M = 0.2$ for Suction, $M = 0.8$ for Clearing: Excessive internal duct noise could cause transition of the boundary layer. To minimize noise and to reduce pressure losses in the ducts, a maximum internal air velocity of $M = 0.2$ was established for suction. During clearing operations, Mach number was limited to 0.8 to avoid compressibility effects and choking.
- c. Aircraft Baseline Condition of $M = 0.8$ Cruise at 35,000 feet: The baseline condition is representative of a typical cruise condition for scheduled commercial flights including future laminar flow control (LFC) aircraft.
- d. One psi Differential Clearing Pressure: The basic ice protection contamination avoidance fluid is propylene glycol methyl ether (PGME). Environmental tests with PGME showed that a differential pressure across the porous surface of 1 psi is sufficient to clear the holes of any residual PGME (Reference 1).

4.3 FLOW REQUIREMENTS

4.3.1 Suction Requirements

The suction levels required to achieve laminar flow over the wing were established by aerodynamic analysis (see Appendix I). The amount of suction required varies with chordwise location (Figure 3.7). Suction flow is expressed as suction velocity, $V_w = C_q V_\infty$. Close to the leading edge a mean suction velocity of 0.47 ft/sec is required to overcome cross flow instabilities associated with steep pressure gradients and wing sweep.

The required suction velocity drops to 0.10 ft/sec over the wing box region where Tollmien-Schlichting instabilities dominate. In the trailing edge region, the required suction level increases substantially (to 0.70 ft/sec) due to crossflow conditions with a severe adverse pressure gradient.

4.3.2 Clearing Requirements

The clearing system must provide sufficient positive pressure at the underside of the porous surface to prevent inflow of liquids. The system must also be able to clear any residual liquid from the holes after a fluid has been applied. The porous skin may be subject to fluid application during operation of the contamination avoidance/ice protection system, during rain, and in icing encounters. In each instance, the clearing system first functions to prevent the inflow of liquid, and then, when the encounter is over, to clear the fluid from the holes by supplying sufficient pressure to overcome surface tension and viscosity. A clean, clear surface is a prerequisite to successful LFC.

Based on studies using PGME as the contamination avoidance/ice protection system liquid, a differential pressure of 1.0 psi is sufficient to clear the porous surface. This pressure is more than adequate when the liquid is water. For surface protection, contamination avoidance/ice protection liquid will be applied from takeoff to 5,000 feet. A positive clearing pressure will be used from takeoff and will be continued up to the initial cruising altitude. Up to 5,000 feet, this positive clearing pressure will minimize the system ingestion of the contamination avoidance/ice protection system liquid, and above 5,000 feet to cruise altitude, it will clear any liquid from the surface.

4.4 CONCEPTS

4.4.1 Suction System Concepts

During suction, air is drawn from the boundary layer, through porous surface, and into flutes in the substructure. From there it is routed through collection channels into ducts and back to the compressor (Figure 4.1).

The wing upper surface was divided into 17 suction panels (Figure 4.2) as determined by structural and manufacturing concerns. The airflow from each panel was calculated and used to size the ducting for the suction and clearing system.

The suction system design concept was to integrate collector ducts into the structure as efficiently as possible. Both chordwise and spanwise collection systems were investigated. In both cases, air from the collector ducts was metered through manifolds into the suction pump. The pump is located at the aerodynamic break on the wing and the suction air is exhausted from the pump at freestream pressure and velocity.

SUCTION SYSTEM MANIFOLDING

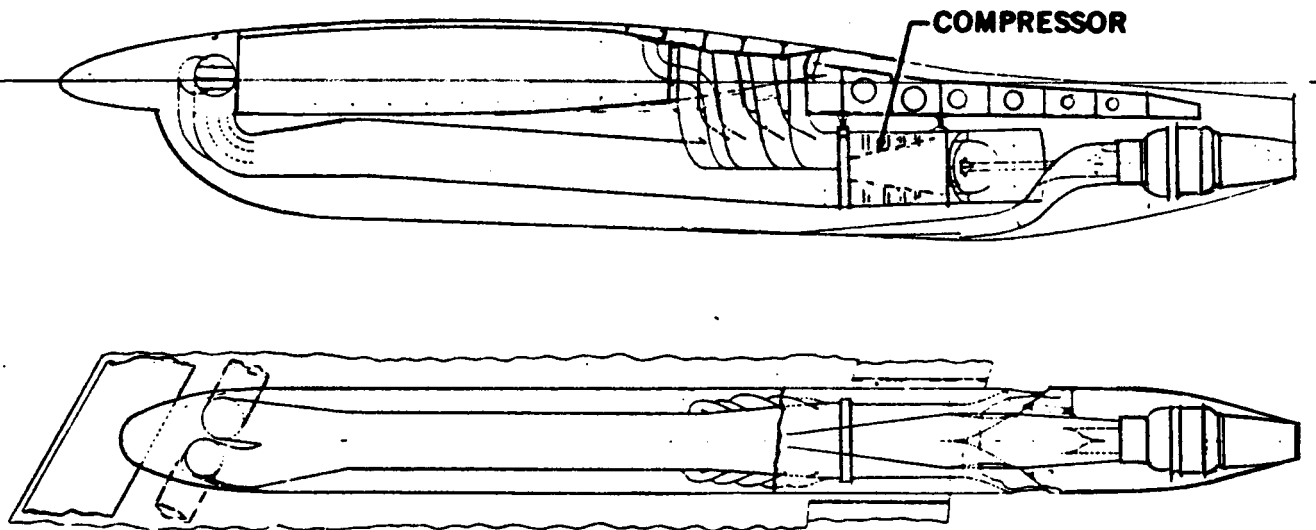


FIGURE 4.1

WING SURFACE PANELS

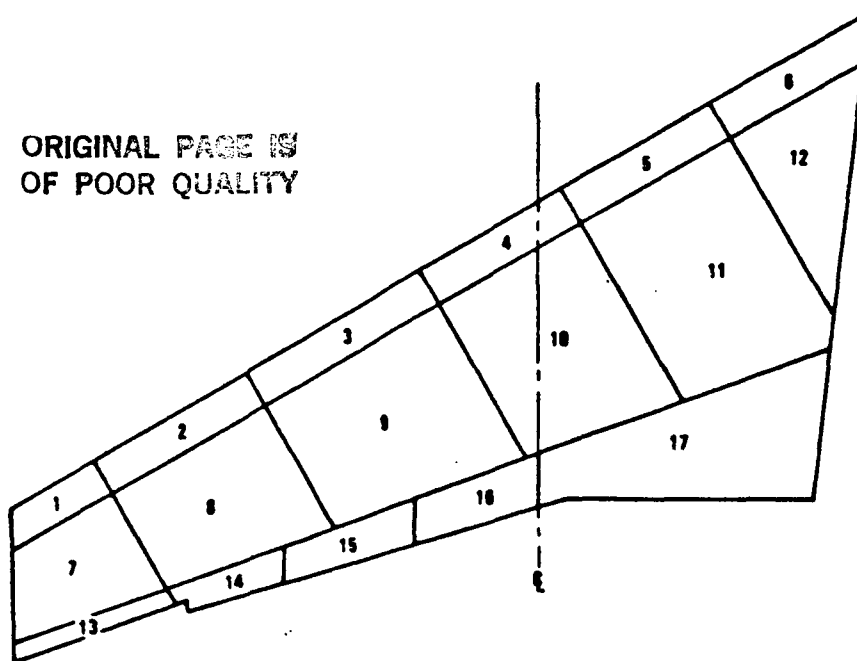


FIGURE 4.2

4.4.2 Clearing System Concept

Although the suction system definition was completed, the clearing system pressure source was not fully defined. Several concepts, such as wing tip or wing root airscoops were considered as possible sources.

4.4.3 Configuration Studies

Two subsurface suction/clearing system configurations were studied. The first was a spanwise air collection system which was developed as the baseline system under Contract NAS-14632 for a 300 passenger transport aircraft with 5,000 mile range. The second system was an equivalent chordwise collection system which is actually a hybrid system using spanwise collection in the leading and trailing edges and chordwise collection over the wing box area. Both these systems were analyzed to see which was the most efficient in terms of airflow, duct design, and adaptability to the clearing function.

The concept of a chordwise air collection system was investigated because of potential structural advantages and improved air collection efficiency.

With the spanwise system, air was routed to and from the surface panels by spanwise channels located beneath the panels (Figure 4.3). The air from these channels was routed to a dry bay located at the mid point of the wing semi-span where it was manifolded into the suction pump (Figure 4.4). In the wing box region, the collection channels were formed by the external stiffeners of the main wing box structure. These channels ran the length of the wing. Because of the length of the channels (54 feet), the large surface area, and pressure gradients, it was necessary to use control valves to meet both suction and clearing requirements. An analysis of the air distribution system (Section 4.5) led to an estimate that 1056 control valves would be required for each airplane. This large number of control valves increased the weight and complexity of the spanwise collection system and decreased its efficiency due to energy loss from excessive pressure drop. Deeper channels were required to accommodate the control valves and to limit the internal velocity to $M = 0.2$. The increased channel depth reduced the effective wing structural depth and the space available for fuel.

WING ARRANGEMENT FOR SPANWISE COLLECTION OF SUCTION AIRFLOW

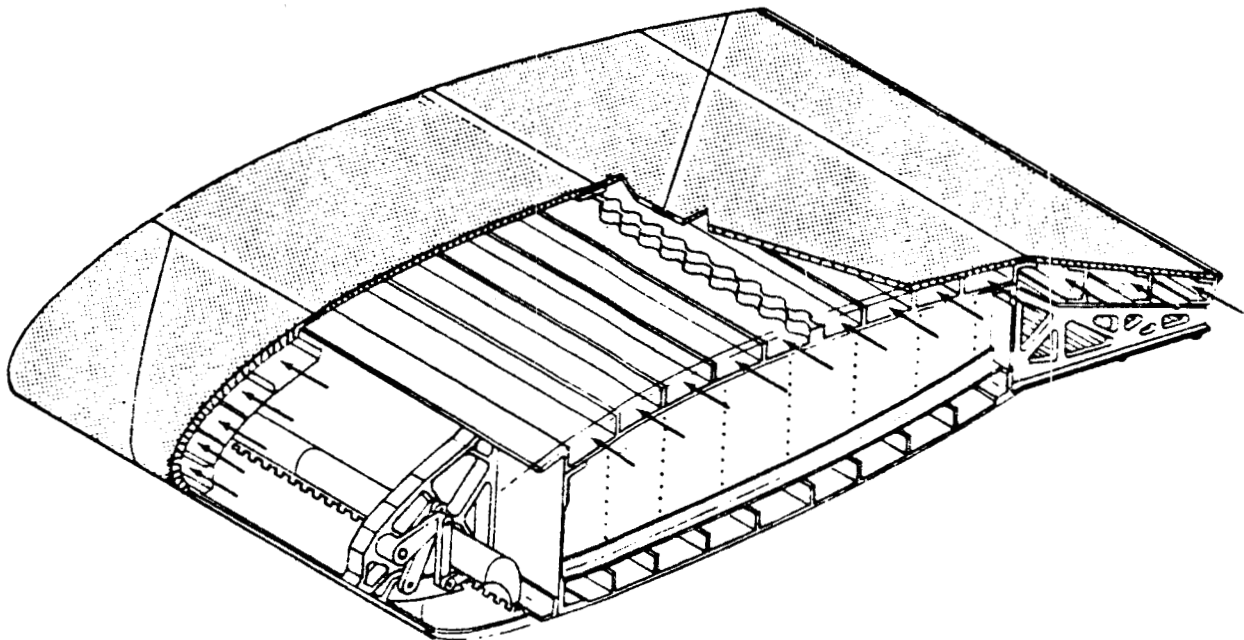


FIGURE 4.3

SPANWISE AIR-COLLECTION SYSTEM

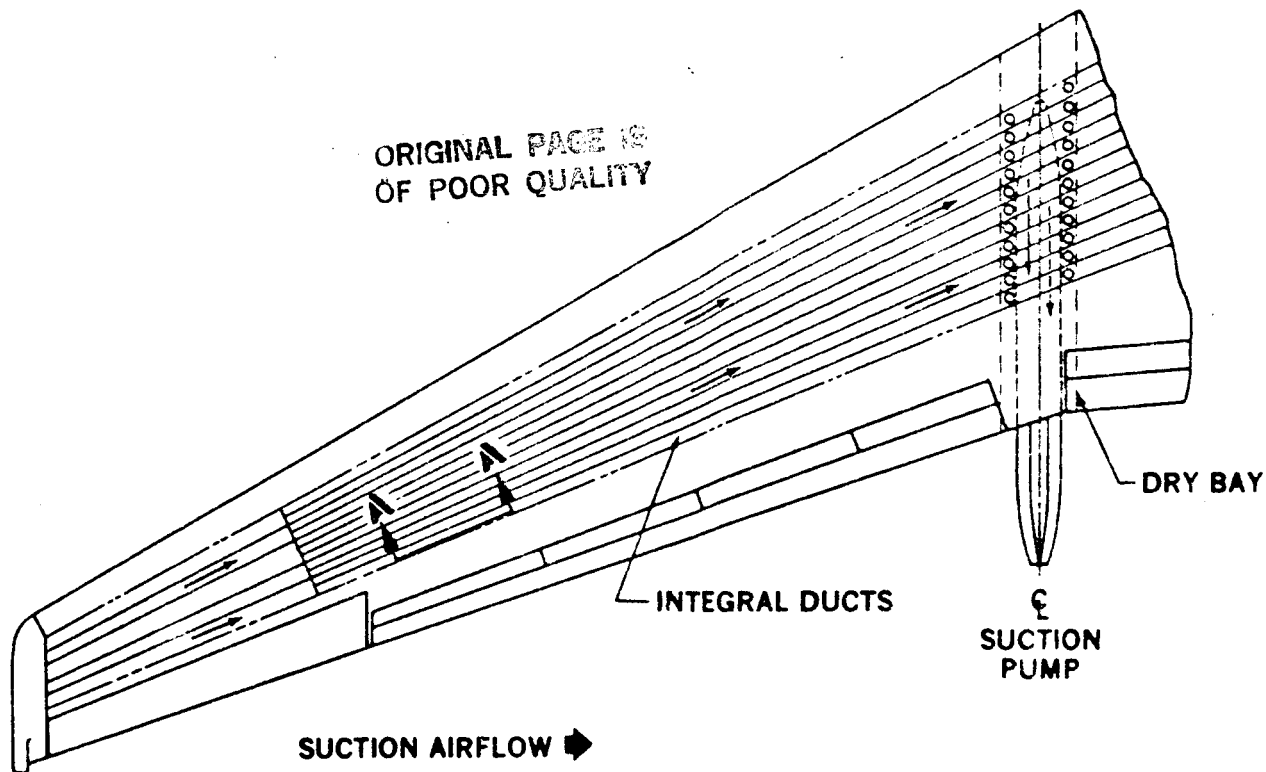


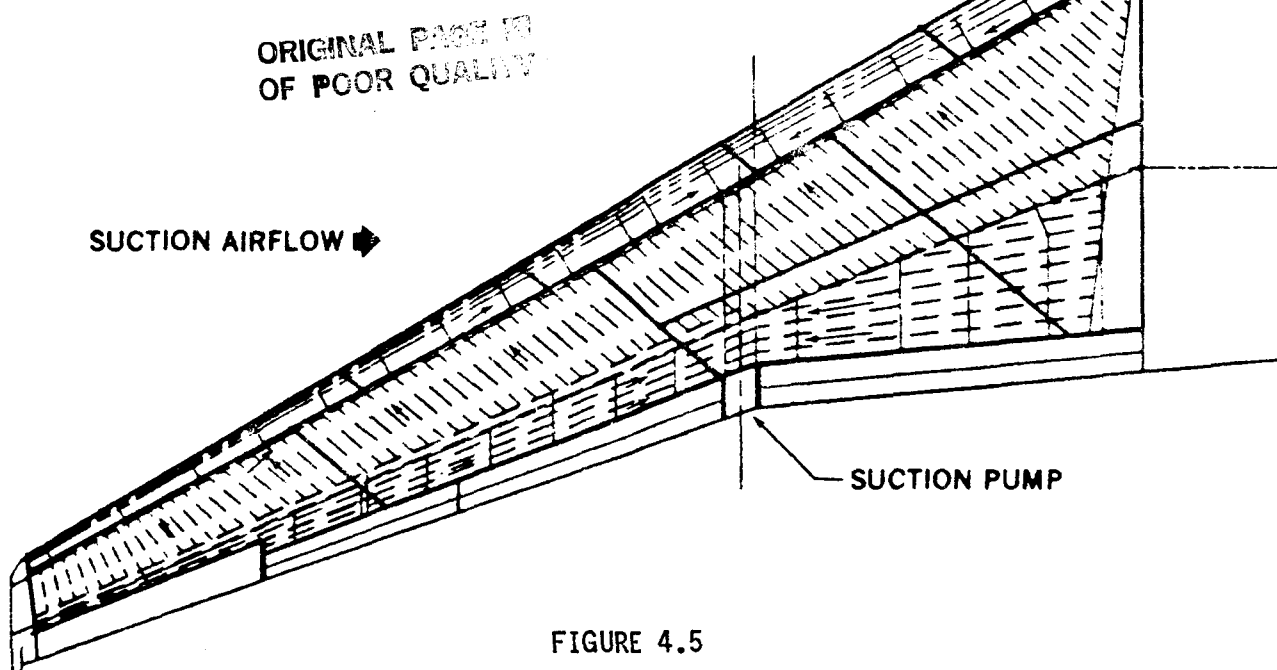
FIGURE 4.4

Despite the seeming advantage of integrating the channels into the wing structure, the spanwise collection design actually resulted in a heavier system than the one subsequently developed for chordwise collection.

A new configuration using chordwise collection channels in the wing box area was studied. Spanwise ducting was retained in the leading and trailing edges. Chordwise collection in the wing box area is possible because both suction airflow requirements and external pressure in that region can be kept fairly constant (see Figure 4.5).

The chordwise channels were much shorter than any spanwise collection channel and the system did not require any control valves to match suction and clearing flows. If, due to clearing source constraints, a sequencing procedure is used for clearing, few control valves would be required. These could be mounted forward of the front spar for easy access. Since the channels were shorter and no control valves were necessary, the required channel depth was much less. Chordwise channel depth could be as small as 0.4 inch compared to a required 2.0 inch depth for the spanwise collection system at the dry bay. This allowed

CHORDWISE AIR-COLLECTION SYSTEM



a deeper, more effective wing box structure and an increased fuel volume within the wing section. Since fewer control valves were required, the chordwise collection system was lighter and more reliable.

With the spanwise design, the flow control valves would be inaccessible. With the chordwise collectors over the wing box area, all the air is routed forward into the leading glove and any metering of the air is done there. The leading edge suction flow is also routed spanwise through ducts. The placement of all this ducting in the leading edge glove improves accessibility to the flow distribution system. With the shield extended and the lower panel removed, good access is provided to the ducts and the control valves (see Figure 3.8).

A preliminary analysis was conducted comparing the chordwise air collection design with the spanwise air collection design for the suction/purge system. The chordwise system, by virtue of its shorter collector channels, is a more efficient design. The suction and purge airflow requirements are more easily matched with the shorter ducts of the chordwise system, simplifying the design task. The very elaborate manifold required for the spanwise system would be replaced by a relatively simple, if long, collector duct which would be

ORIGINAL PAGE 12
OF POOR QUALITY

readily accessible through the leading edge access panels. Elimination of the dry bay in the chordwise design simplifies the wing structure and the fuel system and increases fuel capacity.

The current channel depth of 0.4 inch is more than adequate to provide suction and purge airflows within the design parameters at any wing station. The mismatch in the flute to channel orifice size required to meet suction and purge airflow requirements (Figure 4.6) is increased by the chordwise variation of wing surface pressures. Varying the surface porosity, which can be achieved by programming the electron beam perforating machine, would relieve this situation (see Section 4.5.2).

4.5 ANALYSIS

4.5.1 Suction/Clearing Flow Calculation

The wing was broken down into 17 suction panels (Figure 4.2). Using the suction levels required to achieve laminar flow over the wing as established by aerodynamic analysis and the required clearing differential pressure of 1 psid, the airflow from each panel was calculated. These airflows per panel were then used to size the ducting for both the suction and clearing systems. The airflows calculated for each panel are shown in Figure 4.7. Note the disparity between the flow rates for suction and clearing.

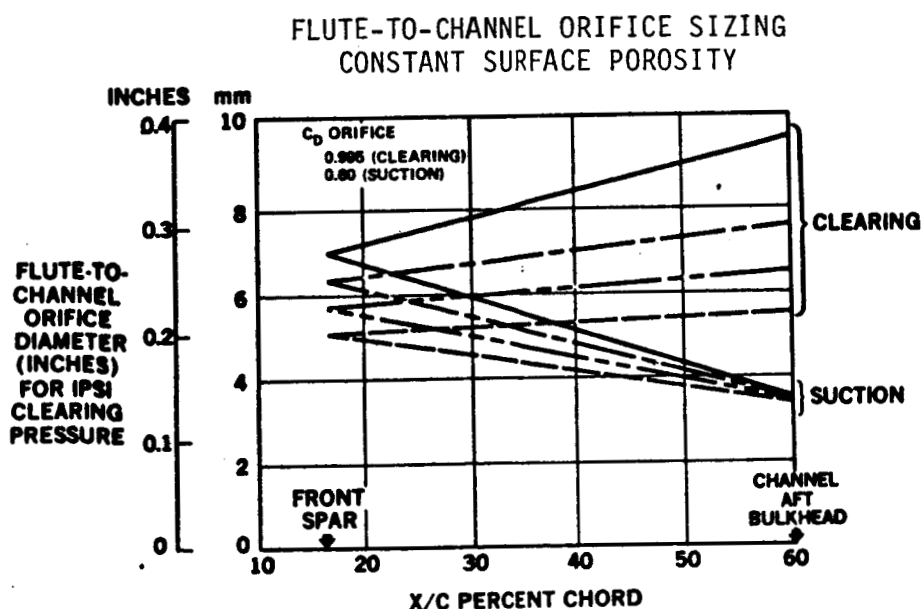


FIGURE 4.6

SUCTION AND CLEARING AIRFLOW REQUIREMENTS

ORIGINAL PAGE IS
OF POOR QUALITY

PANEL NO.	SUCTION FLOW (LB/SEC)	CLEARING FLOW (LB/SEC)
1	0.059	0.767
2	0.123	1.572
3	0.151	1.928
4	0.153	1.945
5	0.173	2.214
6	0.169	2.161
7	0.118	2.884
8	0.179	4.401
9	0.230	5.640
10	0.327	8.020
11	0.380	9.329
12	0.132	3.253
13	0.311	1.712
14	0.428	2.361
15	0.549	3.025
16	0.799	4.40
17	2.49	13.62
TOTAL	6.771	69.233

FIGURE 4.7

4.5.2 Porosity Study

Variation of surface porosity was considered as a possible way of reducing that part of the mismatch between suction and purging orifice requirement due to external pressure variation. Reducing the porosity from its base value at the front spar to 50 percent of this at 60 percent chord allows the system to be matched for both suction and purge (See Figure 4.8). Controlling the airflow at the surface by varying the porosity not only overcomes the orifice problem, it also results in reducing suction airflow and power requirements because the pressure drop at the surface is matched to the external pressure gradient and airflow requirements (Figure 4.9). This feature, in conjunction with the reduction or elimination of other pressure drop metering controls, would result in a minimum pressure drop throughout the suction system. Varying the porosity in either the chordwise or spanwise direction was not anticipated to be a practical problem.

Porosity tailoring allows the clearing airflow requirement to be reduced by 25 percent. The flute-to-channel orifices could then be sized to match both the suction and clearing requirements (Figure 4.8).

FLUTE-TO-CHANNEL ORIFICE SIZING WITH VARIABLE SURFACE POROSITY

ORIGINAL PAGE 12
OF POOR QUALITY

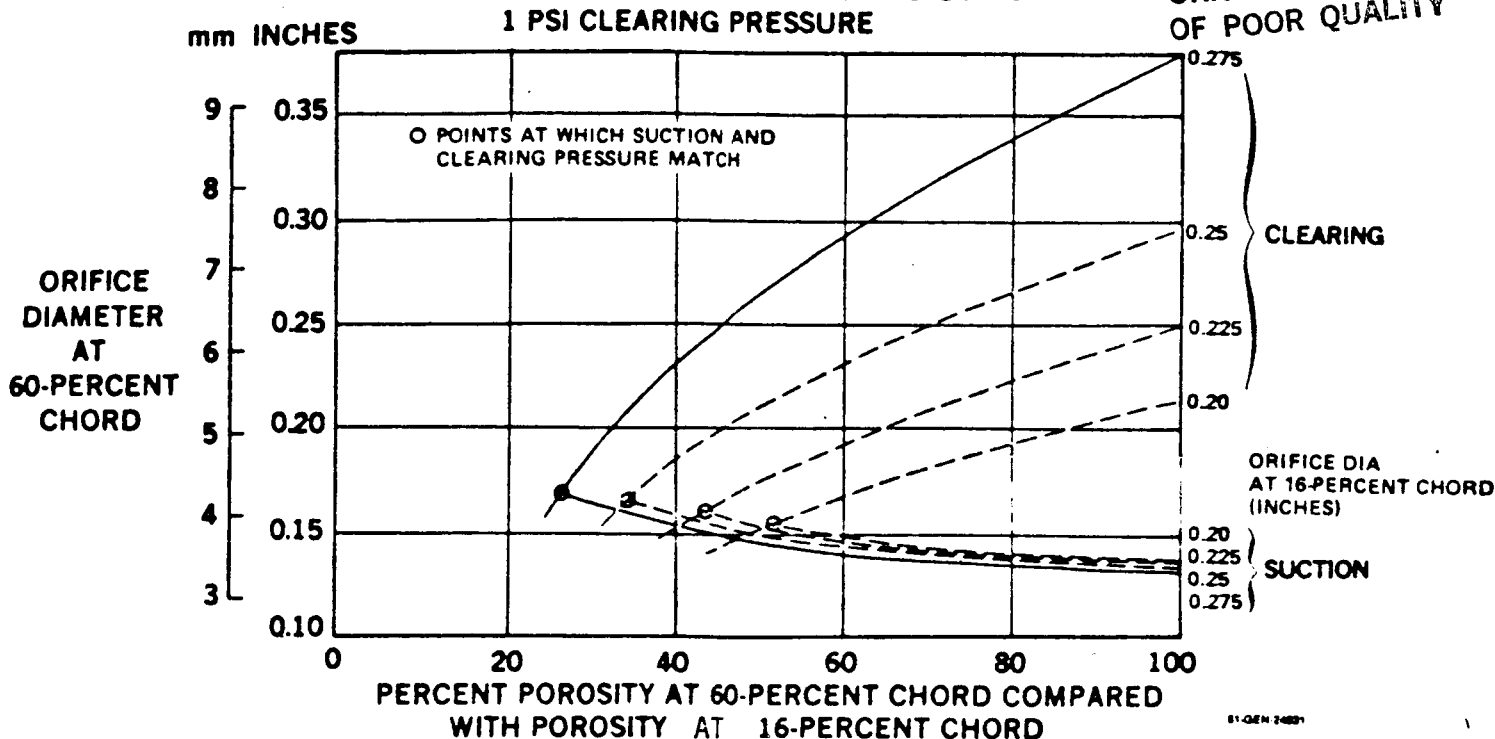


FIGURE 4.8

SURFACE POROSITY REQUIREMENT

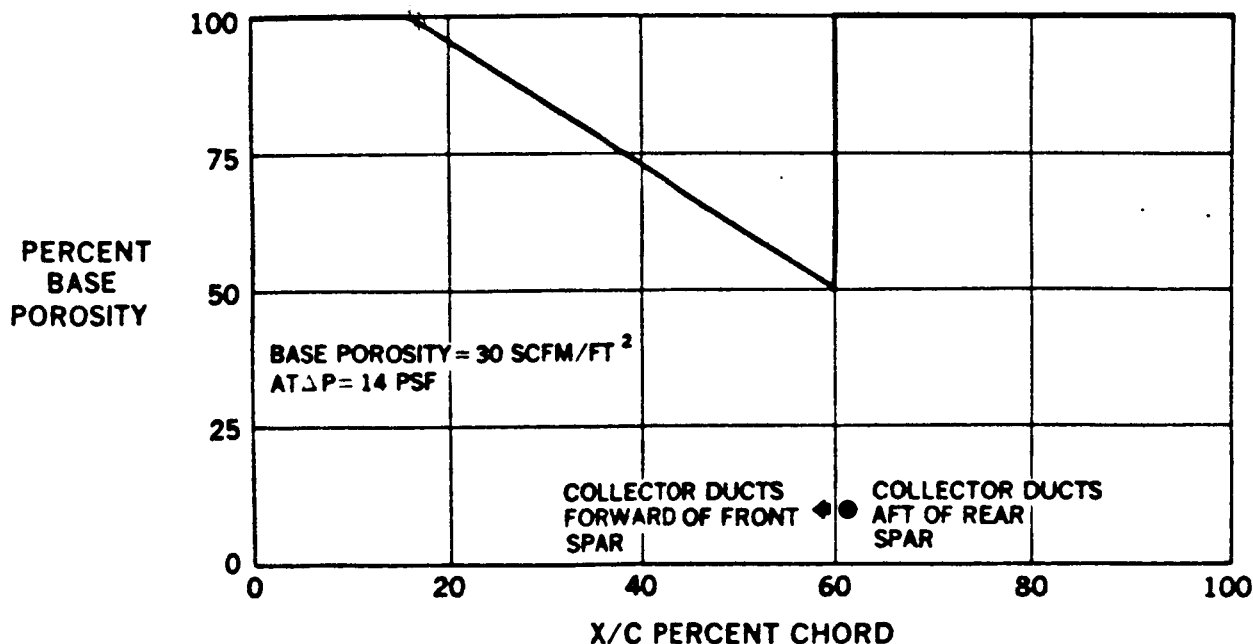


FIGURE 4.9

4.5.3 Control Valve Study

A study was done on the spanwise collection system to determine how many control valves would be required to match the channel sizes for the suction function with those of the clearing function assuming that the entire porous surface would be cleared at once.

In this analysis, it was found that 1056 control valves would be required per airplane. Also, the channel depth would have to be increased to maintain the internal air velocity during suction of $M = 0.2$. To lessen the number of control valves needed, and to reduce the clearing source airflow pressure requirement, a sequencing procedure for clearing was studied. With this method, the surface is cleared in stages. The number of stages depend on the capability of the clearing source to meet the required pressure differential across the surface, the disparity in flows, and differences in channel size requirements between suction and clearing operations. Clearing in sequence prolongs the time needed to clear the system before suction can be applied. Some additional hardware is also needed to control the sequencing operation.

Sequencing was studied on an earlier contract and would have been used for the spanwise collection concept because it resulted in a more efficient, if slower, system. The use of decreased porosity (Section 4.5.2) reduces the number of sequencing stages needed because any increase in pressure drop through the surface reduces the flow rate through the porous surface for the required pressure differential and a larger area can be purged with the same airflow.

Sequencing was not required for the chordwise collection system.

4.6 DETAIL DESIGN

4.6.1 Ducts and Channels

For the spanwise collection system, air is drawn through the perforated skin and subsurface flutes into collection channels running spanwise the length of the wing and routed directly to a dry bay before being manifolded into the suction pump. The maximum channel length is 54 feet.

With the 'chordwise' collection system ultimately chosen, the integral collection channels run chordwise over the wing box area. The air is routed forward and manifolded with flow from the leading edge. The combined flow, from the attachment line to 60 percent chord, is then routed in spanwise ducts (Figure 4.10) to the suction source. The airflow from the surface further aft is collected in spanwise ducts aft of the rear spar. The ducts were sized so that the internal airflow should not exceed $M = 0.2$. The required size for the main duct increases from a nominal 1 inch diameter at the wing tip to a maximum of 9 inches at the mid-semi-span of the wing. The smaller ducts that collect air from the leading edge flutes range from 1 inch to 3.75 inches diameter (Figure 4.11). For this 'chordwise' collection system, the main transport ducting is located forward of the front spar. During suction, these ducts route air to the midpoint of the wing, then penetrate the lower surface and run aft to a mixing chamber which is at the suction pump intake. The airflow from the integral spanwise ducts in the trailing edge are metered through manifolds directly to the suction pump. The suction air is exhausted from the pump at freestream pressure and velocity (Figure 4.1). This ducting system is much simpler than that required for the spanwise system.

LEADING EDGE AIR COLLECTORS

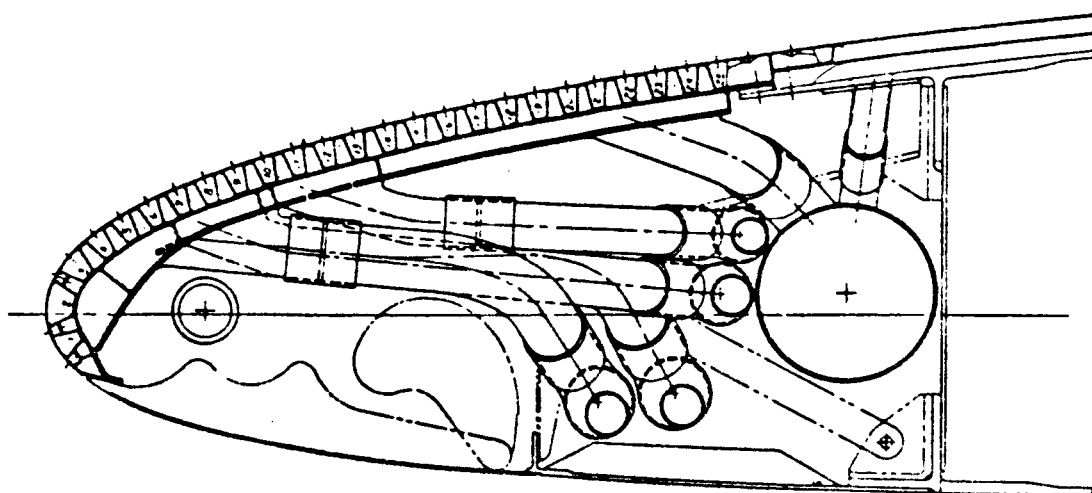


FIGURE 4.10

ORIGINAL PAGE IS
OF POOR QUALITY

DUCT SIZING

ORIGINAL PAGE IS
OF POOR QUALITY

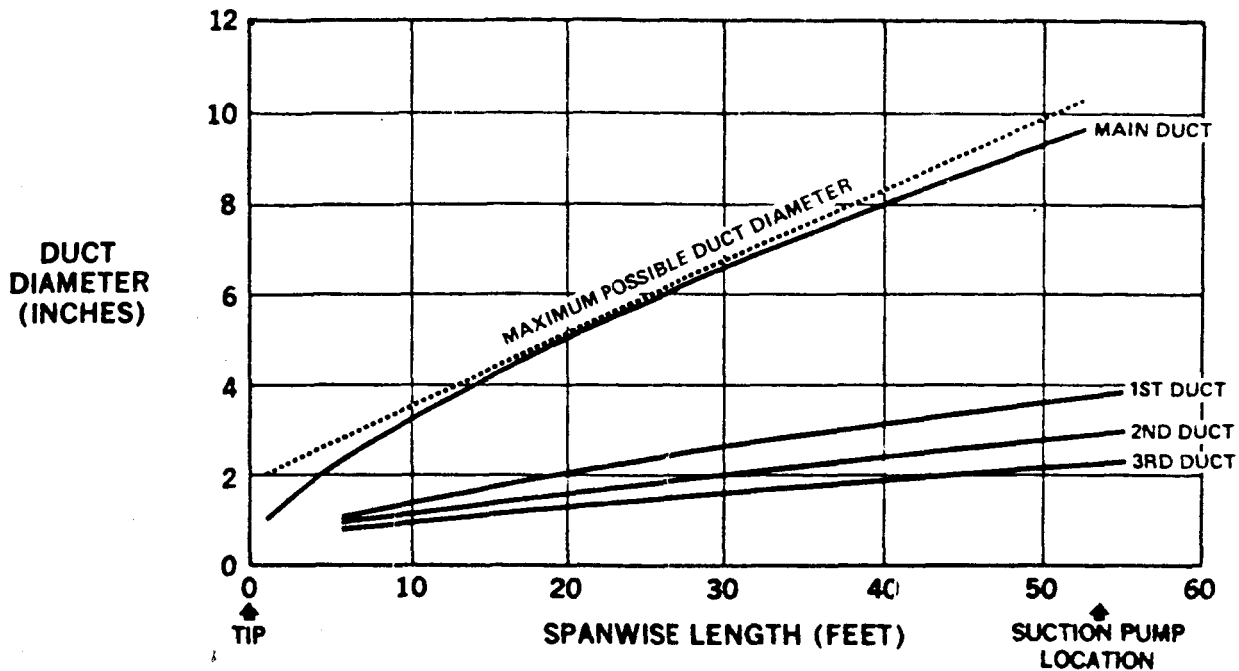


FIGURE 4.11

4.6.2 Orifices and Valves

In either the spanwise or chordwise collection systems, metering orifices are located at the bottom of the flutes. Air passes through the porous surface into the flutes and then through the orifices into the channels. The orifices are designed such that for suction flow when a substantial metering effect is required, the discharge coefficient is 0.68, but for clearing, when minimum pressure drop is required, the coefficient is 0.99. This is achieved by using an orifice with a smooth, well rounded inlet for clearing and a sharp edged inlet for suction.

For the spanwise air collection system considered originally, control valves were located in the collector channels at about two foot intervals. The valves controlled the air flow from the flutes of the surface panels to the channels. Each valve spanned about three to five flutes and was orificed to further meter or control the flow in the suction direction. The orifice in the control valve was designed for low flow energy loss and was positioned on a flapper-like door (Figure 4.12). During suction the valve was seated and all the air flowed through the orifice. When clearing pressure was applied, the flapper-like door opened and reduced the flow resistance. The integral

CONCEPTUAL VALVE DESIGN

SPANWISE AIR COLLECTION CONCEPT

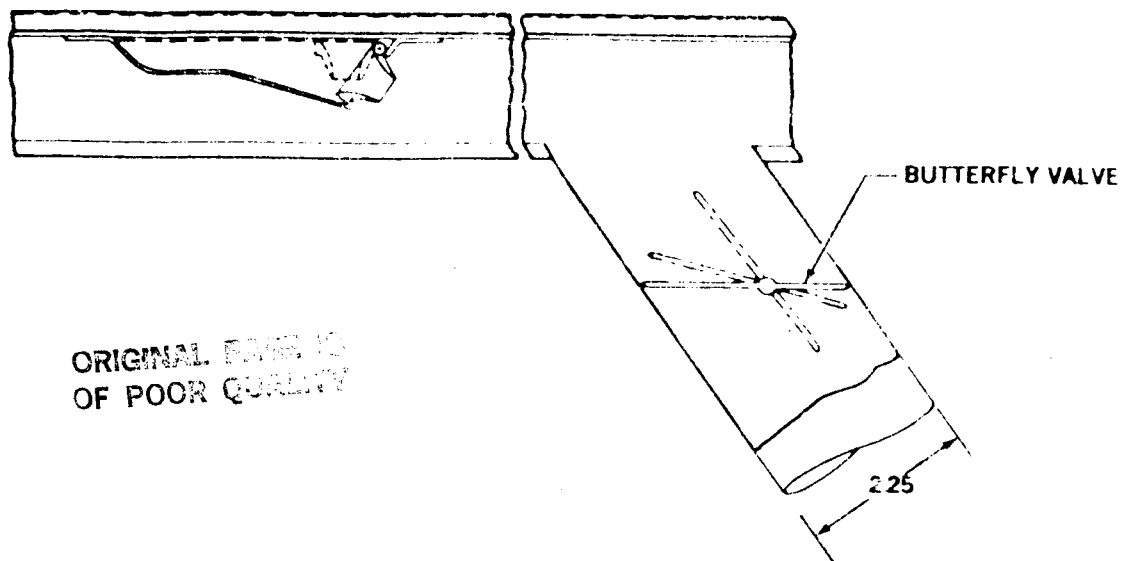


FIGURE 4.12

channels ducted air to a dry bay and butterfly valves in the ducting to the dry bay were used for coarse balancing of airflow and as shutoff valves for clearing in sequence.

The chordwise collection system had no dry bay and if several retractable ram air scoops were used along the span of the wing, clearing sequencing and control valves would be unnecessary. If sequencing were used, accessible control valves could be mounted forward of the front spar.

4.7 CONCLUSIONS AND RECOMMENDATIONS - SUCTION AND CLEARING SYSTEMS

The chordwise system of ducting air over the main wing box offers the following advantages over a spanwise ducting arrangement:

- o The system is simpler with far fewer control valves.
- o Section system components are readily accessible for maintenance and adjustment.

- o Shallower ducting requirements result in reduced weight due to increased effective wing structural depth and increased fuel volume.
- o Dry wing bays are unnecessary, resulting in increased fuel volume and avoidance of fuel bulkhead weights.
- o Multiple cutouts in the upper panel and large cutouts in the lower wing panel for ducting air to the suction pump are avoided, resulting in weight reduction.
- o Complicated duct manifolding to the suction pumps is avoided.

With these advantages, the chordwise ducting system was selected for any future LFC configurations that require LFC suction over the main wing box.

5. ICE PROTECTION AND CONTAMINATION AVOIDANCE SYSTEM ANALYSIS AND DESIGN

5.1 INTRODUCTION

The primary objective of this part of the WSSD Program was to investigate and update concepts of supplemental contamination avoidance and ice protection. This was to ensure that the design of the LFC panel structure being developed and tested would be compatible with proposed ice protection and contamination avoidance systems. The study was to include considerations of operation, performance, design, and fabrication to ensure feasibility of the concepts and permit a choice for further development work.

Under an earlier contract for NASA in which systems for laminar flow control (LFC) on subsonic aircraft were studied (Reference 1), DAC evaluated numerous concepts that would provide contamination avoidance (CA) and/or ice protection (IP) for laminar flow aircraft wing. As a result of this study, DAC selected a retractable shield as a primary protection system. The shield is stowed in the underwing region just aft of the leading edge and is extended to provide protection and lift augmentation during takeoff, climb, descent, and landing.

The preliminary studies also identified two alternative means of providing a supplemental CA/IP system for the wing leading edge, both based on a protective liquid film. One system used a spray (mounted on the aft face of the extended shield) to provide a liquid film on the wing. The second system used a porous dispenser mounted in the fixed wing leading edge and integrated with the suction system. A retractable shield is used with either system and is protected as described in Section 5.2.2.

Insect contamination is most likely to occur between sea level and 5,000 feet. To avoid excessive debris buildup on the wing leading edge, the liquid system can be applied during this period to supplement the shield protection, if necessary.

The ice protection system selected for the shield itself is the TKS deicing system (Reference 2). In this system, an ethylene glycol/water solution is

dispensed through a porous leading edge section of the high lift shield. Contamination of the shield itself is acceptable for the proposed LFC system because it retracts into the lower surface aft of the attachment line where LFC is not required.

The configuration of the DAC Leading Edge Test Article (LETA) being tested on the Leading Edge Flight Test (LEFT) program (Reference 1) uses the shield supplemented by a spray system for contamination avoidance and ice protection.

Using a freezing point depressant (FPD) liquid, the liquid systems can also be used for ice protection of the wing leading edge. If icing conditions are encountered, the shield can be deployed for anti-icing. If a spray system is used, sufficient capacity exists for operation in a de-icing mode. During icing encounters, the shield should be extended with the ice protection on. The detailed operational procedures and the need for a supplemental liquid contamination avoidance system will be investigated during the Leading Edge Flight Test (LEFT) program currently going on at NASA Dryden. The spray system concept was selected for the LEFT program because it does not complicate the leading edge structure and LFC suction system and utilizes off-the-shelf hardware. Preliminary studies of the supplemental liquid film indicated that the glycol-based fluid selected, propylene glycol methyl ether (PGME), will provide excellent contamination avoidance properties and also act satisfactorily as a freezing point depressant for ice protection.

Integrating the liquid dispenser into the wing leading edge and suction system complicates the design, but the possibility of more economical use of the protective liquid and improved operational flexibility make this concept attractive. Two possible methods of implementing the liquid film dispenser concept were considered. These were intermittent chordwise dispensing or an integrated liquid dispenser/suction arrangement. In the intermittent chordwise system, described in Section 5.3.1, dispensers distribute the liquid through the perforated titanium skin from spanwise flutes located between the suction flutes. The integrated liquid/suction system utilizes the spanwise flutes for both suction and to distribute the liquid as described in Section 5.3.2.

The secondary objective of this part of the program was to develop design and operating data pertaining to the liquid dispenser and perforated titanium suction concepts. In particular, analyses and tests were undertaken to:

- a. Determine the relationships between pressure drop and the flow of air or liquid through the perforated titanium (see Section 5.3.3)
- b. Determine the susceptibility of the proposed perforated surface material to clogging from atmospheric contaminants, the effectiveness of cleaning methods, and the ability to clear the surface of any liquid in the perforation (see Section 5.3.4).

5.2 CONTAMINATION AVOIDANCE AND ICE PROTECTION SYSTEM REQUIREMENTS

5.2.1 Fixed Leading Edge

The major considerations for contamination avoidance were the distribution of characteristics of airborne insects, the extent to which smoothness must be maintained, compatibility with other LFC systems and structures, and operation and maintenance procedures.

- a. Insect Population and Characteristics - Most insects are confined to the so-called terrestrial zone, from ground level to (91.4m) 300 feet, although insects can occur up to (1,500m) 5,000 feet above ground on rare occasions.

A contamination avoidance system that is effective at altitudes below (305m) 1,000 feet should be adequate in a temperate climate, but some data indicate that protection up to (1,525m) 5,000 feet may be required under semi-tropical conditions. Each of the systems should, therefore, be evaluated on its ability to provide contamination protection up to (305m) 1,000 feet altitude as a minimum and up to (1,524m) 5,000 feet as a design goal.

- b. Roughness Criteria - The permissible roughness is a function of cruise altitude, the chordwise distance from the attachment line (stagnation point with two dimensional flow), and the type of roughness. The contamination avoidance system has to prevent adhesion of contaminants that would trip the boundary layer. A maximum allowable height of (0.102mm) 0.004 inch was used for system evaluation and preliminary design.
- c. Ice Protection - The ice protection system must prevent or remove ice accumulation near the leading edge and not allow water to run back onto an LFC area where it could subsequently freeze. The ice protection system must meet the requirements of FAR 25 and be certifiable by the FAA. Laminar Flow would have to be maintained after encountering continuous maximum icing condition or intermittent maximum icing conditions as defined by FAR 25.

The ice protection system selected for the shield itself is the TKS deicing system (Reference 2). In this system, an ethylene glycol/water solution is dispensed through a porous leading edge section of the high lift shield. Contamination of the shield itself is acceptable for the proposed LFC system because it retracts into the lower surface aft of the attachment line where LFC is not required.

- d. Compatibility - The contamination avoidance system must be designed within the space constraints of the leading edge box and be compatible with the space requirements of the structure, the suction system, the retractable shield that must also be properly sized and located for aerodynamic performance, and the shield actuating mechanism. Another potential conflict of requirements is liquid dispensing versus suction area requirements, especially in the region of attachment line travel.

It would be highly desirable to use the same liquid for the contamination avoidance and ice protection. To effect this integration, the porosity requirements of the two systems and the spreading characteristic of the liquid must be compatible. Also, a method must be devised to clear the liquid from the porous surface before applying suction. The ducting for the CA/IP system and the suction system could be common or separable.

- e. Aircraft Operation and Maintenance - The contamination avoidance system should not require special flight procedures that would significantly degrade performance or affect safety. Consideration must be given to crew workload, worldwide availability of protective liquids, environmental pollution, and ground maintenance including the ability to replace all system components.

5.3 PERFORMANCE AND DESIGN STUDIES

5.3.1 Intermittent Chordwise Design

One method of applying liquid to the surface is to use spanwise dispensers welded to the skin and spaced intermittently in the chordwise direction. To minimize interference with the suction capability, the liquid dispensers are located in the region between the suction strips, as shown in Figure 5.1. Four dispensers are shown with fluid tubes attached. The titanium dispensers would be seam welded to the skin after the initial forming operation and the graphite substructure subsequently bonded to the skin and dispenser assembly.

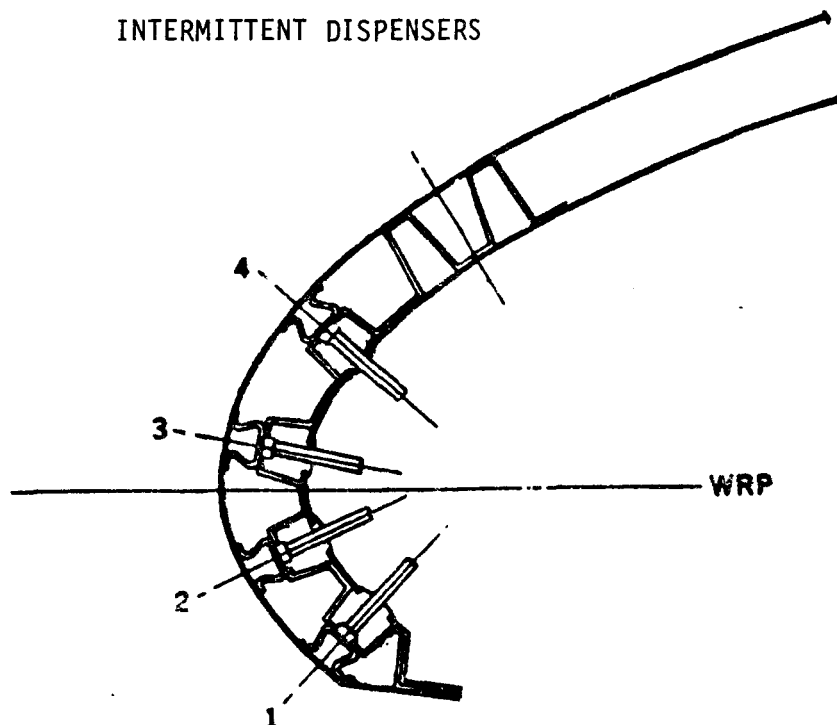


FIGURE 5.1

OFFICE OF
OF POWER

A collar is swaged onto the liquid supply tube and this assembly is bonded to the titanium at a predrilled location. The area of the graphite substructure adjacent to the tube is filled with a sealant.

During low altitude operation, the shield would be extended and aerodynamic forces would cause all of the liquid to flow upward, providing contamination avoidance and ice protection. A disadvantage is that if icing conditions are encountered when the shield is retracted (e.g., during cruise), ice could form between the two dispensers on either side of the attachment line. However, the intermittent chordwise concepts offers two advantages over the spray system:

- a. The dispensers are more economical in the use of liquid firstly by providing uniform distribution, and secondly because unlike the spray system, all of the liquid contacts the surface.
- b. The dispensers provide a measure of ice protection when the shield is retracted.

The major disadvantage of the concept is that it increases the complexity of design and manufacturing of the wing leading edge.

5.3.2 Integrated Suction/Contamination/Ice Protection Design

An alternative method of dispensing liquid through the perforated skin would use a plenum that integrates liquid dispensing with the suction/surface-clearing function. The titanium dispensing plenum would be made using the superplastic-forming and diffusion-bonding process. It could be resistance-welded to the titanium skin at its extremities where sealing is required and could be capacitor-discharge welded in between at the liquid passage spacers.

The center area of the plenum which encompasses the region of attachment line travel during cruise would provide liquid for ice protection and suction for laminarization. The outer plenums are needed for ice protection at extreme angle of attack and dispense liquid only. The tubular ducts would be welded or brazed to the plenum (see Figure 5.2).

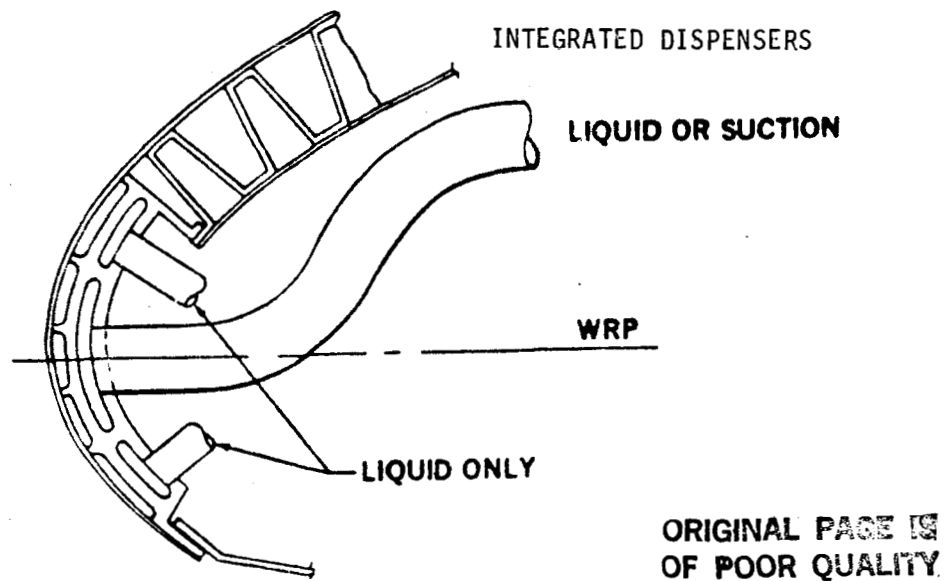


FIGURE 5.2

5.3.3 Pressure Drop Through Perforated Titanium

No data was available for the influence of liquid properties on the pressure drop characteristics of perforated titanium with slightly conical holes and a length-to-diameter ratio between 5 and 10. Testing was, therefore, conducted to verify analytical conditions. The flow in the perforations should be laminar at the calculated Reynolds numbers and the corresponding friction factor was used. A typical result was plotted as liquid flow versus pressure drop for the tested LFC surface with 0.0026 inch diameter holes (Figure 5.3).

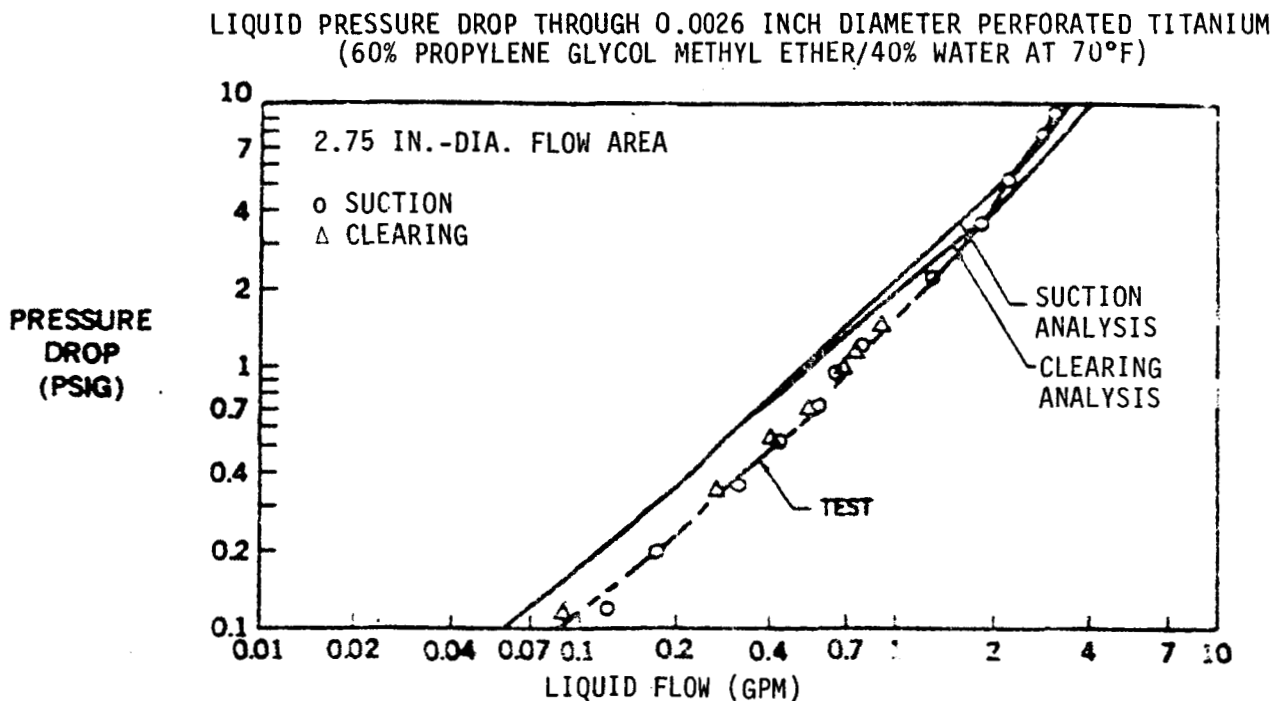


FIGURE 5.3

The results were compared with the following theoretical equations derived previously.

$$\Delta P_d = 0.5q_i + q_e = 0.5625q_i \quad (\text{Suction Flow})$$

$$\Delta P_d = 0.1q_i + q_e = 1.0256q_e \quad (\text{Clearing Flow})$$

Where: ΔP_d is the total dynamic pressure loss, q_i is the inlet dynamic pressure, and q_e is the dynamic pressure at the outlet.

The frictional losses can be calculated using the Darcy equation.

$$\Delta P_f = \frac{4 f l}{d} q$$

Where: f is the friction factor, l is the length, and d is the diameter.

For a mixture of 60 percent PGME and 40 percent water, the analysis predicted a pressure drop 60 percent higher at 70°F than the measured value at typical design flow rates. The slope of the curve for the test data increases rapidly at high flow rates indicating higher dynamic losses than estimated or losses due to transition to turbulent flow.

Since it was not possible within the scope of the program to determine the cause of this discrepancy, a set of pressure curves (Figure 5.4) was empirically derived from tests. These curves provide pressure drop data over the temperature range -40°F to +120°F at flows between 1 and 30 gpm of liquid per square foot of surface area. These curves are recommended for use in design.

5.3.4 Environmental Contamination

Environmental contamination tests were conducted to determine the susceptibility of perforated titanium to clogging due to atmospheric particles. Figure 5.5 shows that a significant reduction in airflow occurred after the specimens were exposed to atmospheric contaminants at the Long Beach Airport for several weeks. Steam cleaning using a simple hand-held wand restored the original porosity of all specimens, including several that had been exposed for 13 to 15 weeks. Periodic steam cleaning at 100 flight hour intervals would prevent significant clogging under typical environmental conditions. Because the steam cleaning temperature was below the curing temperature of the bond, no degradations of the bond should occur after repeated steam cleaning. A visual inspection showed no degradation of the bond.

LIQUID PRESSURE DROP ACROSS 0.025 INCH PERFORATED
TITANIUM WITH 0.0026 INCH DIAMETER AT 0.026 INCH SPACING
USING 60% PGME PLUS 40% WATER AT VARIOUS TEMPERATURES

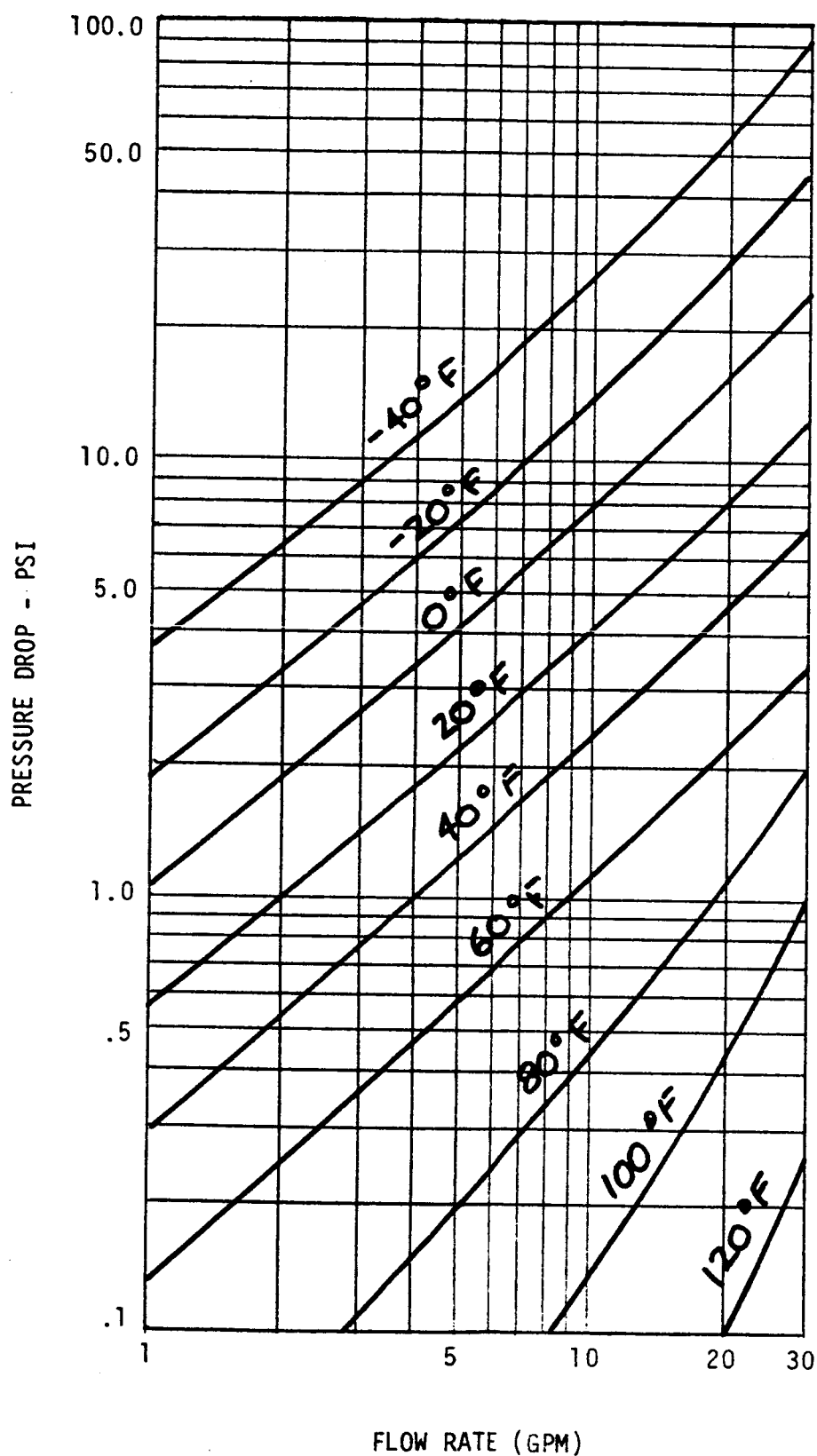


FIGURE 5.4

ORIGINAL PAGE 18
OF POOR QUALITY

ENVIRONMENTAL CONTAMINATION OF 0.0026-INCH-DIAMETER PERFORATED TITANIUM SPECIMEN NO. 1

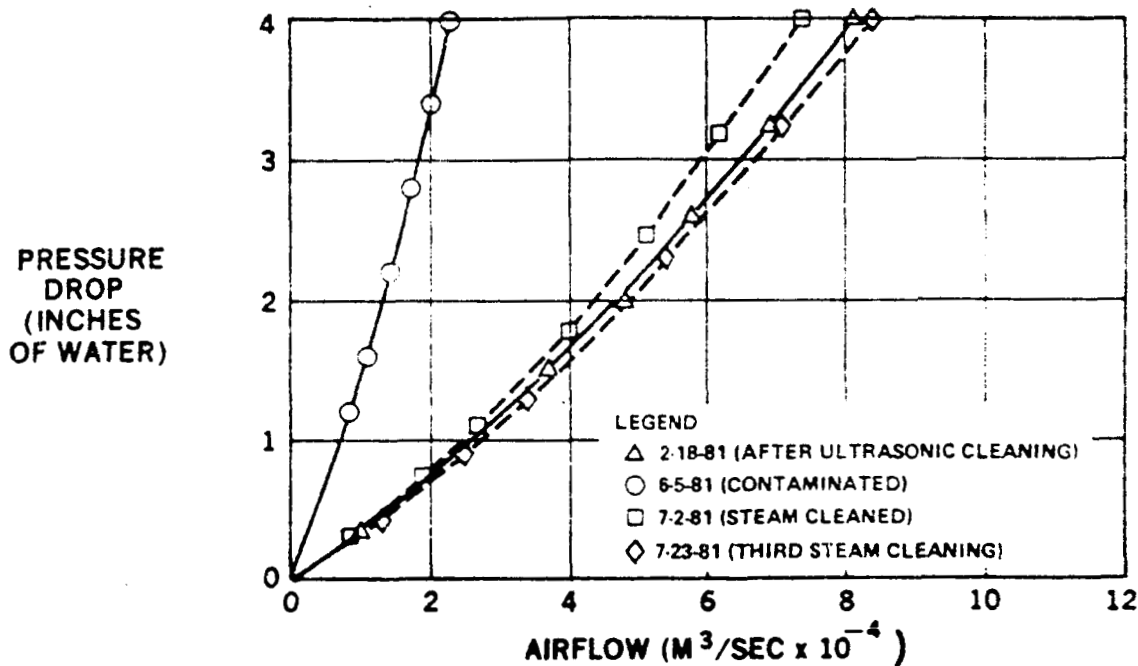


FIGURE 5.5

ORIGINAL PAGE 16
OF POOR QUALITY

The porosity of an almost identical specimen was degraded only to about half the extent of the previous sample in the same time period, as shown in Figure 5.6. This indicated, the variability in the rate of clogging of porosity that can occur under apparently similar conditions. A single steam cleaning again restored the porosity completely.

5.4 CONCLUSIONS AND RECOMMENDATIONS - ICE PROTECTION & CONTAMINATION AVOIDANCE

- o The proposed electron beam perforated suction surface appears to be practical from the aspect of clogging and cleaning in service.

ENVIRONMENTAL CONTAMINATION OF 0.0026 INCH DIAMETER
PERFORATED TITANIUM
SPECIMEN NO. 2

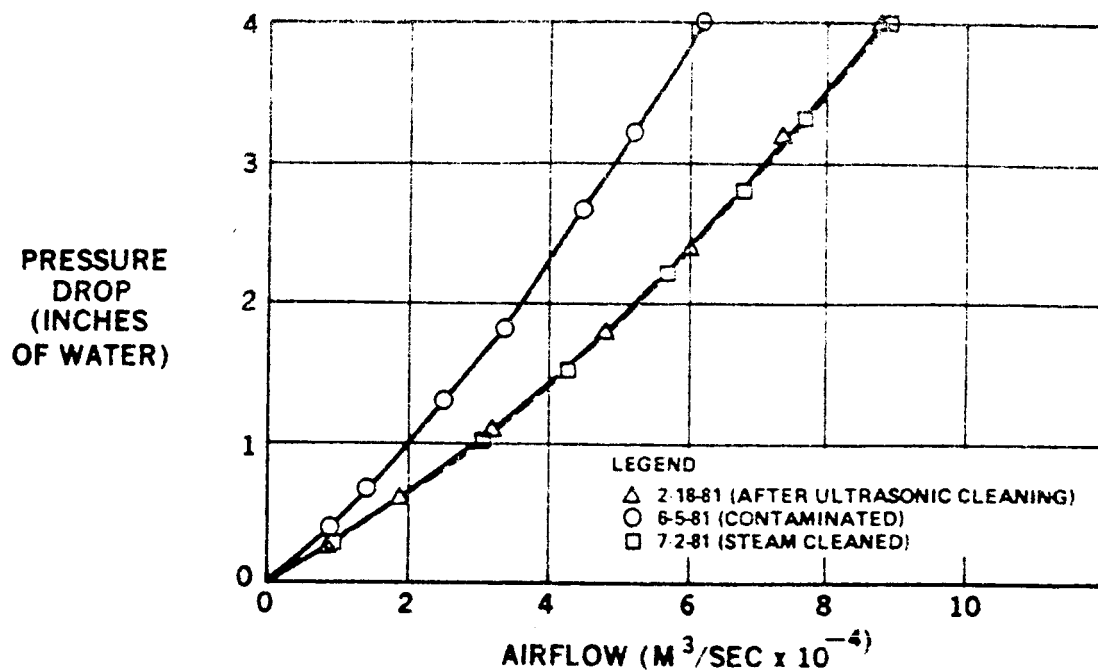


FIGURE 5.6

A design using either integrated liquid/suction or intermittent chordwise liquid dispensing concepts has the potential for development as a practical liquid dispensing system for protection against icing and contamination. Either system could be used for ice protection without deploying the shield and less liquid would be required than with a spray system. Further design studies and testing are needed to develop a practical arrangement.

ORIGINAL PAGE IS
OF POOR QUALITY

6. FABRICATION DEVELOPMENT

6.1 INTRODUCTION

As the design of the LFC porous surface panels matured, it developed from a complex multilayered fiberglass structure which was sewn and bonded together to the simpler design shown in Figure 3.3. This design has a composite molded substructure that is bonded to an electron beam perforated titanium skin in a separate operation. The development of this design required the solution of several fabrication problems, including the following: How could curved panels having this cross-section be fabricated to contour accurately without the aid of very expensive tooling? What could be done to improve the reliability of the bond between the titanium and the substructure? Why did the panels not maintain the mold shape?

6.2 FABRICATION TOOLING FOR CURVED PARTS

In the late stages of the initial LFC contract (NASI-14632), a simplified corrugated substructure was designed to support the porous surface. This simple section was layed up as shown in Figure 6.1. The expansion of silicone rubber mandrels with temperature provided the pressure necessary to squeeze out the volatile gasses and to compact the layup against the hard tool during cure. The method worked well enough for flat or slightly curved panels, but for a highly curved surface such as a leading edge, a collapsible or disposable tool would be required to prevent the molded part from being locked in place on the tool as shown in Figure 6.2. A teflon tool, as shown in Figure 6.3, was devised to solve these problems. The substructure would be layed up on the teflon mandrel tool which was sufficiently flexible to conform to the mold shape. Once the part was cured, the part and the teflon tool could be removed together from the mold and theoretically the teflon tool could be peeled from the molded part.

The prototype tool was composed of machined trapedzoidal teflon mandrels mechanically fastened to a 0.032 inch thick teflon sheet. The tool proved to be too stiff to allow a peeling process to separate it from the part. In addition, during cure the resin tended to run into the joints between the

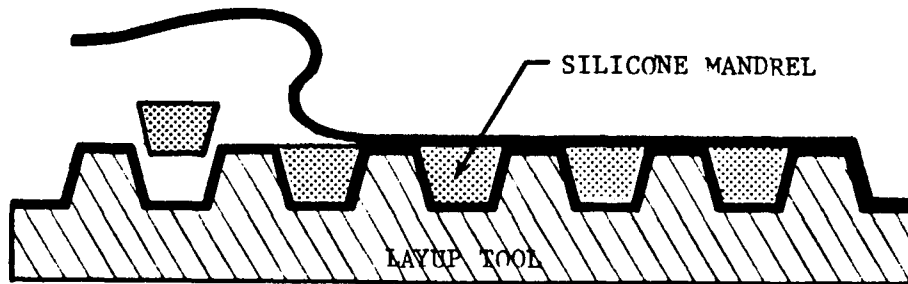
CORRUGATED PANEL FABRICATION STEPS

STEP 1 LAYUP CORRUGATIONS



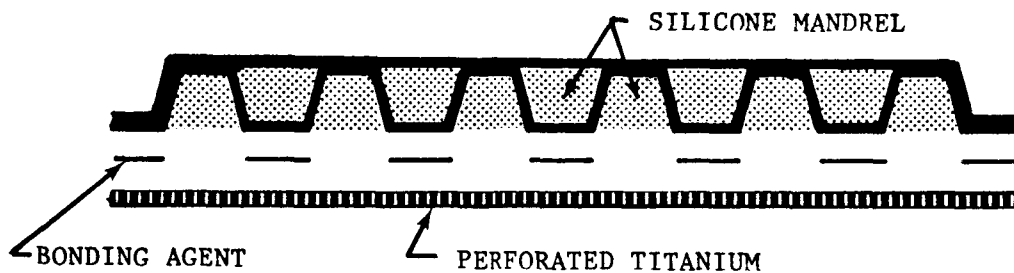
STEP 2 DENSIFY CORRUGATIONS

STEP 3 LAYUP FACE SHEET



STEP 4 BAG AND CURE SUBSTRUCTURE

STEP 5 ASSEMBLE SUBSTRUCTURE AND TITANIUM



STEP 6 BAG AND CURE SUBSTRUCTURE AND TITANIUM



FINISHED PANEL

(MANDRELS ARE PULLED OUT
THROUGH THE OPEN ENDS)

STEP 7 REMOVE MANDRELS FROM CURED PANEL

FIGURE 6.1

ORIGINAL PAGE IS
OF POOR QUALITY

HARD TOOLING FOR CURVED PANELS

ORIGINAL PAGE IS
OF POOR QUALITY

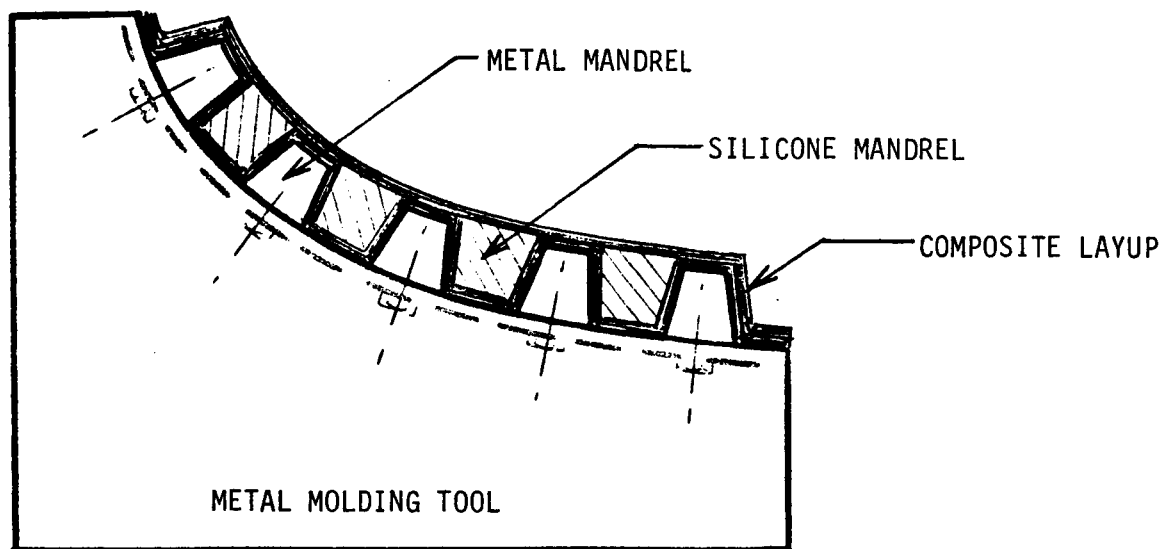


FIGURE 6.2

FLEXIBLE TOOLING FOR CURVED PANELS

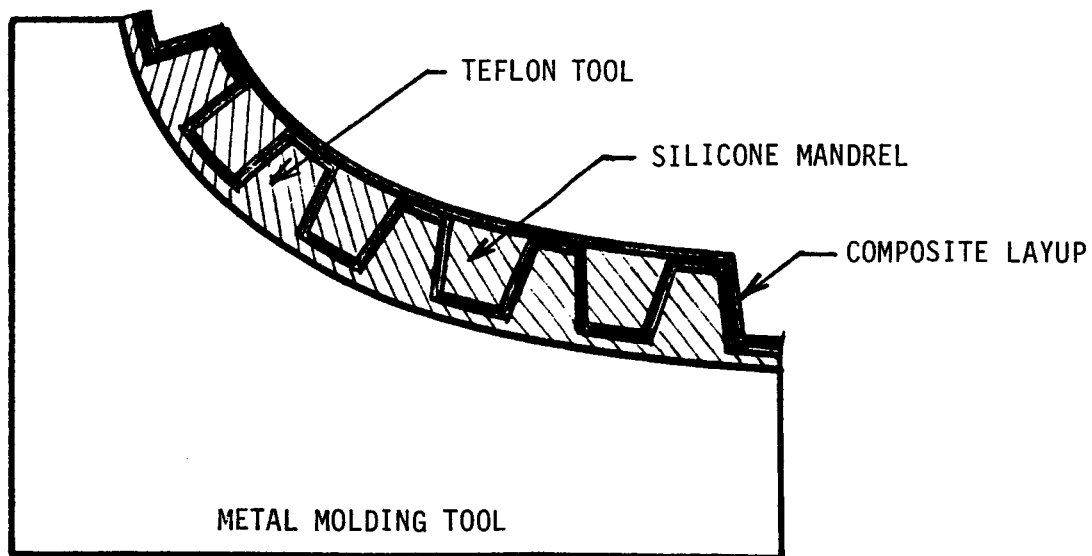


FIGURE 6.3

mandrels and the sheet causing flash which made removal even harder. Unscrewing the mandrels from the sheet to remove the tool was a tedious task, but allowed use of the separated mandrels during subsequent bonding of the perforated titanium outer sheet. A more flexible material and molded or bonded construction was needed to reduce the tool cost and to allow easy separation.

A second tool was made entirely of silicone rubber. Sections of rubber extrusion, trapezoidal in cross section, were bonded to a 0.063 inch thick silicone rubber sheet to form a monolithic flexible tool. This tool was easily separated from the cured part and the parts produced on it were nicely compacted and free of porosity indicating that uniform pressure had been applied. It was felt that the flexible tool concept needed additional development for production use, but all the test panels for this program were fabricated using flexible silicone rubber tools even though no curvature was involved.

The layup and curing processes came under close scrutiny during the search to find out why the panels would not retain their proper shape when removed from the mold (see Section 3.3). About 35 sample substructures, each about 8 x 10 inches, were made before this problem was solved. Initially the fabrication related areas of investigation included the effects of unbalanced layups, possible resin imbalances throughout the substructure, and the temperature distribution during the cure cycle.

The material used to make the initial test specimens was Narmco 5208/T300 preimpregnated biwoven cloth. It is an eight harness satin weave cloth which is woven as shown in Figure 6.4. This weave has an inherently unbalanced distribution of material and is known to warp when layed up in thin sections. This was thought to be a possible source of the panel distortions. Substructures were made using carefully balanced layups of eight harness cloth, a combination of eight harness cloth and unidirectional tape, and a balanced plainweave type of cloth. All of these specimens still exhibited the bowing across the corrugations which was evident in the initial panels. Resin samples were taken from panels made with tape and from those made with cloth.

EIGHT HARNESS SATIN WEAVE CLOTH

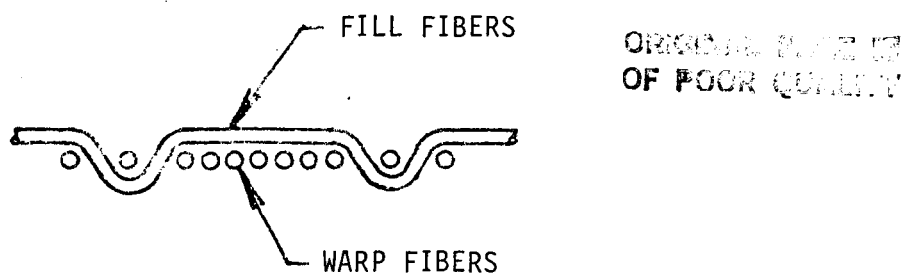


FIGURE 6.4

The resin content of samples taken from various areas of the parts varied only a few percent from one another for any specimen and was insufficient to have caused panel bowing. Thermocouples were placed in the layup to determine temperature distributions during the cure cycle. These showed an even distribution throughout the layup during the entire curing cycle. These tests showed the basic fabrication processes were being done correctly and that consistent laminates were being produced. The problem was finally resolved by balancing the stresses locked in to the bends of the corrugation by wrapping the mandrels as described in Section 3.3. See Figures 3.20 and 3.22.

The fabrication of these panels provided an opportunity to explore various methods of speeding up the layup procedure and to assess what additional problems might be encountered in laying up larger, curved panels. The original panel substructure design had corrugations which were layed up as one piece as shown in Figure 6.1. This would not be a difficult task with fiberglass, but carbon fiber with its much higher modulus of elasticity was too stiff to be forced easily into the flutes. The eight harness satin weave cloth proved to be the easiest material to work with because it could be bent more easily, but considerable time was still required to push the material down into the corners of the corrugations in such a way that it would stay put.

When the mandrels were individually wrapped to prevent the panel from distorting, the fabrication time increased significantly. This design does not appear to lend itself to a production situation, however, techniques such as braiding carbon fiber tubes to fit each mandrel might allow the panels to be produced at reasonable cost.

Another problem which was encountered was that the inner surface of the panels developed a series of ridges as shown in Figure 6.5. These ridges were caused by expansion of the rubber mandrels which is a function of the curing temperature, the volume of the rubber, and the intensity of the autoclave pressure resisting the expansion. The ridges would not affect strength or LFC performance, but rib attachments would need to be molded to the uneven surface because bonding could result in varying bond thickness which would not be conducive to good bonds. Several of the specimens made to investigate the bowing problem were also used to find a way of eliminating the ridges. Two methods were found to be satisfactory.

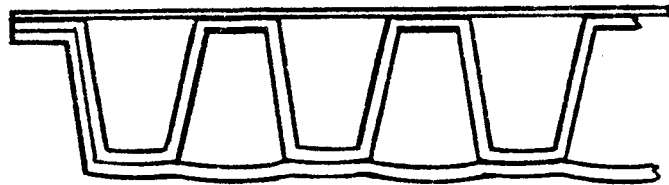
1. Using silicone mandrels extruded with a hole in the middle to reduce the expansion pressure reduced the ridges to an acceptable level. The hole reduced the rubber volume by 8.9 percent and allowed the material to expand inward as well as outward. This method is applicable to larger panels, curved panels, and high production rates.
2. The use of a local caul plate (Figure 6.6) produced a good flat surface on flat panels but would not transfer pressure uniformly on very curved surfaces such as the wing leading edge.

In a production situation, panel interchangeability requirements may dictate that matched tooling be used to control the overall thickness of the panels to close tolerances, at least in local areas. This, of course, would automatically give flat surfaces at those places where the panel would be attached to the supporting structure.

ORIGINAL TOOL
OF POOR QUALITY

RIDGES CAUSED BY SILICONE EXPANSION

TOOL SIDE



BAG SIDE

FIGURE 6.5

CAUL PLATE TOOLING

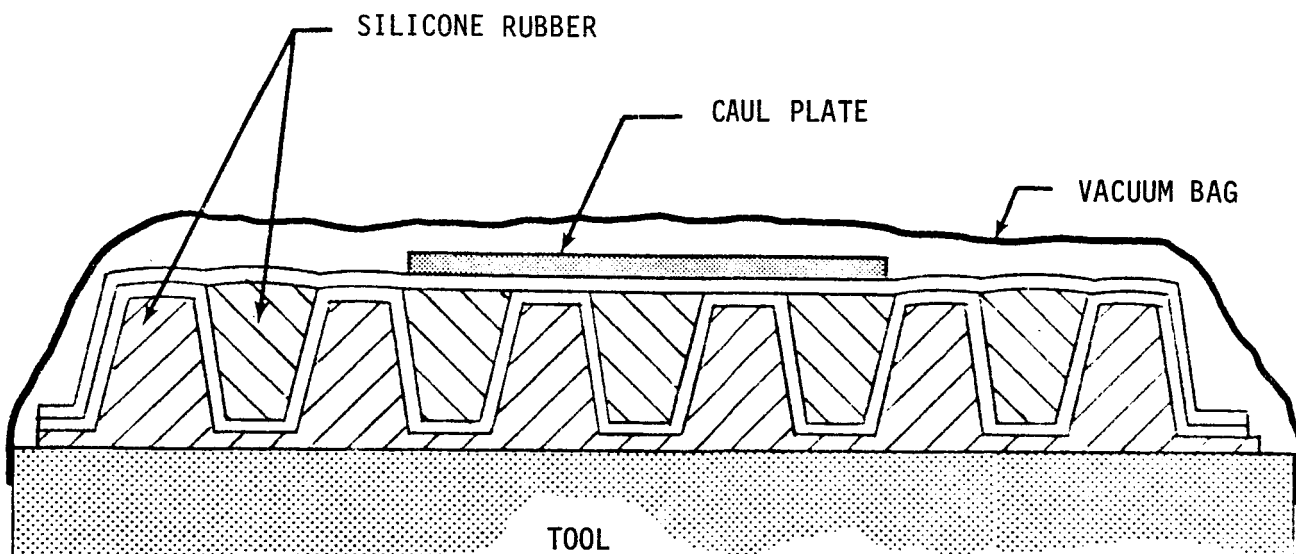


FIGURE 6.6

6.3 TITANIUM WELDING, PROCESSING, AND BONDING

6.3.1 Titanium Welding and Forming

The electron beam (EB) drilled material, as received from Pratt & Whitney, was 0.025 inch thick 6AL 4V titanium sheet material with a perforated area 17 x 54 inches. Since the major test specimen was to be 60 x 70 inches, it was evident that some technique for joining the sheets together would be needed. Welding seemed to be the obvious choice and several test specimens were made to determine whether this would be practical. The results showed that both electron beam and tungsten inert gas (TIG) welding could produce satisfactory welds. The EB weld produced narrower bead but is a more expensive process. As expected, both methods caused distortion of the sheets due to the high local temperatures involved. This "oil canning" was not acceptable and a method of removing it needed to be developed for welding to be used.

The welded sheets were successfully flattened by a method akin to the super plastic forming (SPF) process in which the material is heated in an inert gas atmosphere until it becomes plastic. Gravity or pressure is then used to form the material over a die, in this case a flat surface. In a production situation the panels would be heat formed to contour and if distortions due to welding were present, they would be removed during this process. For a smaller program, flattening the sheets to remove any distortions then rolling them to contour is less expensive, but is a more difficult and less accurate way to produce parts with the required curvature.

6.3.2 Titanium Processing and Bonding

The initial tests of the titanium/composite bond described in Section 3 showed a significant amount of data scatter. The process for bonding titanium and carbon fiber was being developed for the DC-10 Composite Vertical Stabilizer (CVS) program, but was not yet perfected as a Douglas standard process. As a result, the bonding process was unsatisfactory on some of the early lap shear and peel test specimens and this caused some specimens to fail prematurely. The CVS process used FM300K, an epoxy, as the bonding material and it was necessary to determine if the process would have to be modified for the AF31

adhesive which is a phenolic resin system which was more resistant to attack from PGME liquid. The process for bonding titanium to carbon fiber using AF31 adhesive finally consisted of:

1. an alkaline etch and phosphoric acid anodize of the titanium surface,
2. priming of all faying surfaces, titanium and composite, using an epoxy based primer, and
3. bonding of the parts within 72 hours of priming.

This process is essentially the same as that used for epoxy adhesives such as FM300. Use of this procedure did not raise the bond strength but did produce bonds of near maximum strength regularly, thus producing consistent results in subsequent tests. The use of AF31 adhesive also improves the bonding process because it does not tend to run out of the bond area. Because it does not plug perforations outside of the bond area, it not need be as precisely located during fabrication as the high flow epoxies.

6.4 CONCLUSIONS AND RECOMMENDATIONS - FABRICATION DEVELOPMENT

From a fabrication viewpoint, fiberglass would be a better material for the substructure than carbon fiber. It is much easier to work with and conforms to the tool more readily due to its lower modulus of elasticity. It would be of particular advantage if individually wrapped mandrels could be eliminated.

The flexible mandrel concept has proved to be an excellent method of tooling for the porous panel and is usable in a production situation. For those applications where the flutes must be accurately located, a method of stabilizing the tool dimensionally may be necessary.

Nothing inherent in any of the fabrication processes would limit the size of the panel that could be produced, however, panel cost versus size relationships have not yet been established.

The titanium surface material must be carefully prepared to obtain good bonds to the composite substructure and the necessary processing has been developed.

7. SUMMARY OF CONCLUSIONS AND RECOMMENDATIONS

7.1 CONCLUSIONS

- o The chordwise air collection method, which actually combines chordwise and spanwise air collection, is the best of the designs conceived up to this time for full chord LFC. Its shallower ducting improved structural efficiency of the main wing box resulting in a reduction in wing weight and it provided continuous support of the "chordwise" panel joints, better matching of suction and clearing airflow requirements, and simplified duct to suction source manifolding.
- o Laminar Flow Control (LFC) on both the upper and lower surfaces was previously reduced to LFC suction on the upper surface only, back to 85 percent chord (see Reference 1). The study concludes that, in addition to reduced wing area and other practical advantages, this system would be lighter because of the increase in effective structural wing thickness.
- o Panel size will ultimately be limited by design, cost or maintenance, repair and interchangeability considerations rather than anything in the manufacturing process.
- o Thermal analyses and tests were conducted which verified that it was possible to select combinations of titanium and carbon fiber that when bonded at 250°F would stay within the waviness and bowing criteria under flight ambient temperatures.
- o Whirling arm rain erosion/impact testing of small representative LFC panel specimens indicated that with flute widths up to 0.65 inch, a prolonged flight in heavy rain at a true airspeed of 400 miles per hour will not damage the LFC surfaces.
- o Impact damage tests of 50 inch pounds on both the bonding land and center of the suction flute caused significant delamination and splintering of the carbon fiber substructure. More testing in the 20 to 50 inch pound range would establish the level at which the damage to the substructure begins to occur.

- o Propylene glycol methyl ether (PGME) is the preferred freezing point depressant (FPD) liquid for ice protection and contamination avoidance (IP/CA). PGME was found to attack the FM 73 epoxy adhesive used initially, but a phenolic based adhesive (AF 31) maintained a strength of about 2000 psi and was selected for bonding the titanium surface to the substructure.
- o The suction levels required to achieve laminar flow over the wing were established.
- o It is desirable for the clearing system to provide sufficient positive pressure at the underside of the porous surface to prevent inflow of liquids. A positive pressure of 1 psi beneath the perforations is sufficient to avoid inflow of liquids and clear any residual liquid from the holes after a fluid has been applied.
- o The proposed electron beam perforated suction surface appears to be practical from the aspect of clogging and cleaning in service.

7.2 RECOMMENDATIONS

- o Use LFC suction on the upper surface only, back to 85 percent chord (Reference 1).
- o Use the chordwise collection method (which actual combines chordwise and spanwise air collection).
- o Use the titanium EB perforated outer surface supported by a bonded combination of carbon fiber and fiberglass support flutes to stay within the waviness and bowing criteria.
- o Continue the analyses, development, and testing of a fiberglass substructure with carbon fibers introduced in sufficient quantity to balance the thermal expansion.
- o For production components, investigate an all titanium panel. Compare surface smoothness, cost, and weight to the fiberglass substructure for a production quantity of 250 aircraft.
- o Continue material properties tests, small and large compression panel tests, rain erosion tests, and impact damage tests.
- o Establish criteria for allowable deterioration in service of the LFC surface from erosion roughness, indentations, and any porosity deterioration.
- o Investigate repair techniques, allowable blockage from dents, and maintenance intervals recommended.
- o To reduce the effects of the thermal expansion between the titanium surface material and the substructure material (which affects the surface smoothness), investigate a woven combination of glass and carbon fibers to achieve a coefficient of expansion equal to that of titanium.

- o A major design effort should be directed to develop panel joints to carry the expected loadings while maintaining the necessary joint smoothness and suction continuity. Development should include design and testing of joints, panel interchangeability, and integration of an IP/CA fluid dispensing system into the structure.
- o Porosity tailoring was considered as a possible way of matching suction and purging orifice requirement due to external pressure variations. Varying the porosity also reduces the suction airflow and power requirements. Further study of porosity tailoring should be done. This will influence the design of the clearing system.
- o More design development and testing is needed on joints, panel interchangeability, integration of an ice protection/contamination avoidance (IP/CA) fluid dispensing system into the structure, and final definition of the clearing system.
- o Further experimental development should proceed using a fiberglass substructure with carbon fibers introduced only in sufficient quantity to balance thermal expansion.

8. REFERENCES

1. Pearce, W. E., et al, Evaluation of Laminar Flow Control System Concepts for Subsonic Commercial Transport Aircraft, NASA Contractor Report 159251, June 1983.
2. Joubert, C., Laminar Flow Control Leading Edge Flight Test Shield Ice Protection System Specification, NASA Report ACEE-21-SP-1505.
3. Dagenhart, J. R., Amplified Crossflow Disturbances in the Laminar Boundary Layer on Swept Wings with Suction, Masters Thesis, North Carolina State University, August 1979.



9. APPENDIX I

SUCTION AIRFLOW REQUIREMENTS

An aerodynamic analysis of the wing geometry provided by contract NAS1-14632 was completed using the Douglas Jameson 3-D transonic potential flow program. Upper surface pressures are shown in Figure AI-1 for a wing lift coefficient of 0.56. The corresponding isobar map is provided in Figure AI-2. These pressure profiles were used with the MARIA (Reference 3) boundary layer stability analysis to develop suction requirements for laminar flow. An example of the MARIA output for the 93.5 percent semi-span station without suction is shown in Figure AI-3

Note that the inboard portion of the wing has an undesirable shockwave pattern. A refined aerodynamic design could have alleviated this condition if a complete wing were designed, however, such refinement was not within the scope of this program. Wing upper surface pressures outboard of 40 percent semi-span are in close agreement with the pressure profile of the generic two dimensional airfoil.

Updated suction requirements were determined for the WSSD wing using the MARIA boundary layer stability code. Design point conditions for $M = 0.80$, 35,000 feet altitude, and $C_L = 0.56$ were used to establish the baseline suction values. The acceptability of the values were checked at representative off design lift coefficients.

The upper surface chordwise pressure and suction distributions, along with the amplification factors for the two cross flow regions at the 50 percent semi-span station, are shown in Figure AI-4. This is a representative result of the MARIA stability analysis for the characteristic suction distribution having three regions of constant C_q .

The first suction region (leading edge) begins at the attachment line, typically forward of $X/C = 0.04$. A relatively high suction coefficient is necessary in this region due to the strong cross stream pressure gradients and consequent boundary layer crossflow instability. In the second region,

extending from $X/C = 0.04$ to $X/C = 0.60$, cross-stream pressure gradients are minimal and streamwise Tollmien-Schlichting boundary layer instability is the primary boundary layer transition mechanism, hence a relatively low suction level is adequate for maintaining laminar flow in this region. Aft of $X/C = 0.60$, cross stream pressure gradients are again significant and the streamwise gradients are adverse (positive). This region, therefore, requires a high level of suction in order to sustain laminar flow in the presence of the strong cross flow instability combined with the adverse streamwise gradient.

Suction requirements for the WSSD WING, as a function of spanwise station, are shown in Figure AI-5. These suction values were obtained by analysis of several spanwise stations using the MARIA stability code. It should be noted that, compared with previous suction estimates using the X-21 criteria, a substantial reduction of total suction required in the aft region is achieved by starting the increased suction at $X/C = 0.60$ instead of $X/C = 0.65$.

The increasing C_q requirement inboard, along the attachment line in the leading edge region, is compatible with the need for suction along the attachment line of a swept wing as indicated by the earlier X-21 data. This was due to attachment line instability generated when the attachment line Reynolds number (R_0) exceeds a value of approximately 100.

UPPER SURFACE PRESSURE DISTRIBUTION
D3128LFC WING LFC ON 85% C UPPER SURFACE ONLY, ALPHA-.23655D
EG MACH NO. = 0.800 ALPHA = -0.237 DEG. REF : JAMESON(22)+N/H
REY-MAC = 37.61 (MILLION) CL = 0.559 08/20/81

ORIGINAL FILED
OF PCOR QUALITY

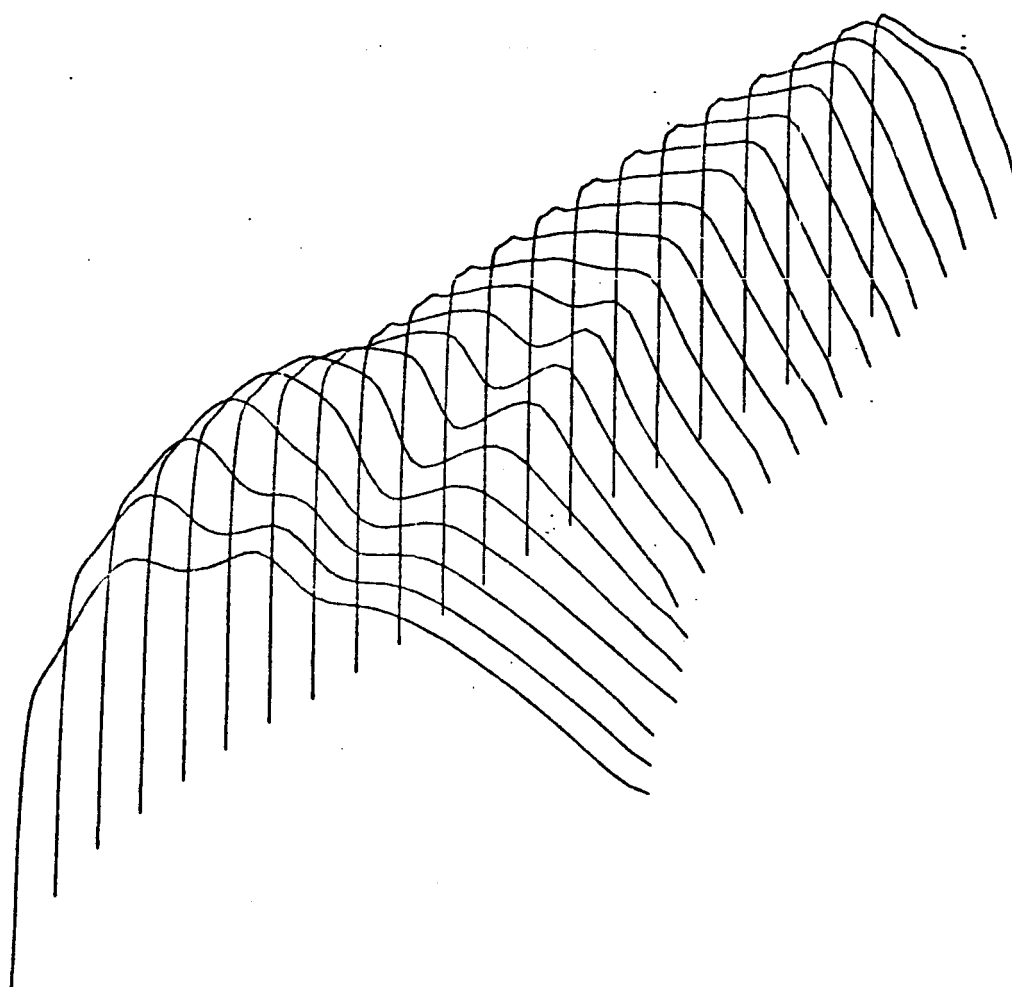


FIGURE AI-I

ORIGINAL PAGE NO.
OF POOR QUALITY

UPPER SURFACE ISOBARS

D3128LFC WING LFC ON 85% C UPPER SURFACE ONLY, ALPHA-.236550

EG MACH NO. = 0.800

ALPHA = -0.237 DEG.

REF : JAMESON(221)N/M

REY-MAC = 37.61 (MILLION) CL = 0.559

08/20/81

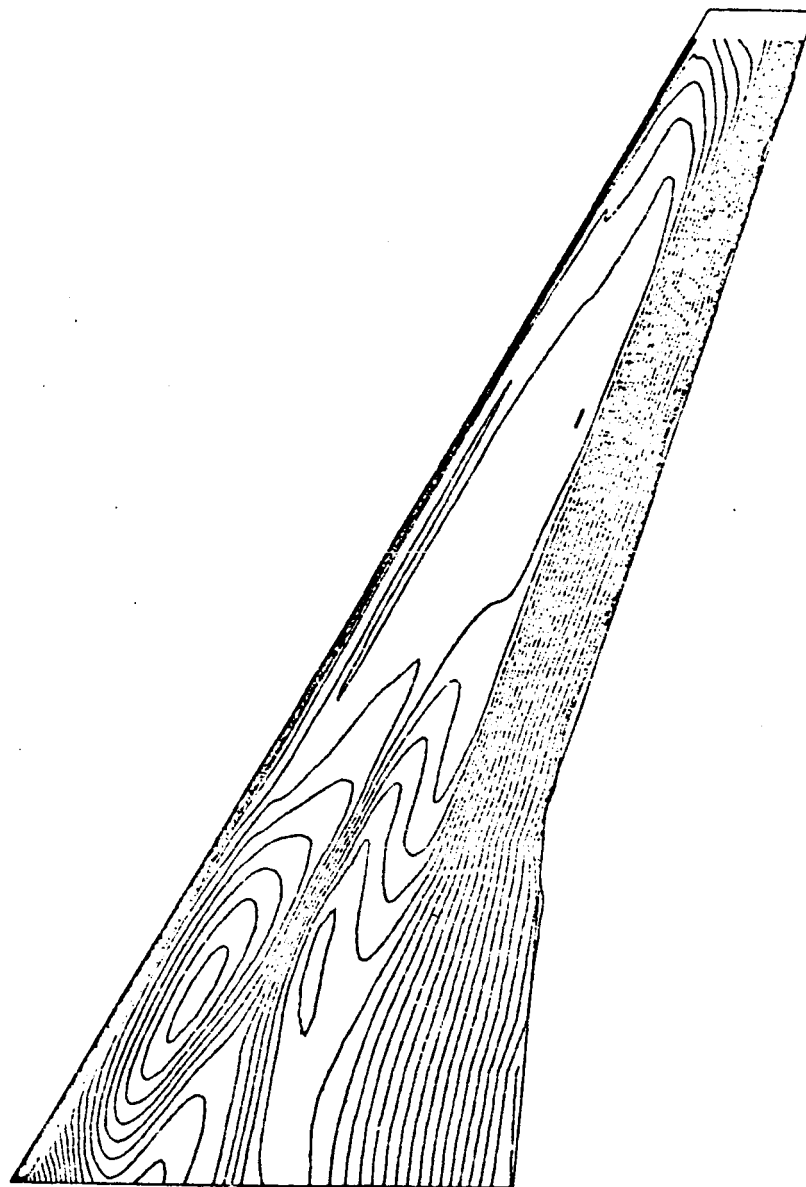


FIGURE AI-2

MARIA CROSSFLOW STABILITY ANALYSIS (NO SUCTION)

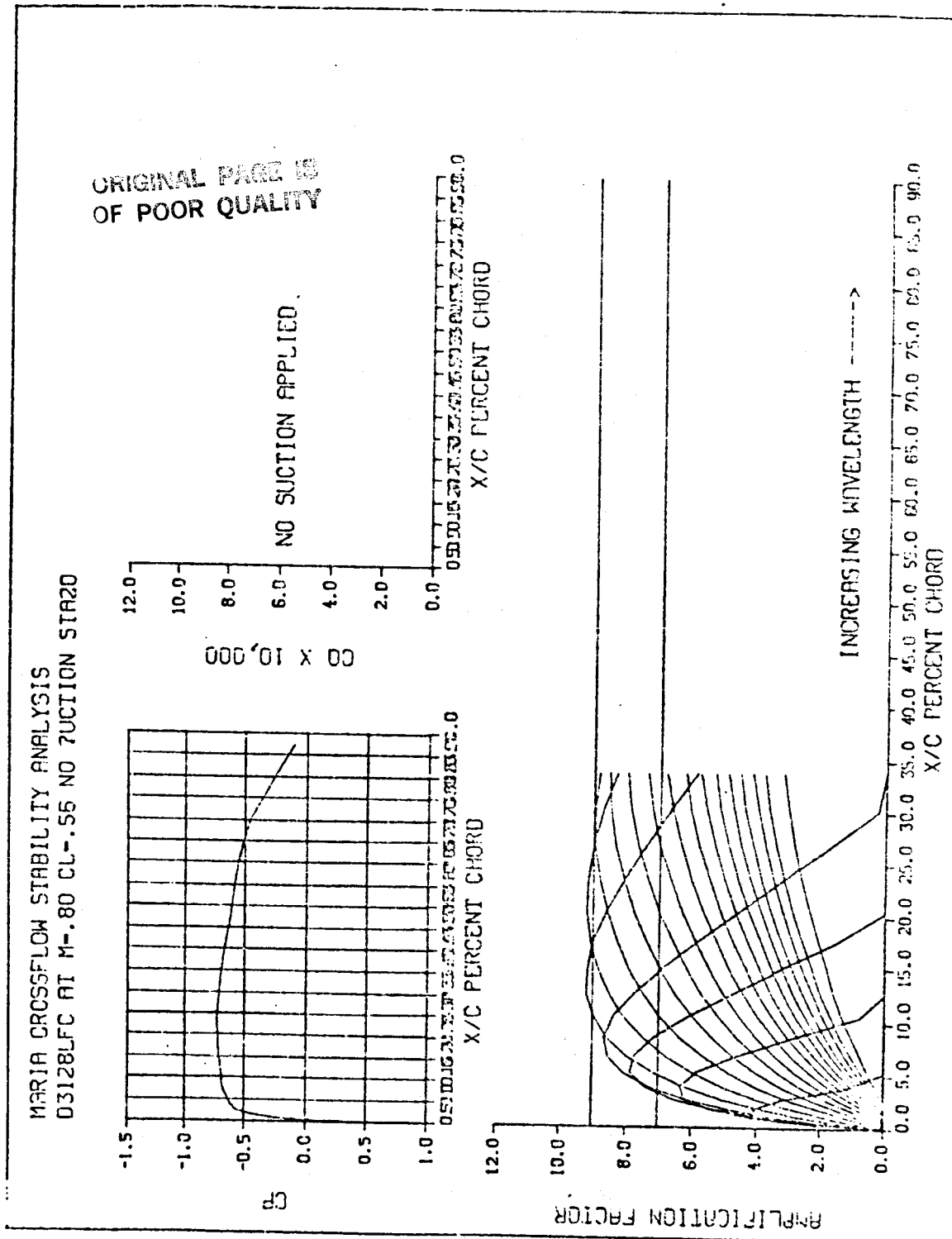


FIGURE AI-3

MARIA CROSSFLOW STABILITY ANALYSIS (WITH SUCTION)

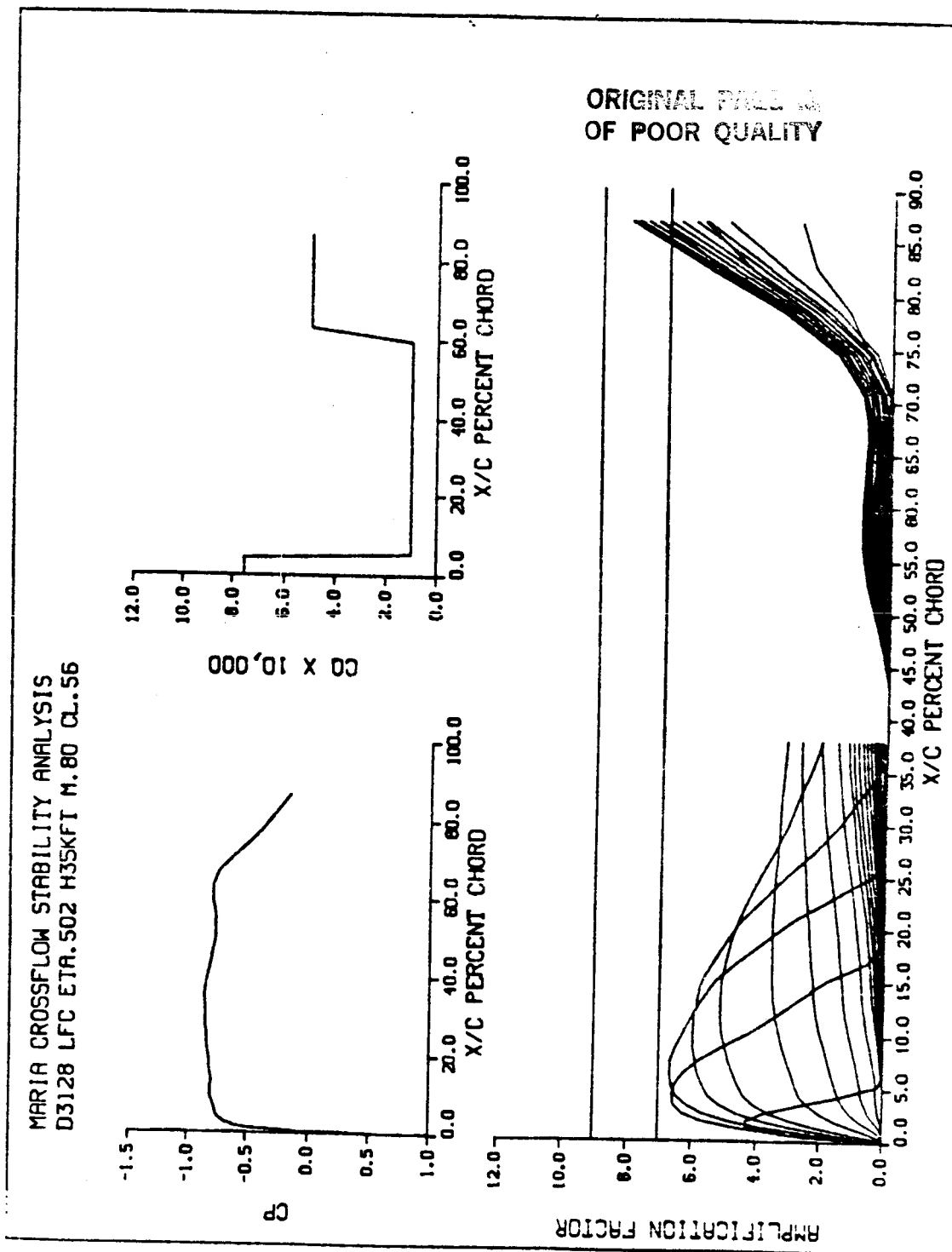


FIGURE AI-4

ORIGINAL PAGE IS
OF POOR QUALITY

WSSD D3128 SUCTION REQUIREMENTS
LAMINAR FLOW UPPER SURFACE TO 85% CHORD

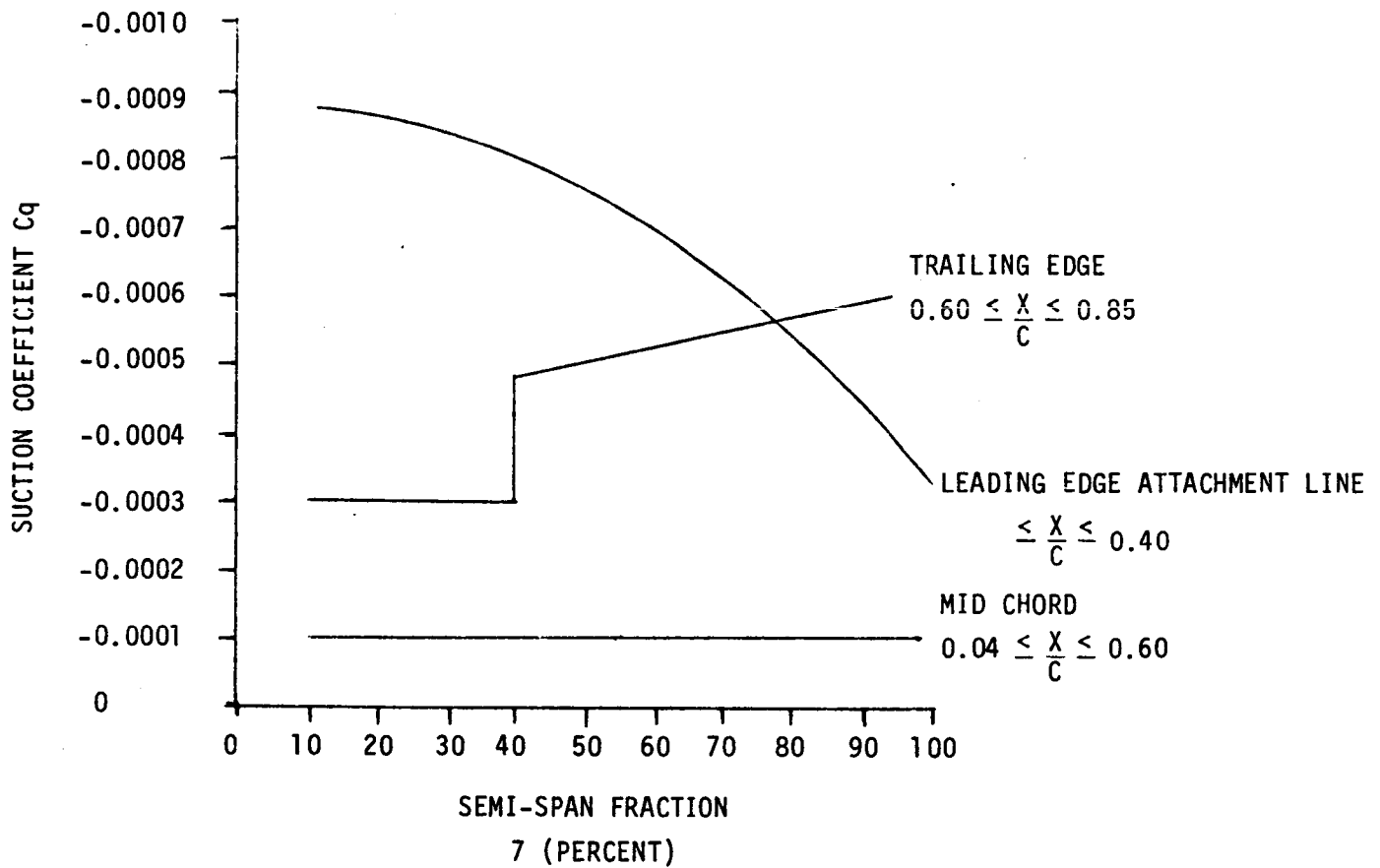


FIGURE AI-5

1. Report No. NASA CR 172424		2. Government Accession No.		3. Recipient's Catalog No.	
4. Title and Subtitle DEVELOPMENT OF LAMINAR FLOW CONTROL WING SURFACE POROUS STRUCTURE			5. Report Date July 1984		
			6. Performing Organization Code		
7. Author(s) C. B. Anderson, et.al.			8. Performing Organization Report No.		
9. Performing Organization Name and Address Douglas Aircraft Company McDonnell Douglas Corporation Long Beach, California 90846			10. Work Unit No.		
			11. Contract or Grant No. NAS1-17506		
12. Sponsoring Agency Name and Address National Aeronautics and Space Administration Langley Research Center Hampton, VA. 23665			13. Type of Report and Period Covered Contractor Report		
			14. Sponsoring Agency Code		
15. Supplementary Notes Langley Technical Monitors: J. Cheely and D. Maddalon, Final Report					
16. Abstract The preliminary design phase of the WSSD contract involved refining the design of the LFC panels and the panel supporting structure. The suction/clearing system and the ice protection/contamination avoidance systems for the wing configuration were included in the study to ensure systems compatibility. After investigating the various design options, the decision was made to use chordwise collector ducts over the main wing box and to retain spanwise collection ducts in the leading and trailing edge regions. This action not only improved structural efficiency, but made the matching of suction and clearing airflow requirements much easier, simplified the suction manifold-ing design, and allowed easy access to metering controls. A unique method of using low cost tooling of silicone rubber was developed to fabricate the laminated substructures for the porous panels. Two designs were created for dispensing liquid through the porous surface. The durability of the surface material was verified and the effects of the glycol based contamination avoidance liquids on various adhesive and laminate combinations were investigated. A nitrile-phenolic adhesive system was found to be more resistant to prolonged exposure to the liquid and was selected for bonding the titanium skin to the laminated structure.					
17. Key Words (Suggested by Author(s)) Laminar Flow, Electron Beam, Perfor- ated Titanium, Air Collection, Bonding, Ice Protection/Contamination, Silicone Rubber, Low Cost Tooling, Durability, Erosion, Thermal Distortion, Waviness.			18. Distribution Statement Subject Category 01		
19. Security Classif. (of this report) Unclassified		20. Security Classif. (of this page) Unclassified		21. No. of Pages 91	
22. Price					

Available: NASA's Industrial Applications Centers